博士論文

Stabilization and Functionalization of Bicelles (Magnetically Orientable Biomembrane Models) Using Tailor-designed Surfactants (界面活性剤の精密設計に基づくバイセル (磁場配向能を持つ平板状生体膜モデル) の安定化と機能化)

松　井　領　市

Stabilization and Functionalization of Bicelles (Magnetically Orientable Biomembrane Models) Using Tailor-designed Surfactants

A DISSERTATION

SUBMITTED TO THE UNIVERSTY OF TOKYO

by

Ryoichi Matsui

October 2016

Preface and Acknowledgements

Preface and Acknowledgements

The present thesis is the collection of studies that have been carried out between 2010–2016 under the direction of Professor Takuzo Aida at the University of Tokyo and RIKEN, Advanced Science Institute. The studies in this thesis are concerned with design of novel surfactants that offers unprecedented stabilization and functionalization of bicelles, new biomembrane models bearing planar lipid bilayer geometry.

A number of people have helped the author during his course of the work. First of all, the author would like to express his profound and foremost gratitude to Professor Takuzo Aida for his inspiring guidance and great support throughout this work. The author is also deeply grateful to the other members of his thesis committee: Professor Kazuaki Kudo, Associate Professor Masafumi Yoshio, Lecturer Hiroshi Sato, and Dr. Yasuhiro Ishida (team leader, RIKEN).

The author extends his sincere gratitude to Dr. Yasuhiro Ishida for his valuable advice, guidance, kind help, and fruitful discussions. The author would like thank him for kind guidance of the unsatisfactory and disrespectful student for such a long time. The author could not obtain a degree without him.

The author also feels grateful to Professor Kazushi Kinbara for guidance on the first year in his research life and teaching him basic attitude as a scientific researcher and methodology on presentation. The author would like to give cordial gratitude to Assistant Professor Yoshimitsu Itoh for teaching him basic skills on organic synthesis. Grateful acknowledgement is also made to the following Collaborators. Assistant Professor Masataka Ohtani gave the author the first idea concerning the usage of cholic acid-derived surfactant for bicellar systems. Ms. Kuniyo Yamada kindly helped the author by mass scale synthesis of surfactant precursors. Dr. Hiroyuki Koshino (unit leader, RIKEN) and Dr. Takashi Nakamura (RIKEN) gave great efforts for highly reliable solid-state NMR spectra of quite temperature-sensitive and unstable polymerizable bicelles, and also gave the author fruitful advice on skills in NMR measurements throughout the course of the works. Dr. Noriyuki Uchida (RIKEN), Ms. Arisu Shigeta, and Dr. Izuru Kawamura kindly accepted urgent need of additional solid-state NMR experiments, and had tough,

speedy and fruitful works soon before submission. Dr. Yoshiki Yamaguchi (team leader, RIKEN) gave the author meaningful advice on properties and know-hows in treatment of bicelles. Without his kind help, the author could not complete any paperwork.

Associate ProfessorAkihiko Tsuda, Associate Professor Norifumi Fujita, Senior Lecturer Hendrik Oktendy Lintang, Assistant Professor Yoshiaki Shoji, Assistant Professor Kou Okuro, Assistant Professor Nobuhiko Hosono, Assistant Professor Tsuneaki Sakurai, Dr. Daigo Miyajima (team leader, RIKEN), Dr. Junko Aimi, Dr. Joon-il Cho, Dr. Terutsune Osawa, Dr. Jeongho 'Jay' Lee, Dr. Kohei Sato, Dr. Takahiro Fukino, Dr. Michio Matsumoto, and Mr. Hiroki Arazoe gave me practical advice as well as helpful suggestions for which the author strongly acknowledge. In addition, the author would also like to express his appreciation to the members of RIKEN groups directed by Professor Takuzo Aida. Especially, Professor Takanori Fukushima, Professor Xigang Wang, Professor Mingjie Liu, Professor Yi-Tsu Chan, Associate Professor Takashi Kajitani, and Assistant Professor Ammathnadu Sudhakar Achalkumar gave me kind advice and fruitful suggestions throughout the author's doctoral course. The author also would thank all laboratory members for kind, delightful, and fruitful (drinking) communication with him.

The author also wishes to show his gratitude to Naoko Saito, Naoko Suyama, Sayuri Tatsuzaki and Mari Oguro for their extremely kind help with official business in the University of Tokyo, and also Mayumi Nagata, Aya Numata, and Reika Luo for their extremely kind help with official business in RIKEN. The author also wishes to show his gratitude to RIKEN Junior Research Associate Fellowship and his uncle Mitsuo Matsui for his financial support during his doctoral course.

The author also thanks to his dear friends; friends from his bachelor course (Faculty of Liberal Arts); Kei Ohashi, Assistant Professor Saeko Okada, Assistant Professor Yuki Imura, Mrs. Kazuhito Tanaka, Shigeyoshi Sato, Maki Mizuno, Hiroko Okamura, Tetsuro Fujita, and Dr. Yoshitaka Moriwaki, friends from his bachelor course (department of Chemistry and Biotechnoligy and related department); Dr. Tomohisa Hirano, Ms. Mariko Mitsuhori, and Ms. Tomomi Oguma, and friends tied

with peculiar relationships; Drs. Yutaro Kashiwagi, Sho Inomata, Kenta Yoshida, and Ms. Mizuki Kashiwagi. The author finally could reach here to write this thesis by their heartwarming supporting hands and friendship. They supported and encouraged him anytime when he was depressed or delighted. And the author reinforced the enthusiasm to science through frank communication with them. Especially, without Dr. Imura's supporting lecture of "Basic Modern Chemistry" the author could never notice pleasure of scientific researches.

Finally, the author wishes to express his deepest gratitude for his family. His mother, Fumiko, and his passed father, Matsuo Matsui have raised him up, supported his education, and encouraged him affectionately. His mother financially supported him even after his father passed. His father might not think that he continue to study to reach the doctoral degree. The author is proud to become a scientific engineer/researcher like his father, even though the field is a little bit different. And his wife, Hiroko Matsui, kindly supported and encouraged him during his extended course of the degree. During the course, she was in pregnancy, and could happily bear his and her new family. When she was unwell in pregnancy, the author was often out for completion of the course and caused her some troubles. The author would thank her for enduring such tough situation to keep her and the child's health. At last, the author would especially thank to his daughter Shiho Matsui, who was born during his extended course of a doctoral program. The author feel thank her for coming to his family. Her smiles and healthy growth encouraged him every day. The author dedicates this thesis to his family.

Ryoichi Matsui

Aida Laboratory
Department of Chemistry and Biotechnology
School of Engineering
The University of Tokyo
October 2016

Table of Contents

Table of Contents

General Introduction

1.1. Membrane proteins and biomimetic membrane models

Cells in all living organisms have cell membranes that divide themselves from exterior environment. Cell membranes have two contradictory important functions; to prevent some unnecessary materials from flowing into the cell, and to give and receive materials between interior and exterior of the cell. To fulfill such contradictory requests at the same time, the cell incorporates elaborately designed membrane proteins into its cell membrane. Membrane proteins are known to interact with some kind of signaling agents to function, and many coenzymes, bacteria, viruses that inhibit function of membrane proteins or denaturation of them, are revealed up to now. That is, elucidation of function of membrane proteins and mechanisms of signal transfer directly leads to important studies to know vital function and therapeutic management of diseases.

Rate of membrane proteins in all organisms (from Bacillus coli to human) is known approximately 30% of all proteins.[1] And structures, functions, and mechanisms of action are actively being studied. Especially, researchers have competed to study structures of membrane proteins so far, because they have to fully understand their structures before analyzing their mechanisms of action. Before development of molecular biology, methods of structural analysis were limited. As platforms and methods (e.g. mass scale protein synthesis, analytical methods of X-ray diffraction patterns and facilities with highly bright synchrotron beams) are gradually established, number of analyzed proteins is exponentially growing. For example, bacteriorhodopsin, a light-driven proton pump found in the purple membrane of *Halobacterium salinarum*, is one of most important and popular membrane proteins which structure has been elucidated with modern methods of structural analysis.[2] Structural analysis of complex, peculiar, and large membrane proteins e.g. calcium pump proteins, gap-junction proteins[3] and Aquaporin[4], are also succeeded as a result of continuous studies in analytical methods of membrane proteins.

However, analysis of membrane proteins is still difficult compared with that of normal (water soluble) proteins, because they are hydrophobic, they are stable only in lipid bilayers, thus purification and isolation in mass scale is difficult, and thus preparation of single crystals of membrane proteins is much more difficult than that of water-soluble proteins. In addition, flexible water-soluble domains coexist in most of

membrane proteins, which conformation can easily be changed by responding to many stimulating substances. It is quite difficult to analyze structure or function of such water- soluble domains by static analysis like crystallization methods. In order to analyze such kind of domains, we need to incorporate these proteins into model membranes which can be applied to dynamic spectroscopic methods like solution NMR. To address these challenges, many kinds of cell-free model membranes that cannot denature the structures of native membrane proteins, and afford systems in which we can easily analyze proteins, are explored. As these demand of researchers, up to now, micelles, vesicles, supported lipid membranes, lipidic cubic phase, and bicelles are established, and are popularly used (Figure 1). These model membranes, well mimic properties of natural cell membranes in some aspects, however, at the same time have fatal drawbacks which are caused by insufficient mimicry of these model membranes. Therefore, we have to choose proper membrane mimetics for specific analysis, and carefully search the most suitable model for stabilization of target membrane proteins or membrane-acting molecules, with somehow combinatorial way.

Here, especially, the author would like to introduce versatility and utility of Bicelles (bilayered micelle), which have flat lipid bilayers in highly homogeneous solution. Bicelles have been introduced in the 1990s as new membrane mimetics and quickly gained popularity.[5] As bicelle was found later than other model membranes listed above, their structures have not been exhaustively analyzed yet. In addition, bicelles also have other drawbacks mainly on their stability. Yet, bicelles have wide variety of advantages which other membrane models don't have (of course described later), so the author feels that bicelle will be potentially more versatile model membrane if its defects are rectified. In this thesis, the author would like to explain a series of studies that conquer fatal drawbacks of bicelles in order to be able to serve as versatile model membranes. In the study, the author developed a new component of bicelle strategically, and explored the method of extraordinarily stable bicelle compared with existing bicellar systems. Before explaining the author's study in the course of doctoral degree, in the introductory section, here, the author would like to introduce components, morphology, and thermodynamics of biomembranes and model membranes stepwise. In the section of component of biomembranes, the author would like to review physical chemistry of membranes with various natural lipids, and also would like to explain difficulty in development of perfect biomembrane mimicry

and fabrication of highly versatile model membranes. In the section of details in existing model membranes, components and morphology of each model membrane are reviewed, and then advantages and drawbacks of each model membrane are discussed in detail. In the next section, detail of bicelle is reviewed. In this section, the author will explain structure and thermodynamics of bicelles which are understood so far, and then, examples of application to analytical methods for proteins and application to material science. At last, the author will explain "making of stable and versatile bicelle", that he aimed throughout his course of studies. In this section, significance and novelty of the studies, and approaches for realization of the aim are briefly explained.

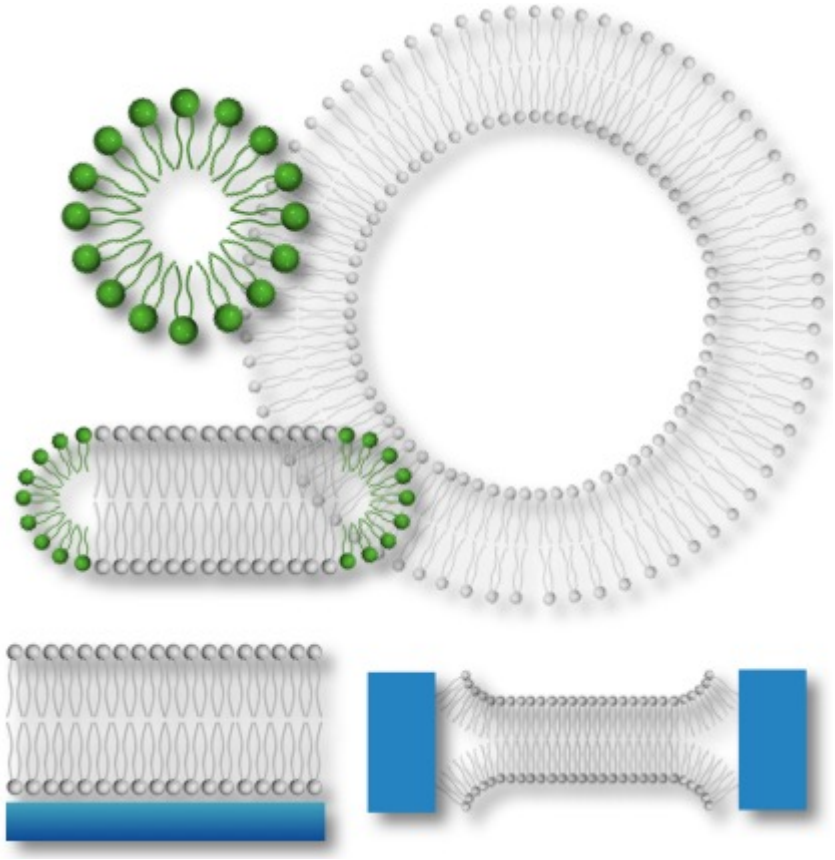

Figure 1. Schematic illustration of biomimetic model membranes.

1.2. Components and chemistry of living cells

As mentioned above, major functions of cell membrane are to separate cell itself from exterior environment, and to take only necessary nutrients from exterior environment only when the cell needs. As described above, main functions of cell membrane are to divide cell itself and exterior environment, and to take in necessary materials only when necessary. The component that realize these two contradictory demands are lipids that comprise cell membrane, and membrane proteins. Amphiphilic lipids forms bilayer in the way that a hydrophilic segment exposes to the surface of the bilayer, and a hydrophobic segment assembles each other in the interior of the bilayer (Figure 2).

Cell membrane exists even on the surface of cell organelle. Each type of membrane has unique composition in lipids and proteins, and the composition of them drastically influences physiological status and morphology. For example, in cell membrane of mitochondria, Gorge apparatus, and endoplasmic reticula, ratio of lipids and species of proteins varies differently, thus each of them can perform each different but important role. Although, component of lipid bilayer is almost common (but ratio is quite different: described later). Component of these membranes is mainly electrically neutral phosphatidylcholine (PC; Figure 3a) such like DMPC (dimyristoyl phosphatidylcholine) and POPC (palmitoyl oleoyl phosphatidylcholine) with unsaturation on its hydrophobic chain, and negatively charged phosphatidylglycerol (PG; Figure 3b). In addition, typically sphingomyerin (SM; Figure 3c), phosphatidylethanolamine (PE; Figure 3d), phospahtidylserine (PS; Figure 3e), and cholesterol derivatives (Chol; Figure 3f) are incorporated into a biomembrane. Difference in the ratio of these lipids is quite important to gain character of each organelle. For example, lipid bilayer membrane in human red blood cell, which is one of best analyzed lipid bilayer, is composed 21% of PC, 29% of PS and PE in sum, 21% of cholesterol derivatives, and so on. On the other hand, mitochondria are composed 40% of PC, 1% of PS, 35% of PE, 1.6% of cholesterol derivatives. Demand of robustness, flexibility, fluidity, or microscopic morphology to express proper functions are quite different between these two cells, so such unique balance of ratio is necessary.

It is undoubtedly clear that lipid bilayer has a lateral fluidity. In 1972, "fluid mosaic model" was proposed by Singer and Nicholson (Figure 4).[6] They proposed that biomembranes consist of lipid bilayers and membrane proteins incorporated into bilayers in a mosaic-like way, and proteins laterally diffuse inside the bilayer. According to this model, not only orientation of lipids but also membrane proteins are located in a way that a hydrophobic surfaces of them are concealed interior to avoid contact with water, and a hydrophilic surfaces are exposed on the exterior of the membrane. In addition, structures of membrane proteins are not fixed in lipid bilayers, but change their conformations flexibly in addition that proteins can "swim" flexibly inside lipid bilayers. Over forty years passed from the proposal, now fluidity of lipids and its local assembly are studied quite actively. As a result, it becomes well-known now that many different functions of lipid bilayers are caused by many different components, ratio, and interactions.[7] Now properties of lipid/protein dynamics can be observed with various analytical methods.[7] Here the author would like to summarize dynamic motions of lipids and their correlation time that is known up to now (Figure 5).

1. Vibrations of bond length and bond torsional oscillations (subpicosecond range)
2. Vibrational motions of bond orientation (picoseconds)
3. Rotations about chemical bonds, gauche/*trans* isomerization (pico- to nanoseconds)
4. Diffusional reorientation of lipid molecules about their long axis (nanoseconds)
5. Wobble of lipids (nanoseconds)
6. Lateral diffusion in the plane of the bilayer (nano- to microseconds for movement over a distance of 0.8 nm, the approximate lateral lattice spacing between two lipids)
7. Undulatory motions of bilayer patches (microseconds to seconds)
8. Flip-flop of lipids between the two monolayers of a bilayer (milliseconds to hours)

As mentioned above, membrane proteins are swimming laterally in a pool of lipid bilayer. By moving about membranes, they relay many materials to other kind of (membrane) proteins, and bind together with other (membrane) proteins or small

(membranous) molecules to exert peculiar functions by concerted mechanisms. For example, G protein-coupled receptor (GPCR), a kind of seven-transmembrane receptors, is coupled to a trimer of G protein that drifts inside the membrane, and then the complex of these proteins finally bind with other target (membrane) proteins to enhance/repress functions of the target. Some kinds of membrane proteins cut off inositol phospholipids enzymatically to utilize products as a media for signal transduction.[8] These chemical events arise effectively because they stick together around peculiar space of lipid bilayer, and proteins and incorporated molecules can easily move laterally in the pool of lipid bilayer. That is to say, many part of motions and functions of proteins are dominated by diffusion properties of lipids. Dynamic motions of lipids are closely related to mechanisms of protein functions. Here, the author would like to explain briefly thermodynamic properties of lipid bilayers with various compositions of phospholipids and other additives. The author will also add the explanation that new assumed models have been emerged based on continuous studies of thermal and dynamic properties since 1980s.

In lipid bilayers, interaction, lateral mobility of lipids, and morphology of bilayer drastically changes thermodynamically. Typically, as temperature gets high, interaction between lipid molecules become smaller, lateral mobility gets higher, and crystallinity gets lower. In mixed system of water/lipids, phase transitions are performed mainly between L_c (crystalline) phase, L_β (gel) phase, P_β (ripple) phase, L_α (fluid, or liquid crystalline) phase (Figure 6). In L_c phase shown at low temperature, crystal-like packing even on hydrophobic long chain can be observed. L_β phase, also called as liquid ordered phase, appears higher temperature than L_c phase. In this phase lipids can diffuse laterally, although diffusion coefficient is slow compared with that in L_α phase because geometry of hydrocarbon chain is still all-trans to tightly pack together. In L_α phase, packing of alkyl chains is significantly disordered, and fast lateral diffusion of lipid can be observed. Such fluidity of lipids and ordered alignment of bilayers, model membranes acquire liquid crystallinity. P_β phase shown at middle temperature range, is unstable phase that has ripple-like, a bit disordered bilayer can be observed. In P_β phase, hydrophobic chains of lipids are a bit packed together like L_β phase. Phase transition between L_β-P_β and P_β-L_α are called pretransition and main transition respectively. From differential scanning calorimetry (DSC) observations,[9] [7] for example, phase transition enthalpies in DMPC bilayer are

estimated as 5.0 kJ/mol and 26 kJ/mol, respectively.[10] Phase transition temperatures are dependent on species of polar group, length of alkyl chains of lipids, and branching or unsaturation of hydrocarbon chains. For example, phase transition temperature of DMPC (number of carbon chain is 14) is 14 ºC (L_β-P_β) and 23 ºC (P_β-L_α) (Figure 7). If the hydrocarbon chains are increased into 16 (DPPC; diparmitoyl phosphatidylcholine, chain number; 16), phase transition temperatures raise up to 35 ºC (L_β-P_β) and 41 ºC (P_β-L_α). Then, when polar group of DMPC is changed to form DMPS (dimyristoyl phosphatidylserine), DMPE (dimyristoyl phosphatidylethanolamine), and DMPA (dimyristoylphosphatidic acid), main transition temperature gets higher (36 ºC, 49.5 ºC, 50 ºC, respectively; Table 1). When unsaturated hydrocarbon chains (such as POPC; 1-Palmitoyl-2-oleoyl phosphatidylcholine) are introduced, phase transition temperature decreases drastically (Figure 8).[11] After morphology and phase transition behavior of lipid bilayers with a single component are revealed, then behavior of bilayers composed of two or more lipids, and sometimes mixed bilayer with lipid and other chemicals are gradually studied. Through the series of studies, artificial membranes can gradually reflect microscopic behavior of biomembrane, and these studies are succeeded in revealing important properties that occur only in such complex systems. For example, when two disaturated PCs with different alkyl chain length, if the difference in chain length are small (typically 1 to 4 methylene), these lipids are perfectly miscible, and phase transition temperature of crystalline to gel state ($L_c \rightarrow L_\beta$) changes almost proportionally to mixture ratio of lipids.[12] On the other hand, if difference in chain length is big (over 6 methylene), phase transition point of crystalline to gel state does not change any more, which indicates that miscibility of lipids are too bad, and thus lateral phase separation in bilayer occurs to generate microscopic domain.[11] (Figure 9) Several factors that dominates miscibility of lipids are known. For example, alkyl chain length (melting point of a chain), unsaturation of alkyl chain (melting point and packing factor),[13] interdigitation[14], species of lipids (interaction or charge of head group. For example, miscibility of PE and PC are different from that of two PCs[15]) are typical and critical factors that change miscibility of lipid mixture.

Recently, selective domain formation that is not depicted in the fluid mosaic model has been found. Major factor of such domain formation is non-lipidic additives that can interact selectively with lipids. This domain formation supports

selective and efficient enzymatic reactions or specific interactions of incorporated proteins, by aggregating needed materials in and around the lipidic domains. For example, a molecule that supports this kind of mixed domain formation is cholesterol. Cholesterols are reported to strongly interact with some kind of lipids to form domain-like aggregates in a mixed lipid bilayer. This kind of interaction to form specific domain is experimentally demonstrated using a kind of model membranes that is composed of two different lipids and cholesterol.[16] (Figure 10) Recently, the lipid/cholesterol domain is believed in also exist in natural biomembrane. It is proposed that some biological events in lipid bilayers are closely linked with translational domains composed of lipids (typically sphingomyelin: SM) and cholesterols called "lipid rafts," which is continuously generated and dissociated (Figure 11).[17] Now, lipid raft is defined as unstable and thus transient assembly composed of lipid, proteins and other small molecules. When membrane proteins come close to (or incorporated into) such assemblies, unprecedented interaction are possible with much higher probability than when they are uniformly dispersed in the membrane. Thus, specific and efficient enzymatic reactions and peculiar multicomponent interactions are thought to be possible. For example, Alzheimer diseases, mad cow diseases, influenza are regarded to be related by lipid raft domains.[18] For that reason, such raft-like domains are regarded as problems needing to be solved. Most of experimental proofs concerning existence of raft-like domains are performed on model membranes. For example, when supported lipid bilayers are prepared by two cholesterol and two lipids with different chain length, "island" with higher height is confirmed to generate by AFM.[19] Similar domains are confirmed with fluorescent optical microscopy.[20] Computational models also support favorable domain formation.[21] Actually, however, existence of lipid rafts in living organisms are now in argument.[17a,22] Yet, there are some trials of direct observation of living lipid rafts using specially prepared microscopy. Hell and coworkers succeeded in observing lipid domains with much slow diffusion property in plasma membranes by using STED (STimulated Emission Depletion) microscopy.[23] [17] Owen and coworkers directly observed cholesterol-dependent ordered lipid assembly by fluorescence lifetime imaging microscopy (FLIM).[24] Supported by these findings, behaviors of lipids are drastically brought attentions by chemists, molecular biologists, and even physical chemists.

As described above, as fundamental insights on lipid bilayers have been accumulated, more insights about behaviors of complex assemblies like biomembranes have gradually been revealed. In detail, translational domains can be formed by mixing multiple lipids with different phase transition behaviors or intermolecular interaction and non-lipidic additives like cholesterols, which cannot be observed in a simple artificial lipid bilayer with single component. Now, Biomembranes are hypothesized to have the same translational assemblies "lipid raft," which environments are favored by specific proteins or target molecules. Each membrane of cell or organelle has a specific composition (Table2, 3), and thus characteristics in physical chemistry varies widely (Table 4). This fact strongly suggests that each cell membrane elaborately create translational environments which are suitable for their functions. Now, many studies highlighted to interactions between lipids and proteins are ongoing.[25] To summarize, as same as proteins that functions, to study function of lipid bilayers that helps efficient function of proteins is quite important.

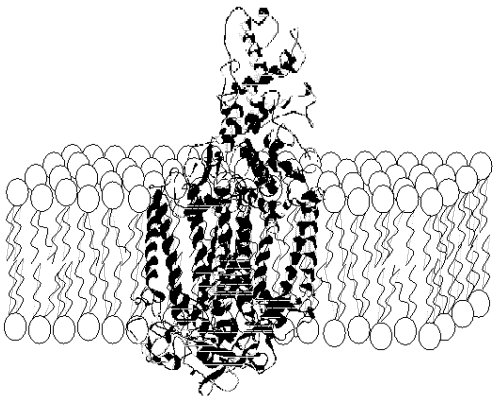

Figure 2. Schematic representation of a biological membrane bilayer with lipids and a transmembrane membrane protein

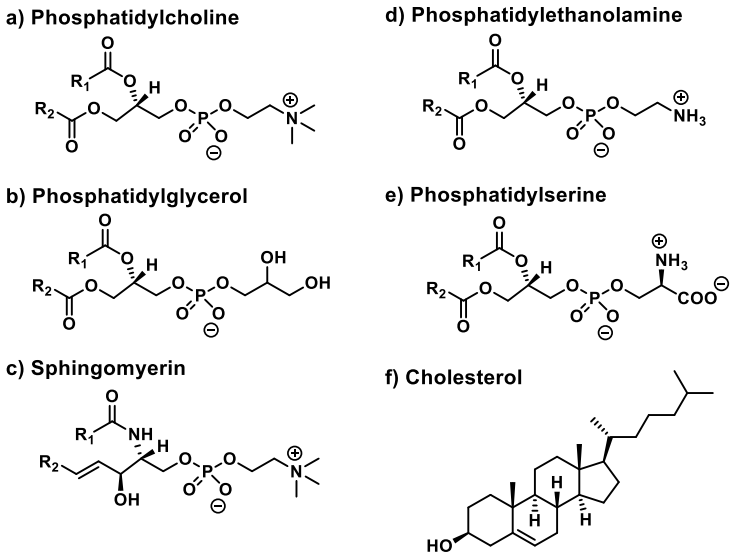

Figure 3. The molecular structures of POPC, DMPC and DMPG. The nomenclature for the positioning of the two fatty acyl chains is indicated for DMPC, as is the conventional numbering and labeling of some of the carbon atoms.

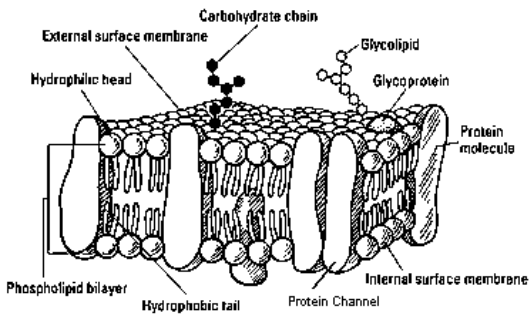

Figure 4. Schematic representation of fluid mosaic model of cell membranes.

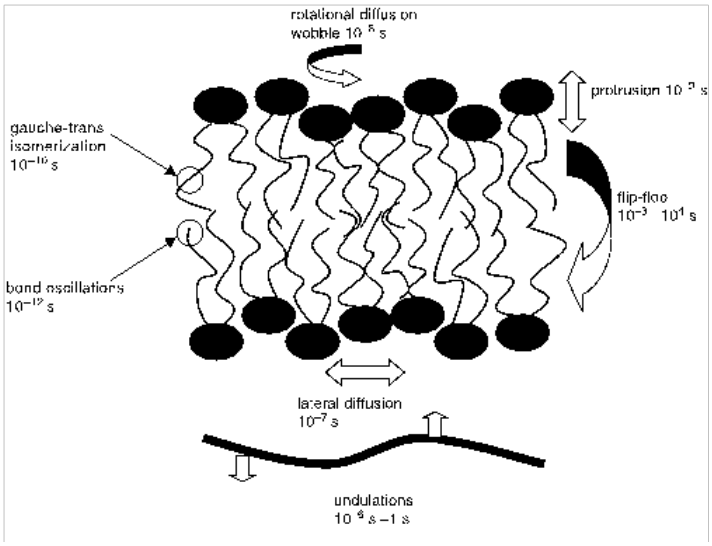

Figure 5. Typical time-scales (correlation times) for different types of motions in a biological membrane (Adapted from Yeagle, P.L, 2005. "The Structure of Biological Membranes" CRC press, Boca Raton)

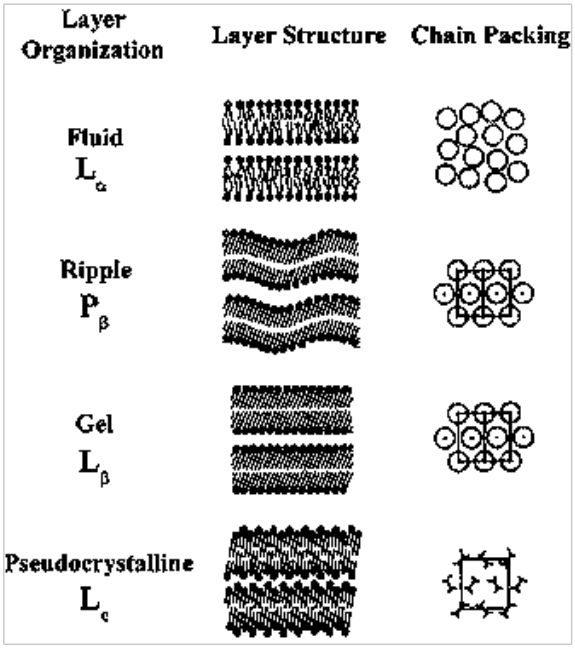

Figure 6. Organization of the lamellar bilayer phases of DPPC in the fluid (L_α), ripple (P_β), gel (L_β) and pseudo-crystalline or subgel (L_c) states. A top view of the packing of the hydrocarbon chains is shown in the last column.

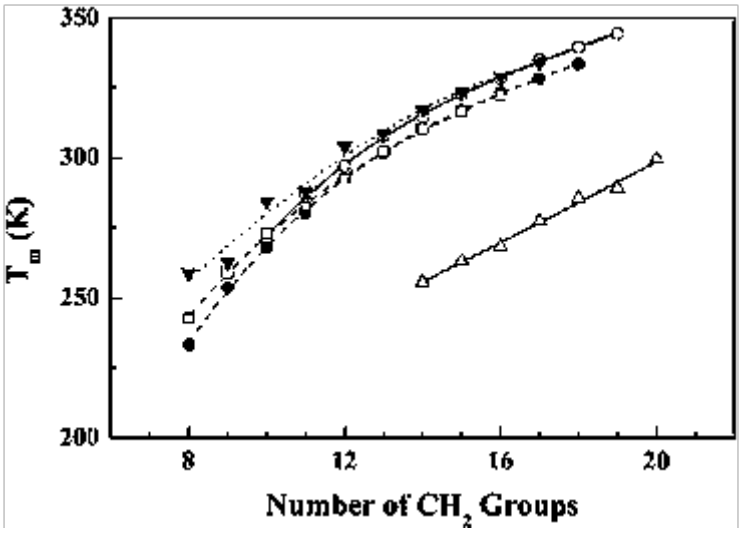

Figure 7. A plot of the gel to liquid–crystalline phase transition temperatures of a group of homologous series of chain-symmetric PCs containing different classes of fatty acids vs. the number of CH_2 groups in the hydrocarbon chain. The symbols are as follows: (○), linear saturated PCs, (●), methyl isobranched PCs, (▫), methyl anteisobranched PCs, (▼), w-cyclohexyl PCs; and (△), *cis*-monounsaturated PCs.

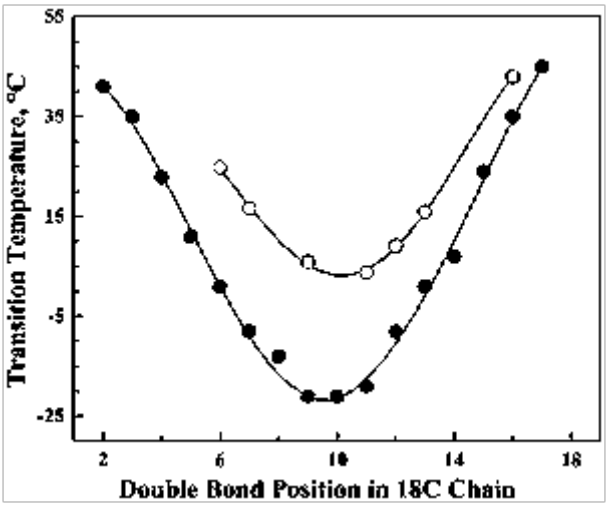

Figure 8. Plots of the apparent gel to liquid–crystalline phase transition temperature of a series of chain symmetric dioctadecenoyl PCs (-●-) and 1-stearoyl-2-octadecenoyl PCs (-○-) vs. the position of the double bond in the *cis*-monounsaturated hydrocarbon chain.

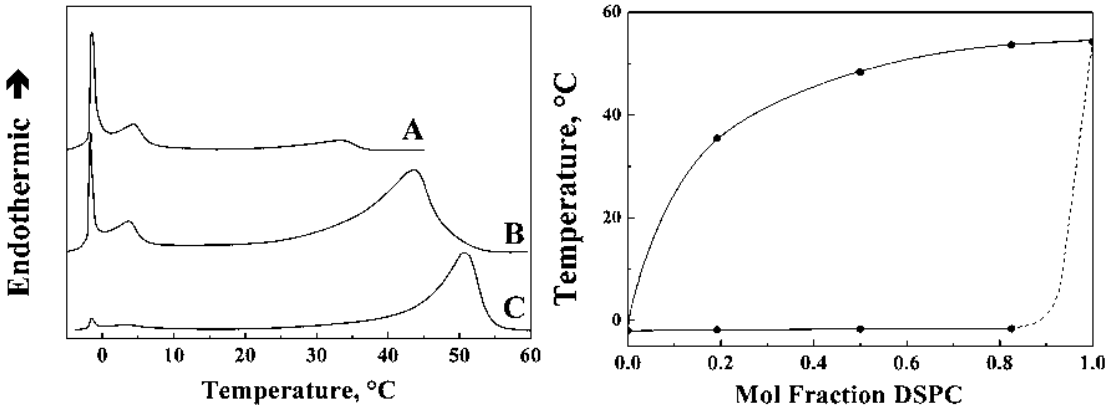

Figure 9. Process of phase segregation of two-component lipid bilayer. Left; Solid curves, dashed baselines: transition curves for DLPC–DSPC mixtures with mole fraction DSPC (XDSPC) = 0.191 and 0.819. Dashed curve, solid baseline: transition curve for XDSPC = 0.498. Right; Phase diagram constructed from calorimetric transition curves.

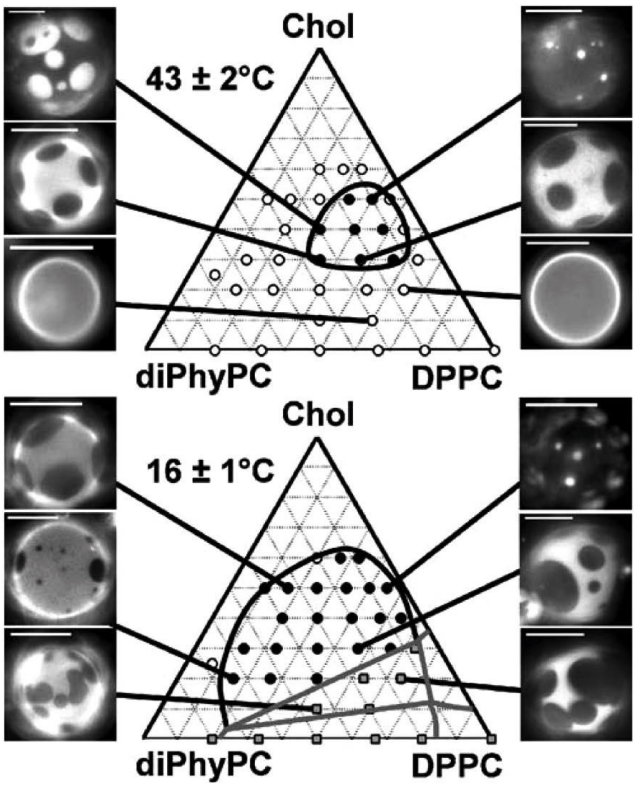

Figure 10. Phase diagrams and microscopic images of three component lipid bilayers (diPhyPC/ DPPC/Chol). ○ is miscible state, ● is liquid/liquid phase segregation state, and in ■ area, gel state lipids are shown in some domains.

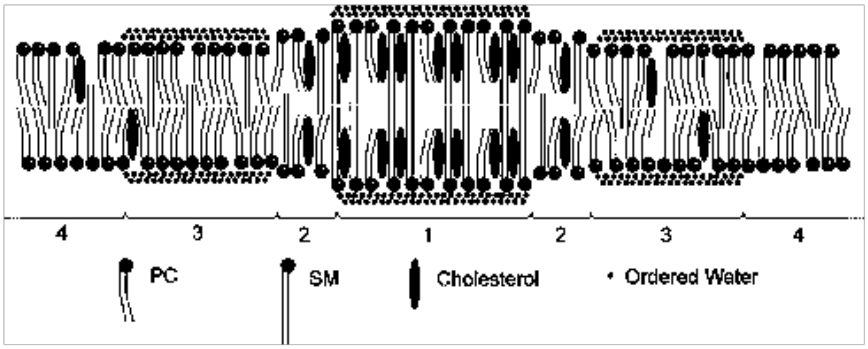

Figure 11. Schematic illustration of artificial lipid raft model composed of phosphatidylcholine (PC) and sphingomyelin (SM) fabricated on solid surface.

Table 1. Gel to liquid–crystalline phase transition temperatures of diacyl and dialkyl glycerolipids (Adapted from Yeagle, P.L, 2005. "The Structure of Biological Membranes" CRC press, Boca Raton)

Sample	T_m (Diacyl)	T_m (Dialkyl)
14:0 PC	23.9[a]	27.0[b]
16:0 PC	41.4[a]	44.2[c]
12:0 PE	31.3[b]	35.0[b]
14:0 PE	50.5[b]	55.5[b]
16:0 PE	64.4[b]	68.5[b]
18:0 PE	74.2[b]	77.0[b]
14:0 PA	50.0[d]	61.5[e]
16:0 PA	67.0[f]	75.0[e]
14:0 N-Methyl PE	42.7[g]	46.0[b]
14:0 N,N-Dimethyl PE	31.4[g]	34.0[b]
14:0 Phosphoryl 3-amino-propane	41.9[g]	46.0[b]
14:0 Phosphoryl 4-amino-butane	34.4[g]	38.0[b]
14:0 PG	23.7[d]	26.0[h]
14:0 β-D-GlcDG	45.5[i]	50.0[j]
16:0 β-D-GlcDG	61.0[i]	63.6[j]
18:0 β-D-GlcDG	71.7[i]	72.0[j]
14:0 α-D-GlcDG	40.5[k]	52.0[l]

Table 2. Lipid Composition of Plasma and Subcellular Membranes. (Adapted from Yeagle, P.L, 2005. "The Structure of Biological Membranes" CRC press, Boca Raton)

	Percentage of Phospholipids*								Phospholipids (μg/mg protein)	Cholesterol (μg/mg protein)
	PC	PE	PS	PI	PA	CL	LGP**	SM		
Rectal gland plasma membrane	50.4	35.5	8.4	<1	—	—	—	5.7	389	n.d.
Brush border membrane	33.3	35.6	7.4	8.2	1.2	n.d.	4.1	10.3	190	50
Cholinergic receptor membranes	37	40.5	17		<1	—	<1	<1	330(480)***	135(190)***
Plasma membrane	39	23	9	8	1	1	2	16	672	128
Mitochondria	40	35	1	5	—	18	1	1	175	3
Microsomes	58	22	2	10	1	1	11	1	374	14
Lysosomes	40	14	2	5	1	1	7	20	156	38
Nuclear membrane	55	13	3	10	2	4	3	3	500	
Golgi membrane	50	20	6	12	<1	1	3	8	825	38
Sarcoplasmic reticulum	72.7	13.5	1.8	8.7	<1	<1	—	1	603	78
										12

* Abbreviations of phospholipids: PC, phosphatidylcholine; PE, phosphatidylethanolamine; PS, phosphatidylserine; PI, phosphatidylinositol; PA, phosphatidic acid; CL, cardiolipin; LGP, lysoglycerophospholipid. ** Values for LGP in excess of a few percent should be viewed with caution. High contents of lysoglycerophospholipids are probably the result of phospholipid degradation during preparation.
*** Values for two different preparations by the same authors.

Table 3. Fatty Acid Composition of Phosphatidylcholine of Some Membranes From Rat Liver (Adapted from Yeagle, P.L, 2005. "The Structure of Biological Membranes" CRC press, Boca Raton)

	Fatty Acids as Weight%										
	14:0	16:0	16:1	18:0	18:1	18:2	18:3	20:0	20:3	20:4	22:6
Rat liver	0.5	29.7	1.0	16.8	10.4	16.8			1.5	18.3	3.4
Mitochondrial (outer)	0.4	27.0	4.1	21.0	13.5	13.5			1.1	15.7	3.5
Mitochondrial (inner)	0.3	27.1	3.6	18.0	16.2	15.8			1.0	18.5	3.8
Plasma membrane	0.9	36.9		31.2	6.4	12.9	tr	tr		11.1	
Microsomes											
Smooth endoplasmic reticulum	0.4	28.6	3.1	26.5	10.6	14.9			1.4	14.0	0.7
Rough endoplasmic reticulum	0.5	22.7	3.6	22.0	11.1	16.1			1.8	19.7	2.9
Golgi	0.9	34.7		22.5	8.7	18.1	tr	tr		14.5	

Note: tr = trace.

Table 4. Diffusion coefficients of selected lipids and proteins in biomembranes.

Component	Membrane	D (cm^2/s)	Method
Phospholipids	Lipid vesicles	$10^{-8}-10^{-9}$	FRAP
	Mitochondria	10^{-9}	FRAP
	Lipid vesicles	10^{-8}	EPR line broadening
	Lipid vesicles	10^{-7}	Pyrene excimers
$Ubiquinone_{10}$	Mitochondria	3.5×10^{-9}	FRAP
	Mitochondria	4×10^{-7}	Fluorescence quenching
Gramicidin S	Lipid vesicles	3.5×10^{-8}	FRAP
Bacteriorhodopsin	Lipid vesicles	$0.15-3.4\times10^{-8}$	FRAP
	Purple membrane	Immobile	FRAP
Lectin receptors	Fibroblasts	$1-10\times10^{-11}$	FRAP
Surface antigens	Mouse egg, unfertilized	1.6×10^{-9}	FRAP
	Mouse egg, fertilized	10^{-11}	FRAP
Rhodopsin	Retinal rod membrane	2.6×10^{-9}	FRAP
Surface antigens	Mouse-human heterokaryons	4.2×10^{-10}	Fusion
ConA receptors	Embryonic muscle	4.7×10^{-10}	Electrophoresis
Mitochondrial proteins		8.3×10^{-10}	Electrophoresis
		$3.7-4.4\times10^{-10}$	FRAP
Integral proteins	Normal erythrocytes	4.5×10^{-11}	FRAP
	Spherocytic erythrocytes	2.5×10^{-9}	FRAP

1.3. Membrane Models

Needless to say, when we analyze function of membrane proteins or membrane-acting molecules, it is necessary to incorporate them into proper lipid bilayers. The best way may be direct spectroscopic observation of whole cell (e.g. in cell NMR[26]), however, such strategy has limitation because so many components associate together in a cell membrane, and thus system itself is so complicated. Thus, when we analyze a particular protein, we have to build simple membrane models to incorporate it. However, fabrication of perfectly suitable system for all analytic methods is unreasonable, so we now select a suitable membrane models for each analysis. Components of membrane models should be simple. However, conversely, too simplified system can't mimic natural biomembranes. To reconstruct properties generated by complex interactions with multiple components (e.g. lipid rafts), membrane models are requested abilities, e.g. to embrace multiple components, to be applied to several kinds of analytical methods, etc. So, versatility of model membrane is quite necessary. As described above, the natural system is found as more complex, so, its mimetics need to be more complex in order to faithfully reflect behaviors of natural membranes. There are several model membranes studied up to now.[27] Examples of typical model membranes established up to now is shown as follows; micelle, vesicle, supported lipid bilayer, lipidic cubic phase, etc. In addition, recently, bicelle, planar lipid assembly with edge-stabilized surfactants has been found, and gradually gain popularity. Here the author will explain characteristics of these assemblies below, and introduce analytical methods in which each model membranes can be suitably applied.

Micelles are the simplest and easiest architecture to solubilize membrane proteins in water. Components of micelles are usually amphiphilic surfactants. They often encapsulate hydrophobic membrane proteins in their hydrophobic interior. Diameter of micelles is usually 6 to 10 nm, enough size to encapsulate membrane proteins (Figure 12). Such varieties of micelles have helped solving structures and characteristics of membrane proteins in the past 15 years. During this period of time, many kinds of surfactants that lightly affects proteins. For example, SDS, DM, DDM, LDAO, DPC, and cholic acid derivatives are well established for use in reconstitution of proteins or membrane peptides (Table 5).[28] However, when proteins are

reconstituted into micelle, some of them denature mainly because interior environment of micelle is not relevant to natural biomembrane.

Vesicles are frequently used as membrane mimetics because they have bilayers on the surface, because they can be made from various lipids that are components of living cell, and because size or hydration can be customized by various preparation methods. Actually, vesicle can be classified as three structures with various size and layered structures; multilamellar vesicles (MLV; ~1μm in diameter), large (or sometimes giant) unilamellar vesicles (LUV; ~100 nm or GUV; 1~10 μm), and small unilamellar vesicles (SLV; 20~30 nm) (Figure 12).[28a]

Multilamellar vesicles (MLVs) are widely used as membrane models because they can be easily prepared and can incorporate various membrane proteins and membrane peptides.[29] MLVs are inhomogeneous in composition, but on the order of 1 μm diameter and up to tens of bilayers.[30] They are often used for NMR analyses of membrane proteins by coupling with solid state MAS (magic angle spinning) system.[29b,31] In spite of such prominent features, however, MLVs are not biologically relevant because they are less hydrated due to their tightly packed multilamellar walls, and much higher concentration and higher protein/lipid ratio compared to natural membrane are necessary. In addition, in reconstitution step of membrane proteins, additional method such as addition of other surfactants is necessary in order to enhance incorporation events of proteins or peptides into lipid layers.[29a,32]

Unilamellar vesicles are divided into several categories by their sphere size. GUVs (giant unilamellar vesicles), LUVs (large unilamellar vesicles) and SUVs (small unilamellar vesicles) are major categories of unilamellar vesicles. They are used mainly in more diluted conditions than that for multilamellar vesicles. Thus, lipid layers are well hydrated to afford a room for moving dynamically. Compared with multilamellar vesicles, lateral diffusion rate is closer to biological membranes.[28a] Thus, unilamellar vesicles are regarded as more relevant system to biological membranes than multilamellar vesicles. LUVs and GUVs are popular kind of unilamellar vesicles. Their size is up to 10μm, thus curvature of their lipid layers is relatively smaller than micelles or SUVs, which makes environment of bilayer relevant to biomembranes. The second advantage is general versatility of lipids used. Much kind of lipids can be used to make LUVs and GUVs.[28a] In addition, diffusion rate of lipid bilayers is found independent on size of vesicles,[33] which makes them more

popular as membrane models. There are several methods to fabricate unilamellar vesicles.[34] Reverse-phase evaporation of organic solvents, extrusion through polycarbonate filters, and sonication method are commonly used.[30] Compared with MLVs, in which lipid bilayers are stacked like onion skin, ULVs can contain watery environment inside the sphere of vesicles, and thus inner environment of the vesicle is highly excluded from exterior environment by single lipid bilayer. When some material transporters are incorporated into unilamellar vesicles, selective transportation of molecules between inside and outside of vesicles can be achieved. Thus, unilamellar vesicles can be utilized for model membranes to know selective ion/molecule permeation events by membrane proteins[35] (Figure 13). They can be also utilized for models of primitive cell,[36] cell division,[37] or lipid rafts.[38] However, as they afford large interior volume, thus actual concentration of lipids in solution is quite lower than that of multilamellar vesicles. Thus GUVs are never used in measurements which require detection sensitivity e.g. NMR of membrane proteins. For the same reason, LUVs are mostly used for studies which are focused on properties of lipid bilayers themselves, not on membrane proteins. SUVs are the smallest vesicles with diameter of around 30 nm, which is an order of magnitude larger than a detergent micelle (Figure 12 a). A few reports utilized SUVs for structure determination of membrane proteins by NMR,[39] however, they are inconvenient because they are too diluted and unstable.[39,40]

Supported bilayers are flat lipid bilayers supported on glass substrates.[41] They are stable under wet condition, and bilayers retain fluid while they are supported. In addition, basically, supported bilayers can be made of versatile composition of lipids. Therefore, they have been mainly utilized as a membrane models with complex composition for microscopic use.[19b] Black membranes are special kind of supported bilayers that are aligned in micro-size pores of glass substrates. They are especially utilized for electrochemical experiments of ion transporting membrane proteins.[42] The major drawback of supported bilayers is difficult preparation methods. Supported bilayers are prepared by soaking diluted systems of unilamellar vesicles with uniform size which is treated with special extrusion machines (Figure 14).[43] Moreover, a reconstitution procedure of membrane proteins is rather complex.[44]

Lipidic cubic phase can be prepared using some kind of monoalkyl lipids, such as 1-monooleoyl-rac-glycerol or 1-monopalmitoleyl-rac-glycerol.[45] They are

known as a new medium for crystallization of membrane proteins (Figure 15).[45b,46] In particular conditions, membrane proteins gradually assemble together in the cubic bilayer, and then they form crystal to drop out from bilayer. This crystallization method is now recognized as a one of established and matured approaches to know structures of large membrane proteins with high atomic resolution. However, owing to a highly curved geometry of cubic structure of bilayers, obtained crystal structures sometimes don't satisfactorily reflect their original structure when they are reconstituted in fluid and flat lipid bilayers. Therefore, the author regard lipidic cubic phase as far from versatile membrane models.

Bicelles (bilayered micelles) are newly found lipid assemblies which have intermediate characteristics of micelles and vesicles. Bicelles have flat bilayer which edge is stabilized by some surfactants. The bilayer is well solubilized by surfactants, so solution is homogeneous, which offers clearly different characteristics from vesicles. Bicelles are much easier system to be dealt with than other model membranes, because bicelles are homogeneous solution with perfectly flat plane, and because preparation method is much easier than other model membranes (just mixing all components). In addition, concentration can be widely adjusted keeping morphology, and size of membrane can be easily controlled by changing lipid/surfactant ratio. Moreover, bicelles have peculiar ability to orient with strong magnetic field (described later in detail), so additional structural information can be obtained when they are utilized for structural analysis of proteins.[5] However, bicelles still have drawbacks that other membrane models don't have, which severely limits situation that bicelles are utilized.

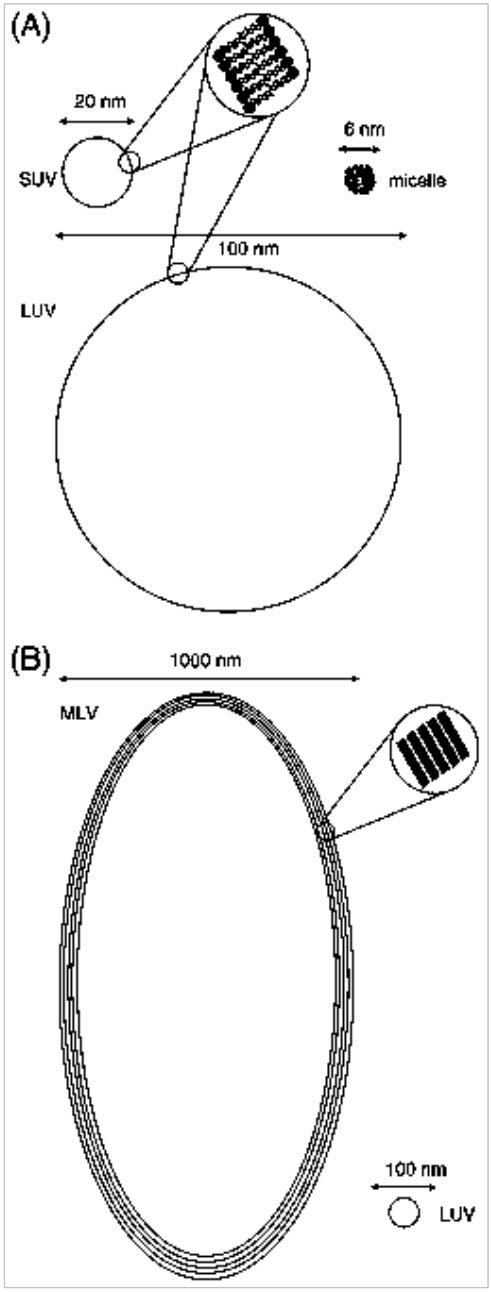

Figure 12. Cartoons depicting several membrane mimetics described in the text. (A) detergent micelle, small unilamellar vesicle (SUV) and large unilamellar vesicle (LUV). (B) large unilamellar vesicle (LUV) and multilamellar vesicle (MLV).

Table 5. Average characteristics of detergents frequently employed for structural NMR studies of proteins.

Detergent	Monomer MW (g/mol)	Monomer CMC (mM)	N	Micellar MW (kDa)	Typical NMR conditions	Some MP structures solved by solution NMR[a]
Non-ionic (mild)						
DDM (C12-DM)	511	0.2	140	72		
DM (C10-DM)	483	2	80	39		
OG (C8-G)	292	20	90	26	200 mM/40 °C	PagP
Zwitterionic						
DPC (C12-PC or FOS-12)	352	1.5	70	25	200 mM/40 °C	GpA, OmpA, PagP, OmpX, OmpG, PLN, DsbB, i3, DAGK, Rv1761c, CD4
LDAO (C12-DAO)	229	1	75	17	300 mM/40 °C	VDAC
*c*7-DHPC (D7-PC)	482	1.5	25	12	100 mM/50 °C	SRII
DHPC (D6-PC)	454	15	35	16	300 mM/40 °C	M2, OmpA, kpOmpA, Pf1
Anionic						
LPPG (L16-PG)	507	0.02	160	81	200 mM/50 °C	DTF
LMPG (L14-PG)	479	0.2	55	26	80 mM/40 °C	KCNE1
SDS (C12-S)	288	3	80	23	500 mM/40 °C	MerF, FXYD1, FXYD4
Mixtures						
DPC/SDS 5:1[b]	–	–	–	–	150 mM *DPC*/30 °C	ZZ
DHPC/DMPC 4:1[b](isotropic bicelles)	–	–	200 *DHPC* 50 *DMPC*	125	200 mM *DHPC*/40 °C	Bnip3, ErbB2, EphA1, αIIb-β3

a Protein abbreviations: ⌴IIb-à3 (Integrin ⌴IIb-à3); Bnip3 (Bnip3 transmembrane domain); CD4 (human CD4); DAGK (diacylglycerol kinase); DTF (G-protein-coupled receptor double transmembrane fragment); EphA1 (EphA1 transmembrane domain); ErbB2 (ErbB2 transmembrane segment); FXYD1 (human FXYD1, Na,K-ATPase regulatory protein); FXYD4 (human FXYD4, CHIF); GpA (human Glycophrin A transmembrane domain); i3 (i3 intracellular loop of the vasopressin V2 receptor); KCNE1 (human KCNE1); M2 (In⌴uenza M2 proton channel); Pf1 (Pf1 major coat protein); PLN (human phospholamban); Rv1761c (Rv1761c from Mycobacterium tuberculosis); SRII (Sensory rhodopsin II); VDAC (human VDAC-1); ZZ (zetazeta transmembrane domain).
B mol/mol ratio.

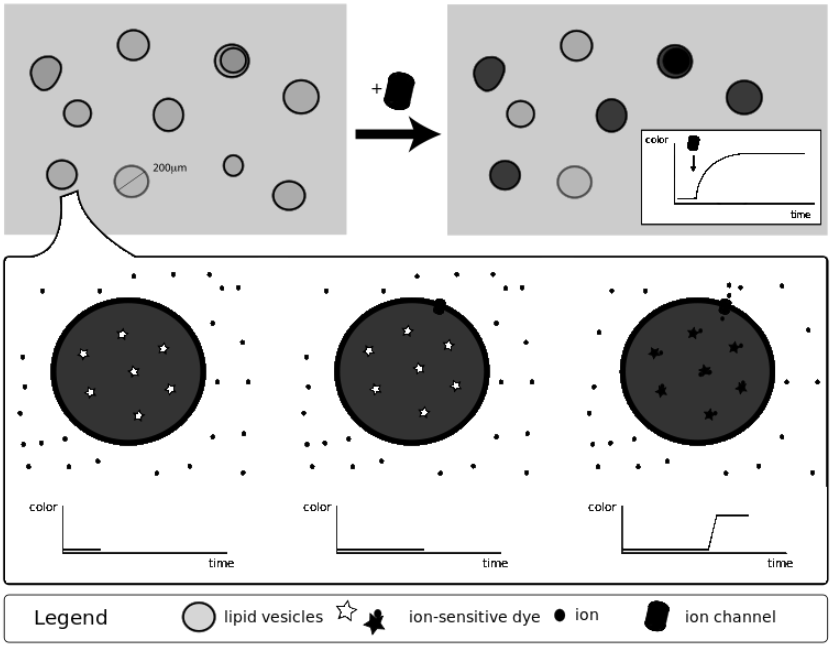

Figure 13. Schematic illustration of ion permeability test of transmembrane ion channel using ion-sensitive dye.

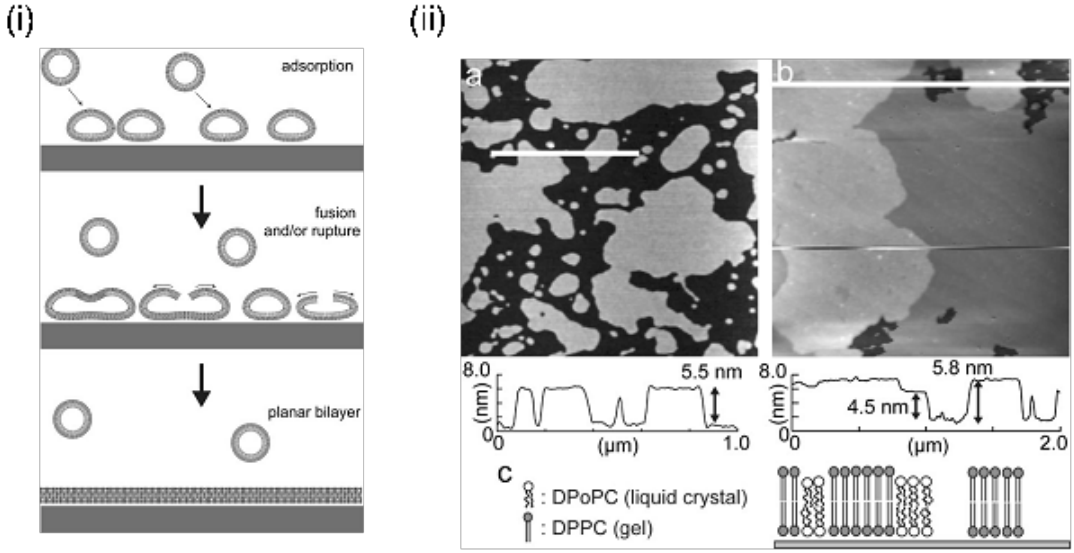

Figure 14. (i) Schematic illustration of the SLB formation processes by the vesicle fusion method. (ii) (a) AFM topograph of DMPC-SLB (in gel phase) on SiO2/Si(100)surface, and the cross section profile at the white line. (b) AFM topograph of DPoPC (liquid crystal) +DPPC (gel) binary SLB on TiO2 (100) surface, and the cross section profile at the white line. (c) Schematic illustration of the profile in (b): Thicker region (5.8 nm) corresponds to the DPPC- rich gel phase domains, and the thinner region (4.5 nm) to the DPoPC-rich liquid crystal domains.

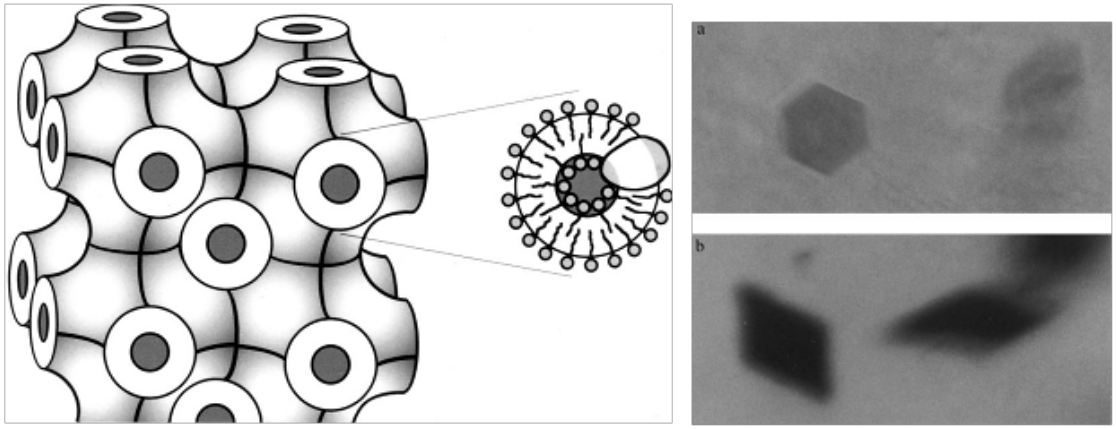

Figure 15. (left) Schematic illustration of lipid cubic phase. (right) Polymorph of bacteriorhodopsin obtanined from lipid cubic phase.

1.4. Bicelle

Since the first structural identification of mixed micelle composed of lecithin and bile acid in 1980,[47] disk-shaped lipid bilayer has gradually been studied further. Mueller and coworkers identified the assembly composed of the 3:1 ratio mixture of lecithin/bile acid as anisotropic non-micellar assembly by dynamic light scattering (DLS) and small angle X-ray scattering (SAXS).[48] From their analyses, they proposed disk-like mixed micelle model, in which lecithin bilayer is surrounded by bile acid. Radius estimated from combination of SAXS profiles and theoretical curve fitting implies that some amount of dimer of bile acid seems to be fused into lipid bilayer to form lipid disk with a little bit larger diameter than that of perfectly segregated model (Figure 16). After the findings, there are several reports about peculiar behaviors of lipid/lipid or lipid/surfactants mixtures.[49]

In 1990s, Sanders II and coworkers investigated mixed micelle composed of DMPC and DHPC (dihexanoyl phosphatidylcholine). They first found that mixed micelles composed of lipids and proper surfactants have ability to align parallel to magnetic flux, when two components are mixed with appropriate ratio.[50] They also mixed a membrane-acting reagent (GM3-ganglioside) into the system, to propose that such kind of mixed micelle can be utilized as a new class of model membrane that can form completely flat, native cell-like, and magnetically alignable lipid bilayer.[51] This way, such kind of lipid bilayer mixed with a certain surfactant was gradually brought into a stage of biomolecular use.

In 1995, the mixed micelle system that can form dispersed (sometimes disk-like) flat bilayer was named “bicelle” by Sanders II and coworkers,[52] because the system has characteristics of both bilayer and micelle. In this report, they found that using NMR with high magnetic field strength, chemical shift anisotropy (CSA) of proteins can be obtained when proteins are reconstituted into the membrane. As bicelles align to the applied magnetic fields, proteins incorporated into bicelles are forcibly aligned. Owing to such alignment, peculiar split NMR signals of proteins can be obtained. Analysis of degree in splitting gives more accurate and detailed structural information of proteins.

Next, Analytical method for water-soluble proteins/biomolecules using bicelle has been established. In 1997, Bax and coauthors reported that bicelle could

be used as an "aligner" of water-soluble proteins when they are solvated in bicelle solution.[53] In this report, they reports that water soluble protein (ubiquitin) can be weakly aligned by wall of bicelle that is oriented by magnetic flux, and that average angle between a specific bond (e.g. amide N-H bond) and director of magnetic flux can be expressed by RDC (residual dipolar coupling) on 2D NMR spectra. This finding was promising because bicelle can be utilized, not only for peculiar lipid aggregates, but also for a new analytical method, an aligner of bio-related large molecules. Since this paper is reported, researches in which bicelles and NMR analyses are linked together increased explosively.

After the series of prominent studies by Sanders II and Bax in 1990s, Bicelles are regarded as a new class of biomembrane models that can be utilized for various analytical methods.[54] As a result of followers' studies, now bicelle can be utilized mainly in two ways: 1. Reconstituting membrane proteins/biomolecules into bicelles to analyze in spectroscopic methods e.g. solution NMR. 2. Solubilizing water-soluble proteins/biomolecules in mixture of aligned bicelles, to obtain secondary structural information by weakly aligning these soluble proteins/biomolecules. However, unfortunately, it is known that morphology of bicelles easily changes by many factors like lipid/surfactant ratio, concentration, and temperature, etc. Thus, we have to understand characteristics of bicelles to appropriately utilize them. In next chapter, the author will explain analysis in morphology of bicelles and application to analytical methods and material science. As described later, the author has studied mainly on magnetically oriented bicelles. Thus, especially, properties of magnetically oriented bicelles will be described in detail.

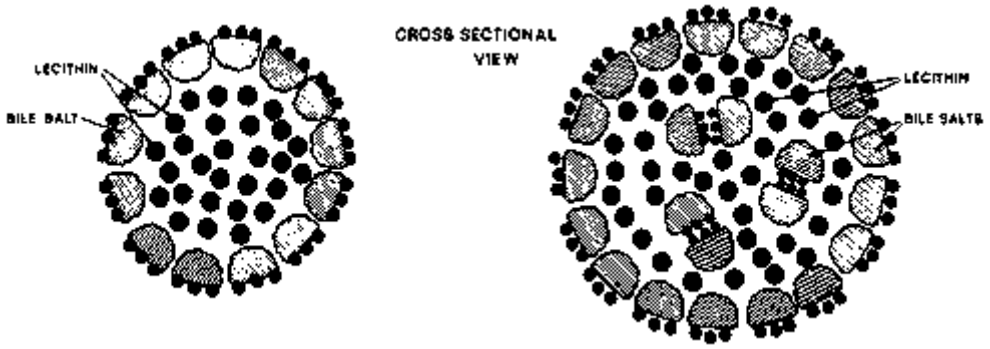

Figure 16. Schematic models for the structure of the bile salt-lecithin mixed micelle, shown in longitudinal (cut through the disk diameter) and cross section (cut through middle of the hydrocarbon steroid parts and fatty acid chains of bile salts and lecithins, respectively). Small's mixed micellar model is shown in Figure **A.** Mixed disk model represented by Carey and coworkers is shown in Figure **B.** Note that hydrogen-bonded bile salts are incorporated within the interior of the bilayer in the mixed disk model.

1.4.1. Morphology and dynamics of bicelles

Bicelle can be synthesized by mixing a certain ratio of lipids and surfactants. However, mixture of lipids and surfactants can form various morphological modes, which are sensitively affected by structure of components, lipid/surfactant ratio, concentration, temperature, pH, kind of salts, etc. Exhaustive analysis have not done yet, however, mainly 6 morphological types in mixed system of phospholipids and surfactants are known up to now[5] (Figure 17): multilamellar vesicles (A), with toroidal pores lined up by detergents (B), extended lamellae bicelles showing magnetic-alignment (C), chiral nematic "worm-like" ribbons, also magnetically alignable (D), flat disk-like bicelles tumbling isotropically (E), and detergent micelles (F) from a system with the largest q value (molar ratio of lipid/surfactant; q = [lipid]/[surfactant]) to the smallest. In assembly (B) to (E) surfactant is delocalized on the rim of the lipid bilayer.[5]

Only three assemblies shown above are defined as bicelle; flat disk-like bicelles tumbling isotropically (isotropic bicelle, also known as fast tumbling bicelle) (E), extended lamellae bicelles showing magnetic-alignment (magnetically oriented bicelle) (C), and chiral nematic "worm-like" ribbons (D). Isotropic bicelle can be formed when ratio of lipid/surfactant is low (generally lower than q=1), while magnetically oriented bicelle can be formed when the q value is above 1 (typically around 3 to 5). Among these three, isotropic bicelle and magnetically oriented bicelle are typically used. These two kind of bicelles can be selected as usage. Isotropic bicelles does not align to magnetic field. On the contrary, owing to much content of surfactants, lateral diameter of isotropic bicelle is kept small and dispersed. Thus, even though isotropic bicelles have lipid bilayers, as solution of isotropic bicelles has enough fluidity, they can be as utilized like a way of micelles. So, isotropic bicelles is known to keep structure of incorporated proteins much more stable than that in micelles. Magnetically oriented bicelle can orient to strong magnetic fields. Thus they are better suited in utilizing detailed structural analysis of membrane proteins in spectroscopic methods. However, because the lateral diameter is quite large and weak interlamellar packing exists, solution of magnetically aligned bicelles are prone to be viscous. So, improvement of spectroscopic methods is necessary, such as

utilization of novel methods of solid-state NMR. Worm like ribbons are distinguished as a kind of magnetically oriented bicelles.

Several variations of combination of lipids and surfactants have been reported up to now. The most popular combination of lipid and surfactant as a component of bicellar structure is DMPC and DHPC (Figure 18). As lipids that can form bicelle, DLPC (diC12PC),[55] DMPC, DPPC(dipalmitoyl phosphatidylcholine),[56] DIOMPC[57] (lipids with ether linker) and even sphingomyelin derivatives (SSM: D-*erythro*-*N*-stearoyl-sphingomyelin)[58] are also known (Figure 19). In addition, TBBPC, which contains biphenyl part at its hydrophobic chain, can be utilized as a peculiar bicelle that can orient perpendicular to magnetic flux.[59] Versatility of lipids is relatively high compared to surfactants, though difference in their thermodynamic properties must be mindfully taken care of. As surfactants, DHPC, diC7PC,[56] CHAPSO,[51] and TritonX 100[60] and so on are known. However, the author have to note that all combination of lipids and surfactants cannot be acceptable for formation of stable bicelles, and that we have to choose carefully their combination from these candidates, and we also have to be careful to concentration of lipids and surfactant, concentration of salts in the system, and q value, and the other factors.

Structure, kinetics and thermodynamic property of bicelle is still not completely clarified, because the assembled structure of the system drastically changes by temperature, some structures are huge and viscous for optical spectroscopy, structures highly depends on concentration, ratio of lipid/surfactant, choice of lipid or surfactant, and so on.[54d, 61] Still, by many researches over two decades, some information of structure and thermodynamic properties are known. From here, structure and applications of two kinds of bicelles, isotropic bicelles and magnetically oriented bicelles, are reviewed respectively.

For analyses of isotropic bicelles, DLS, SAXS and SANS plottings around Guinier regions are also efficient.[62] Predictions based on calculation analysis of SAXS peaks originated from electron density maps of models of aggregation structures can be also examined for isotropic bicelles.[63] Mäler and coworkers established the analytical method to estimate size of isotropic bicelle by measuring diffusion coefficient of DMPC and DHPC with NMR spectroscopy.[64] According to their observations, size of isotropic bicelles composed of DMPC and DHPC (q=0.5) are about 12 nm in diameter, and 6.1 nm in thickness. According to the diffusion

coefficient of DHPC that is clearly different from that of DMPC, DHPC is localized on the rim of bilayer. Through these analyses, sizes of isotropic bicelles and diffusion properties (lateral diffusion coefficient = 2-4 × 10^{-11} m^2/s) have been elucidated almost completely.

On the other hand, for magnetically oriented bicelles, the same measurements as that for isotropic bicelle is not applicable because the lateral size of bilayer is quite larger than that of isotropic bicelle, and because property of magnetic alignment can be generated only at high concentration and at relatively high temperature (typically 35~45 ºC), and because obtained solution is highly viscous. Thus, direct measurement such like TEM, cryo-TEM, or DLS measurement is not always suitable for magnetically oriented bicelles. Instead, SAXS, SANS, NMR, FRET measurements with fluorescent surfactants, and DSC are often used to estimate morphology, dynamics, and kinetics of magnetically oriented bicelles.

Implications about their morphologies have been obtained mainly by ^{31}P NMR, comparing degrees of alignment of phospholipids. For example, a system composed of DMPC/DHPC (q = 3), from ^{31}P NMR, it is suggested that isotropic mixed micelle is formed below room temperature. Only under the temperature of 30 to 40 °C, peculiar aligned structure can be obtained. However, when temperature is raised higher, powdery multilamellar vesicles can be obtained. In the aligned state, two ^{31}P signals are detected, large one of which is identified as planar and magnetically oriented phospholipid bilayer (mainly DMPC), and small one of which as phospholipid surfactant (DHPC) surrounding phospholipid bilayer, thus a peculiar type of segregation takes place (Figure 20). Theoretical calculations support this hypothesis (segregation of DMPC and DHPC). When the phosphor nucleus is oriented to magnetic flux, the NMR signal relevant to the nucleus shifts to a director of (001) due to anisotropic effect.[61,65] This way phosphor peak of bilayer that oriented along magnetic flux can clearly be separated from that of edge (torus) component. Using this nature, integration of these two peaks can roughly estimate molar ratio of lipid used for bilayer and for torus. This nature is supported by a calculational method, which indicates that when both components which comprise bilayer and torus have phosphor atom (e.g. DMPC and DHPC), ^{31}P NMR is applicable as a indicator if intensity and s/n ratio is enough.

Size and morphology of planar bilayer are also studied. For bicelles in dilute condition, TEM can be utilized. And in concentrated condition that are close to condition for practical use, X-ray or neutron scattering can be utilized. van DAM and coworkers directly observed shape of bicelles composed of DMPC/DHPC in dilute condition using TEM.[66] (Figure 21) They explored the condition in which magnetically oriented bicelle is kept stable and less concentrated enough for TEM observation (3 wt% total lipid content. typically 10-20% solution is used for NMR use). They are also succeeded in multiple forms of this lipid mixture in each condition, changing temperature and q value. They suggests that as temperature raises from lower to higher, the morphology of mixture changes from mixed micelles, small discoidal micelles which bilayer of DMPC and edge-stabilized DHPC seems segregated, worm-like micelles, branched worm-like micelles, finally to perforated lamellar layer that seems to be identified as magnetically oriented bicelles. The same morphological change can also be observed by changing q-value. Yang and coworkers estimated morphology of mixture of DPPC/diheptanoylphosphatidylcholine (diC7PC) that drastically changes by raising temperature, in practical conditions using SAXS.[62a] SAXS profiles in Guinier region taken at each temperature are plotted to estimate shape of microscopic assemblies. As a result, as temperature are raised up, shape of assembly of DPPC/diC7PC changes from spherical micelles to discoidal bilayer, and finally forms multilamellar vesicles seemingly due to extremely low miscibility of DPPC and diC7PC at high temperature range. Naito and coworkers applied SAXS to magnetically oriented bicelles.[67] They indicate that stacking between bilayers becomes weaker compared to multilayered vesicular aggregation when the mixture forms magnetically aligned bicelle. They presumed that magnetically oriented bicelle has stacked cluster with two bicellar layers in average. From this stacking property, lipid bilayer of bicelle is much more hydrated than that of multilamellar vesicle. SANS measurement elucidated that morphology of magnetically oriented bicelle can be changed by q-value (ratio of DMPC and DHPC) from chiral nematic worm-like assembly to disk-like (or perforated lamellar) structure.[62b,68]

Phase transition behaviors of lipids in bicelles are studied in detail. Tachibana and coworkers utilized DSC thermogram to confirm phase transition of magnetically oriented bicelle composed of DMPC and DHPC (q=1.8).[69]

Exothermic peak identified as main phase transition of lipids are quite large, and, in addition, small peak are observed in a lower temperature region of main transition peak. This peak implies that structural change of the assembly takes place before phase transition of lipids (ripple-liquid crystal). Many small peaks are observed in a lower temperature than main phase transition of lipid bilayer, which is assumed to be due to subtle structural change of the assembly. (Figure 22) They presumed that above phase transition temperature of ripple phase to liquid crystalline phase of DMPC (23 ºC), "perforated lamellar" structure exists, while below 23 ºC the structure become smaller to form isotropic (small, and not alignable to magnetic fields) bicelles. This phase transition behavior well corresponds to TEM observations by van DAM. Comparing these two seemingly same results obtained by different analytical methods, analysis of morphology of DMPC/DHPC mixture seems highly reliable. Combining these data, DMPC/DHPC mixture forms bicelle only between 30 to 40 °C, between which lipid bilayer is in L_c phase. Morphologies of mixture of DMPC/DHPC in other q value or lipid concentration are also studied (Figure 23). All these studies indicate that temperature range in which mixture of various components forms magnetically aligned bicelles are all above phase transition temperature of L_β to L_c.[51] DSC studies revealed that lower temperature of magnetically-oriented-bicelle phase accords with structural change temperature of lipids, and in magnetically-oriented-bicelle phase lipids are always in L_c phase.[69] In order to form magnetically oriented bicelles, phase of lipid bilayer is a potentially critical factor, which directly influence morphology and fluidity of lipid bilayers.

In a temperature range where magnetically oriented bicelles forms, model cartoons composed of planar (or disc-like) lipid bilayer with perfectly segregated edge-stabilizing surfactants (typically short chain lipids) are often drawn. However, actual behaviors of lipids are a little different. Some implications of kinetic stability about magnetically oriented bicelle composed of DMPC and DHPC using FRET from fluorescent lipid to fluorescent surfactant.[70] Based on a previous bicelle model proposed before this report, lipids and surfactants are considered to be perfectly segregated.[71] However, according to the report, FRET between a fluorescent lipid and a surfactant is active even in the phase of magnetically oriented bicelle, which indicates that a surfactant (DHPC) is easily incorporated into a bilayer of DMPC. In addition, when two bicellar system in one of which fluorescent lipid is incorporated,

and the other fluorescent surfactant is incorporated are mixed, increase rate of FRET at low temperature (17 ºC) is slower than that measured on the temperature range of magnetically oriented bicelle. According to these results, DMPC and DHPC is not perfectly segregated in the magnetically oriented bicelle phase, and dynamic equilibrium between bicellar sheets are continuously occurs. This report offered the important issues about dynamics of magnetically oriented bicelle. Nieh and coworkers supports these hypotheses after analysis of same system by NMR and small angle neutron scattering (SANS).[72] From their results, they presumed that, in a temperature range where magnetically oriented bicelles forms, as temperature raises up, surfactants (DHPC) gradually fuse with lipid bilayers, and thus ratio of segregated edge-stabilizing surfactants decreases. Instead, water breaks into the inter-membrane stacking to obtain more hydration and homogeneity. At higher temperature than region of magnetically oriented bicelles, bicelles destabilize into precipitates that is composed mainly of long chain lipids. At this temperature range (for mixture of DMPC/DHPC with q value of 3.0, above 40 °C), micelles are thought to be likely to stick together with themselves, not with rim of lipid bilayers. (Figure 24) From these discussions, key factors to form magnetically oriented bicelles are combination of following three; lipids are in liquid crystalline phase (L_c), segregation of lipids and surfactants takes place to some extent (lipids can assemble together, and surfactants too), and in converse, hydrophobic segment of surfactants can interact with hydrophobic segment of lipid bilayers to some extent. From the series of researches, here the author can summarize that when structure, combination, and ratio of lipids and surfactants fulfills these three factors, stable magnetically oriented bicelle seems to be achieved.

Lipids in magnetically oriented bicelles are able to move laterally in the membranes. If we mimic biomembranes using bicelles, one of the important factors required for model membrane is the diffusion rate of lipids. Measurement of lateral diffusion is often carried out using hydrophobic molecules which are able to fuse into lipid bilayers. Instead of observing behavior of lipids, a lateral diffusion rate of such molecules is often estimated by SS-NMR. Thus, estimated diffusion rate with this method is derived from hydrophobic molecules incorporated into the membrane models, not lipids. However, if we choose these molecules carefully, almost same diffusion rate as that of lipids can be measured. The criteria might be similarity of

molecular weight, structure, and hydrophobicity, etc. Soong and coworkers incorporated Phronic F68, block copolymer PEG-PPG-PEG, into magnetically oriented bicelles to estimate the lateral diffusion rate of its propylene oxide methyl group. As a result, diffusion rate of F68 is estimated $1.1x10^{-11}$ m^2/s, which corresponds to the diffusion rate of membrane proteins in natural biomembrane. Cho and coworkers utilized mixture of DMPC/POPC/DHPC/Cholesterol to estimate diffusion rate of POPC at various temperature range from 0 °C to over room temperature. At room temperature, POPC and DMPC diffuses uniformly, at which temperature, diffusion rate of POPC is estimated 8×10^{-12} m^2/s, which is the same order as that of vesicles ($2\text{-}4 \times 10^{-12}$ m^2/s).[7,73] This value reflects order of biomembrane, indicating that magnetically oriented bicelles are well-established biomembrane mimetics. Compared to these data, for isotropic bicelle, lateral diffusion coefficient of DMPC is $2\text{-}4 \times 10^{-11}$ m^2/s,[64] which is one order higher than that of magnetically oriented bicelle. This diffusion order does not precisely reflect biomembrane, though, with this high diffusion and fast correlation time, solution NMR of membrane-acting reagents or membrane peptides can be observed with high resolution.

Cho and coworkers also proved that formation of lipid domain is also possible in bicelles. they found that the bicellar system composed of DMPC/POPC/DHPC can be thermally stabilized by adding 13 mol% of cholesterol, and that lateral motion of the system composed of DMPC/POPC/DHPC/Cholesterol at the temperature range between phase transition temperature of POPC (270 K) and DMPC (296 K) is restricted (lateral diffusion coefficient; $4.3\times 10^{-12} m^2/s$) compared to that measured above phase transition temperature of DMPC ($8 \times 10^{-12} m^2/s$).[72b] This implies that lipid domain composed of POPC and cholesterol can be generated only between at the temperature range between phase transition temperature of POPC and DMPC, which is similar to that of lipid raft domains. This may be because two state of lipid bilayer (L_β phase for DMPC, L_α phase for POPC) coexist in bicellar mixture to form raft-like domains in order to stabilize each domain.

From these viewpoints, vectors of applications are different between magnetically oriented and isotropic bicelles. Characteristics of bicelles with representative components are summarized in Figure 25.

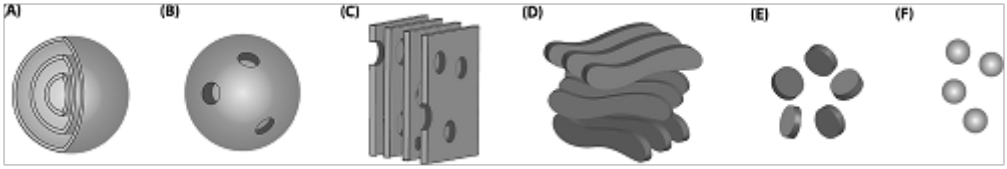

Figure 17. Schematic models for the morphology of bicellar phases with increasing detergent content: multilamellar vesicles (A), with toroidal pores lined up by detergents (B), extended lamellae bicelle showing magnetic-alignment (C), chiral nematic "worm-like" ribbons, also magnetically alignable (D), flat disk-like bicelle tumbling isotropically (E), and detergent micelles (F).

A) **B)**

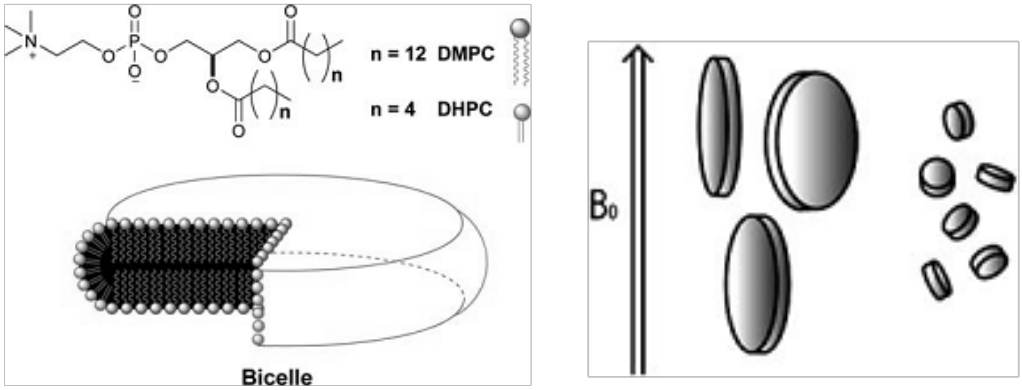

Figure 18. (A) Schematic representation of the DMPC–DHPC bicelle. **(B)** Oriented bicelles (left) and fast-tumbling isotropic bicelles (right) in a magnetic field B_0.

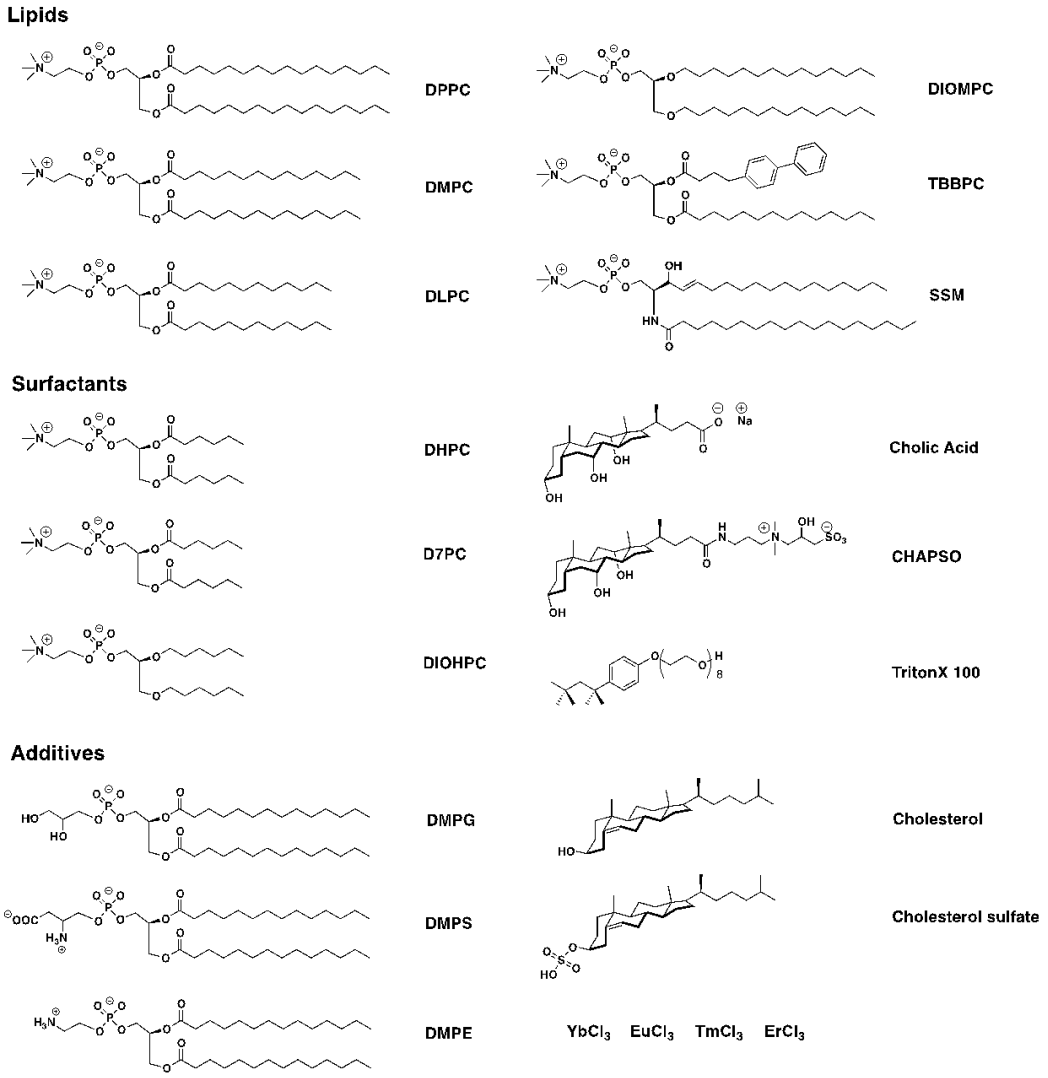

Figure 19. Chemical structures of representative components of bicelles.

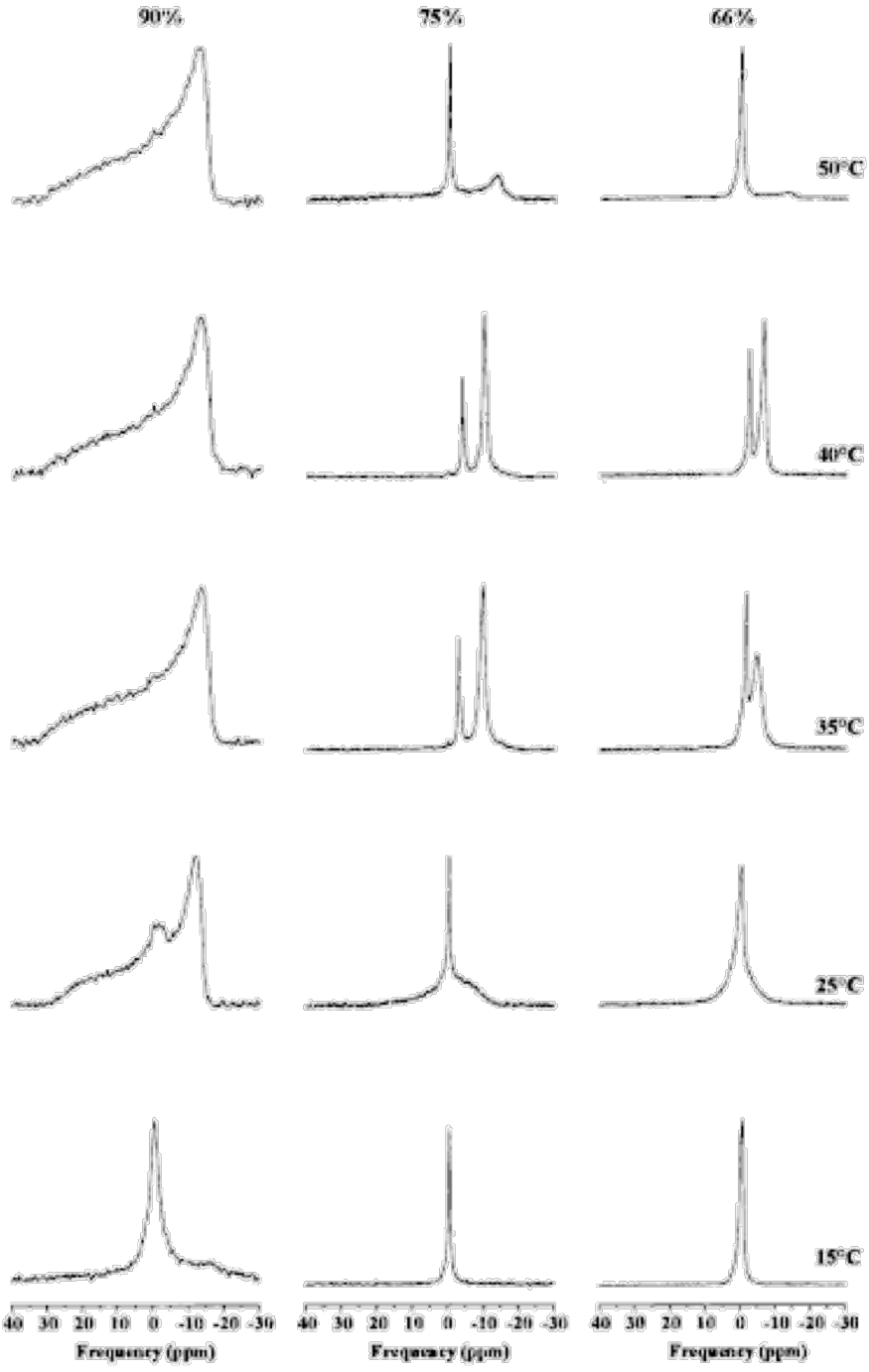

Figure 20. Proton-decoupled ^{31}P NMR spectra of DMPC and DHPC mixtures in 80% (w/w) D_2O. Mole fractions X = [DMPC]/([DMPC] + [DHPC]) are 90%(left), 75%(middle), and 66%(right). Chemical shifts are expressed relative to 85% H_3PO_4 (0 ppm). (adopted from Raffard, G. et.al. *Langmuir*, **2000**, *16*, 7657)

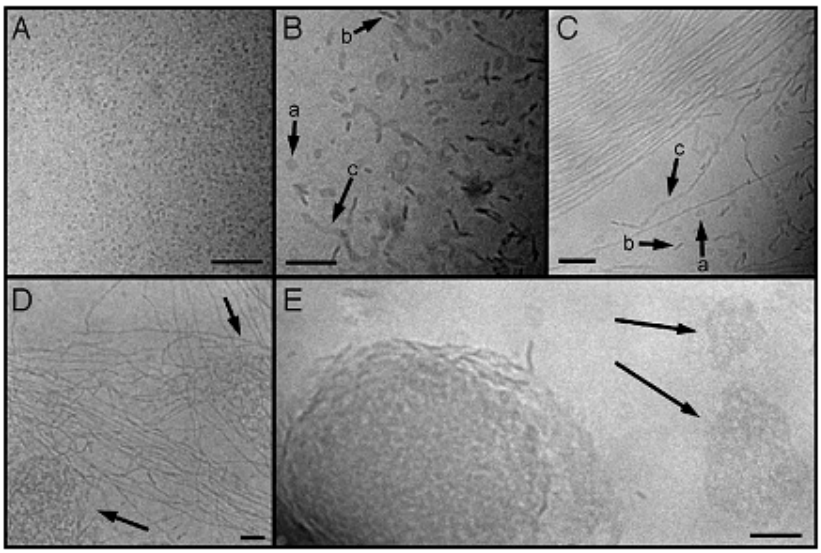

Figure 21. Cryo-TEM images of aggregates formed by DMPC/DHPC mixtures at 25 ºC and cL = 3% for q = 2.0 (A), q = 2.2 (B), q = 2.5 (C), q = 3.0 (D) and q = 4.0 (E). Arrows in B and C point to discs face-on (arrows a) and edge-on (arrows b). Arrow c in B points to elongated distorted discs, and arrow c in C points to a (quasi-)cylindrical micelle where variations in cylinder width are evident. Arrows in D point to large and dense aggregates of branched and entangled (quasi-) cylindrical micelles. Arrows in E point to isolated bilayers which are perforated. Bar = 100 nm in all images (note the different scales).

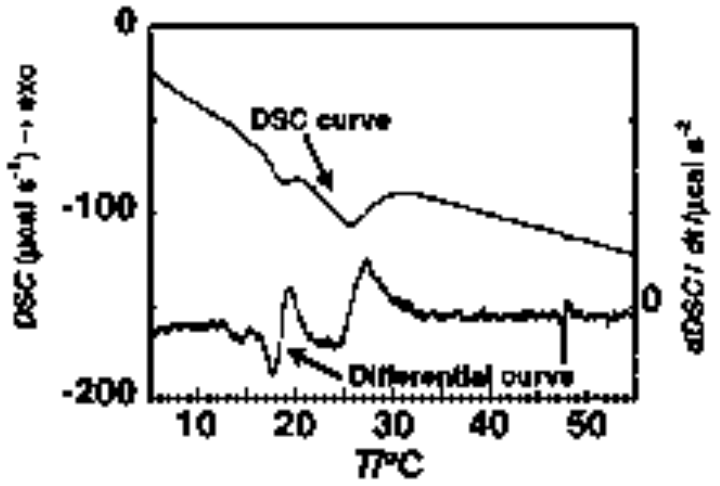

Figure 22. DSC profiles of aqueous solution of DMPC and DHPC (q=xx).

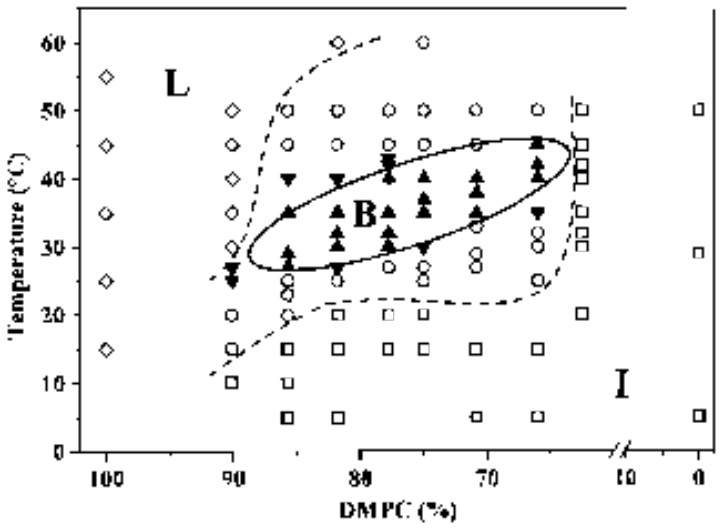

Figure 23. Temperature-composition diagram of DMPC/DCPC in 80% (w/w) D_2O, 100 mM KCl, as determined by ^{31}P NMR: (▲) single phase of bicelles self-orienting into the magnetic field; (▼) self-orienting bicelles coexisting with isotropic or unoriented phases; (○) unoriented plus isotropic phases; (□) isotropic phase (micelles); (◇) lamellar phase. Mole fractions X) [DMPC]/ ([DMPC] + [DMPC]) are expressed in percent. One-phase regions are denoted I, B, and L for isotropic, bicellar, and lamellar phases. Solid and dashed lines are tentatively drawn to help viewing phase boundaries.

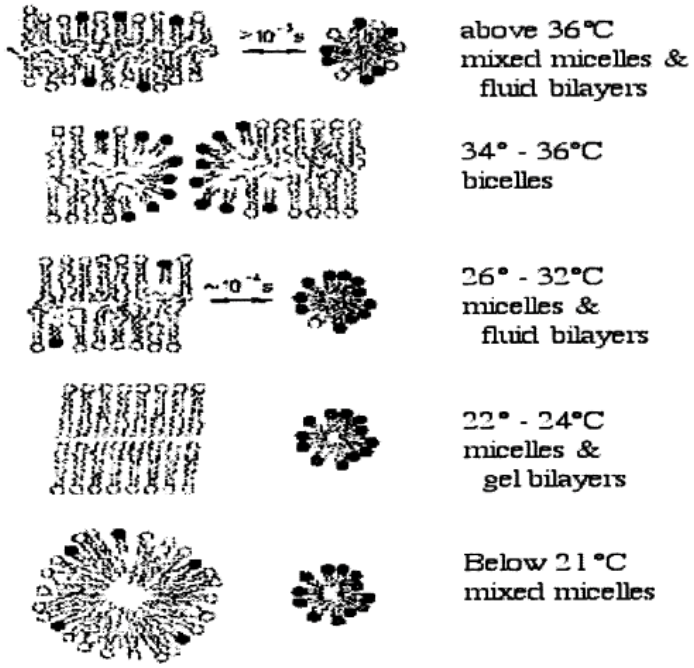

Figure 24. Mixing model of bicelle alignment as a function of temperature. (Adopted from Rowe, B. *et. al.*, *Langmuir*, **2003**, *19*, 2042.)

Properties	Isotropic bicelles	Magnetically Oriented Bicelles
q value ([DHPC]/[DMPC])	0.3~1	2~6
Alignment to magnetic field	No	Yes
Lipid membrane diameter	60~100 nm	>100 nm Sometimes Plate-like
Viscosity	Low	High
Diffusion coefficient of membranes	2-4 × 10^{-11} m^2/s	8 × 10^{-12} m^2/s
Applicable temperature (DMPC/DHPC)	0~ >40 ℃	30~40℃

Figure 25. Properties of isotropic bicelles and magnetically oriented bicelles composed of DMPC and DHPC.

1.4.2. Applications of bicelles

Application of isotropic Bicelles

Isotropic (fast tumbling) bicelle (usually misture of DMPC/DHPC (q=0.5)) can be used as a model membrane system mainly for NMR structural analysis.[74] Because of low viscosity, small-sized aggregation, and high homogeneity, systems containing isotropic bicelle can be analyzed with solution NMR. Taken into consideration that disk radius of isotropic bicelle is about 6 to 10 nm, small membrane-associating molecules are suitable for precise analysis.

Vold and coworkers first found isotropic bicelle as a suitable medium for NMR determination of binding mode and structure of membrane-associated peptides. They determined structure of mastoparan (a 14-residue peptide, INLKALAALAKKIL-NH_2) found as wasp venom by combination of 2D TOCSY, NOESY, and DQF-COSY.[75] In this study the short peptide showed well-defined helical conformation with its long axis parallel to the bilayer plane. After this milestone report, Vold and coworkers published several papers where more precise and complex structure of membrane-acting peptides.[76] After these series of pioneering studies, Mäler and coworkers played an important role in applying isotropic bicelle to cell penetrating peptide.[77] They determined motilin whose sequence is FVPIFTYGELQRMOEKERNKGO. NMR-based structural and dynamics studies revealed that motilin consists of α-helical structure between Glu9 and Lys20 in isotropic bicelle under acidic condition. Importantly, the structure was found to be significantly different from that observed in SDS micelles, where the peptide shows poor helical properties. This indicates that isotropic bicelles are more suitable as a model membrane than micelles. More recently, Nielsen and coworkers studied the membrane bound structure and conformation of alamethicin, a 20-residue peptide provided by the fungus *Trichoderma viride* in lipid bilayers by combination of isotropic bicelles and molecular dynamics.[78] NOESY data for alamethicin in DMPC/DHPC isotropic bicelles supported a transmembrane configuration (Figure 26), but the peptide is not so rigid and has a high degree of dynamics. Hence they compared NMR data with molecular dynamics simulations, thus proposed more plausible picture of membrane-penetrating alamethicin with a flexible dynamics.

Most pharmaceutical compounds and bioactive natural compounds have some affinity to membrane bilayers. Accumulating knowledge about such interaction becomes more important recently. In this case, isotropic bicelles also can be utilized as a model membrane for NMR analysis when such small molecules are incorporated into bilayer membrane. Murata and coworkers determined conformation of erythromycin A (EA), salinomycin (SA), and Amphidinol 3 (AM3) when they are incorporated into bilayer membrane.[79] To check localization of EA in isotropic bicelle, they utilized special lipids that bear paramagnetic substituents on 5' or 12' position of hydrophobic chains (Figure 27).[79a] When paramagnetic compounds are added into the system, NOEs around the substituent are decreased. Combination with such strategic experiments, NOESY and DQF-COSY spectra can show precise information on localization of EA in the isotropic bicelles (Figure 28).

In addition, isotropic bicelles also have ability to stabilize some membrane proteins. Girvin and coworkers reported that Smr (*Staphylococcal* multidrug-resistance protein) in isotropic bicelle (DMPC/DHPC q = 0.5) has the best binding ability of tetraphenylphosphonium (TPP), a known ligand of Smr, above all the other known surfactants that solubilize membrane proteins.[80] In addition, they succeeded in high degree of spectroscopic assignment using ^{1}H-^{15}N TROSY, which indicates that isotropipc bicelle has ability to be utilized for NMR measurement of some kind of membrane proteins.

Murata and coworkers succeeded in obtaining information on interaction of sphingomyelin in isotropic bicelle by NOESY.[58] Interaction between sphingomyelins measured in bicelle may give an implication to mechanisms and structures of lipid raft domains in living cells.

Wüthrich and coworkers proved that isotropic bicelle can also work as a model of lipid raft.[81] β-sheet formation and elongation of a prion protein can occur only when both DMPC and DMPS (dimyristoyl phosphoserine), which form raft-like domains, are used as a component of long chain lipid in isotropic bicelles.

Applications of magnetically oriented Bicelles

As described above, magnetically oriented bicelle has mainly two ways of applications; one usage is aligned solution for water-soluble proteins/ membrane-acting molecules, and the other is forcible aligner for membrane proteins/ membranous molecules.

Since 1997, after Bax's development of bicelle for "alignment media" of bio-related macromolecules, number of reports related to applied measurements and analysis using magnetically oriented bicelles has explosively increased. In this report, development was to induce CSA (chemical shift anisotropy) on ubiquitin using weak interaction between ubiquitin and surface of magnetically oriented bicelle. As a result, proteins acquire weak orientation along with magnetic field. By the effect, for example, chemical shift of carbonyl C in amide bond, which has three chemical shift anisotropy tensor δ_{11}, δ_{22}, δ_{33}, changes according to angles against the director of magnetic field. Anisotropic dipolar interaction generated thereby can be expressed on modulated J-coupling. This amount of changes is called residual dipolar coupling (RDC) (Figure 29).

For the case of a molecule with an axially symmetric chemical shift tensor, the contribution to spin energy levels, which leads to an offset in resonance position from that seen with isotropic averaging, is given in equation (1);

$$C_i = \Delta\delta \frac{\overline{(3\cos^2\theta - 1)}}{2} \gamma_i B_0 I_{zi} \qquad (1)$$

where coefficient $\Delta\delta$ is the difference in chemical shift in directions parallel and perpendicular to the symmetry axis, θ is an angle between chemical bond of two atoms and magnetic force vector, and $\gamma_i B_0 I_{zi}$ is the Zeeman interaction operator.

RDC can be easily expressed on two dimensional heteronuclear NMR spectra, such as HSQC (Figure 30). That is, RDC can be calculated by deducting coupling constant of each peak on non-aligned spectra from that on aligned spectra. Then, by comparison of these data with simulated RDC data calculated from some patterens of 3D protein models, angular information of chemical bonds e.g. C-N bonds or N-H bonds are determined precisely.[82] Through this way, Bax and coworkers

demonstrated utilization of bicelle in order to solve accurate conformational analysis of bio-related macromolecules.[83] Determination of absolute configuration of small molecules is also carried out.[84]

Magnetically oriented bicelles are also effective for detailed analysis of transmembrane proteins or peptides because they can incorporate such kind of proteins/ biomolecules into the planer lipid membranes, and they can align them forcibly perpendicular to magnetic flux. Before magnetically oriented bicelles are utilized as aligned biomembranes, when we need to align transmembrane samples in lipid bilayers, we have to prepare mechanically aligned lipids with many stacks of glass plates with difficult preperation by consuming much time, and measure within limited NMR tools.[85] Compared to such a complex method, magnetically oriented bicelles can be prepared easily,[86] a method for incorporation is simple,[87] and in addition, general NMR tools can be utilized for analysis of target biomolecules.

As mentioned above, it is naturally difficult to obtain sharp spectra from biomolecules in magnetically aligned bicelles with solution NMR because of high viscosity and naturally slow correlation time of lateral lipid motion. As solid state NMR (SS-NMR) is gradually developed recently, magnetically oriented bicelles gradually utilized frequently as tools for alignment media for transmembrane biomolecules, especially for large proteins consisting of several building units. For example, CXCR1, (kind of G-protein coupled receptors (GPCR)),[88] its binding interaction with interleukin8,[89] the transmembrane domain of nicotinic acetylcholine receptor (nAChR),[90] membrane protein p7 from hepatitis C virus,[87a, 91] the membrane spanning domain of Vpu from HIV-1,[92] HIV-1 envelop spike, MerFt (part of bacterial mercury transport protein),[93] multidrug resistance efflux pump EmrE,[94] and cytchrome b_5 [95] have been solved using magnetically oriented bicelles. Of course, magnetically oriented bicelles are also applicable to membrane peptides and membrane-acting small molecules. For example, structure, angular information, dynamics, and interactions of Neuropeptide Met-Enkephalin,[96] D-penicillamine-enkephalin,[97] Islet Amyloid Polypeptides,[98] antimicobial peptides LPcin-I, LPcin-II,[99] antimicrobial peptides extracted from Australian tree frogs,[100] Neuronal $\alpha 4\beta 2$ nicotinic acetylcholine receptor,[101] and even synthesized cytotoxic amphiphilic peptides[102] have been solved using magnetically oriented bicelles.

To extract effective structural information from complicated NMR signals of biomolecules, several custom-tailored NMR sequences specialized on systems of magnetically oriented bicelles have been utilized. In order to know geometry and alignment of peptide groups, two-dimentional separated-local-field (SLF) experiments, which is able to correlate ^{15}N chemical shift and ^{1}H-^{15}N dipolar couplings, have been utilized. Based on the sequence, polarization inversion by spin exchange at the magic angle (PISEMA) experiment was utilized by Ramamoorthy and coworkers as a prototype of a tool to know molecular orientation in bicellar systems.[103] PISEMA experiment affords characteristic patterns on oriented molecules. Especially α-helices give circular patterns known as polarity index slant angle (PISA) wheels, from which tilt angle of peptide helix within the lipid bilayer can be detected (Figure 31). PISEMA experiment is expanded for other mixing sequences e.g. Broadband-PISEMA,[104] HIMSELF (heteronuclear isotropic-frame spin exchange via local field), HERSELF (heteronuclear rotating-frame spin exchange via local field),[105] and SAMMY.[106] Method to enhance sensitivity of SLF experiments is also explored.[107] PISEMA (and SS-NMR for bicelles) now has been gradually popular for determination of dynamic structure of membrane proteins when they are incorporated in biomembranes.

Solid-state NMR measurements with magic angle spinning (MAS) of cytochrome b_5 reconstituted in bicelle and multilamellar vesicles have been investigated.[108] Their measurements indicate that ^{15}N NMR spectra of cytochrome b_5 reconstituted in magnetically oriented bicelle is clearer than that in well hydrated/less hydrated multilamellar vesicles. Using MAS, though, orientational information of the bicellar system is lost, so SS-MAS NMR spectroscopy in combination with several specific sequences (RanpCP for 1D ^{15}N spectra, and CRUC COSY and DARR for 2D ^{13}C-^{13}C spectra) is still suitable tool especially for hydrophilic mobile domain of cytochrome b_5.

Suitability of bicelles as a model membrane compared to other model membrane has also been explored. Tachibana and coworkers found that DMPC in magnetically oriented bicelle is more densely packed than that of mixed micelles, and that structure of bacteriorhodopsin reconstituted in magnetically oriented bicelles is closer to that in purple membranes than that in mixed micelles.[109] This result indicates that large planar structure of magnetically oriented bicelle is suitable for

bio-related macromolecules, and that magnetically oriented bicelles with large area of lipid bilayers are more suitable model membrane system than small bicelles.

Other applications of bicelles except for spectroscopy

Among all supramolecular assemblies regardless of organic or inorganic materials, disk-like or platelet architecture is quite rare.[110] Still, size- and shape-controlled organic architecture is a challenge. Thus disk-like shape of bicelles itself a quite unique character enough. There are several examples of utilization of bicelles for templates to fix disk-like shape onto polymer or inorganic complexes. Shelnutt and coworkers developed platinum nanowheels using bicellar template.[94] Shi and coworkers fabricated disk-like poly(3,4-ethylenedioxythiophene) nanoparticles using bicelle as a template.[111] Pinkhassik and coworkers succeeded in formation of polystyrene disk with uniform size by UV-induced free radical polymerization of styrene and crosslinker (1,4-divinylbenzene) that are incorporated inside the hydrophobic region of bicelle bilayer.[112] (Figure 32) Kikuchi and coworkers achieved permanent fixation of disk shape of bicelle using long-chain lipid bearing siloxane group by sol-gel-reaction.[113] (Figure 33)

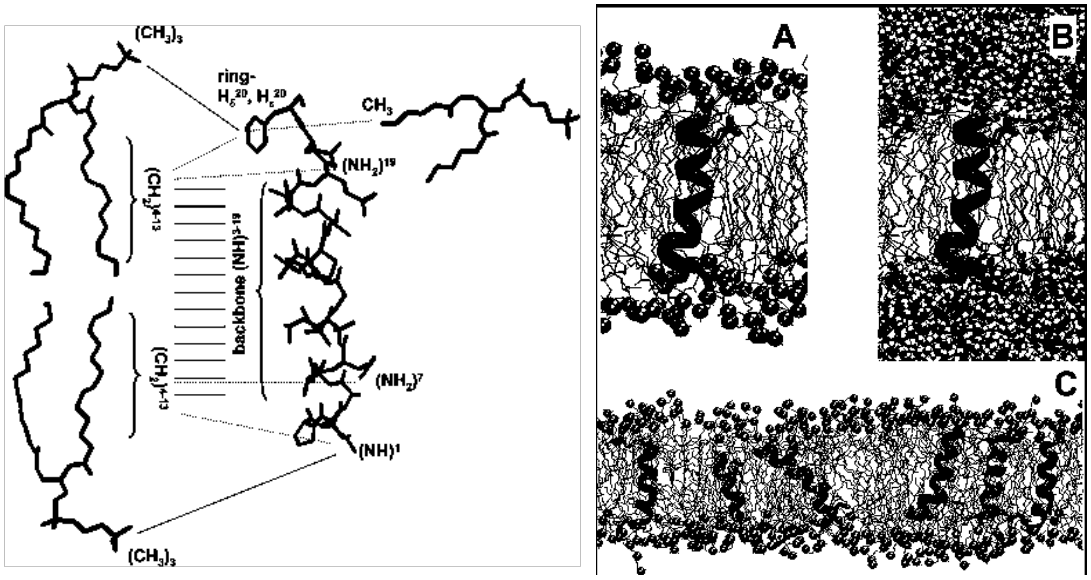

Figure 26. **(left)** Summary of observed NOE connectivities between alamethicin and lipid molecules as illustrated by lines between the involved structural elements of the individual molecules: left, DMPC; middle, alamethicin; right, DHPC. The NOE are between the associated protons rather than heavy atoms shown in this scheme for the sake of visual clarity. Relatively weak cross-peaks are denoted by dotted lines. **(right)** Snapshots from the MD simulations of alamethicin in a DMPC bilayer. The peptides are shown in green ribbon with the N-terminus in the top and the hydrophilic side chains of Gln7, Glu18, and Gln19 are shown in orange licorice. Lipids are colored gray with head groups labeled in blue (N) and pink (P). Panels A and B show the same snapshot, without and with the water molecules, respectively. (C) Illustration of the diversity of both the peptides and the lipids. Pro2 and Pro14 side chains are shown in black licorice.

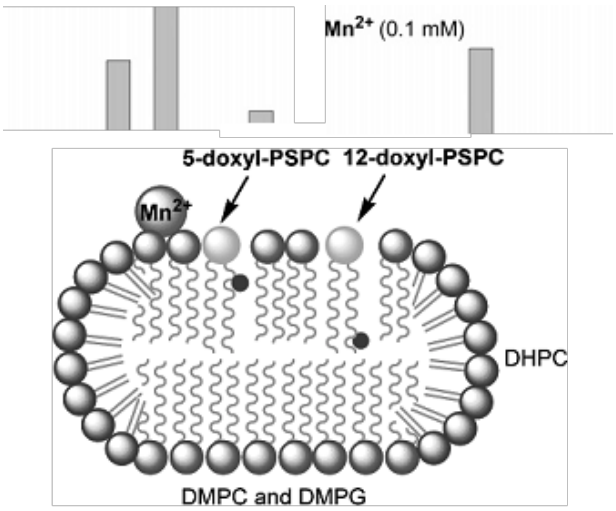

Figure 27. Schematic model of the location of each paramagnetic agent in the isotropic bicelle deduced from the T_{1M} values.

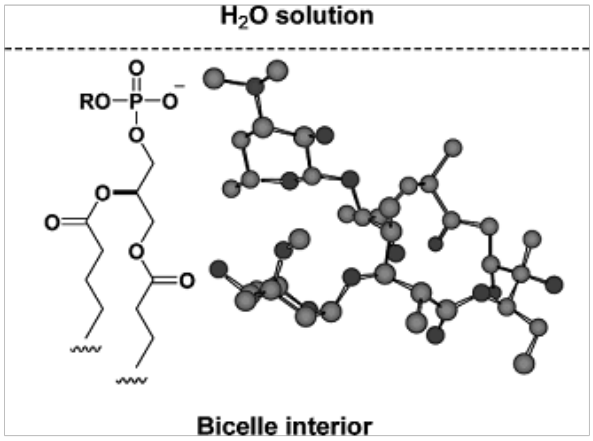

Figure 28. Model representing the position and conformation of EA with respect to bicelle lipid bilayers. The molecular formula of the phospholipid polar region, which is depicted as being almost equivalent to the conformation in the liquid-crystalline bilayer, is also shown to provide an indication of the location of EA.

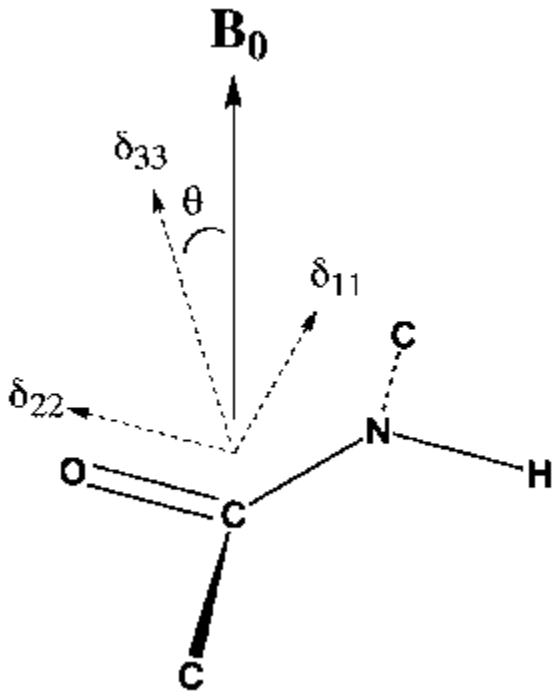

Figure 29. Chemical shift anisotropy of an amide carbonyl carbon. Chemical shift tensor elements, δ_{11}, δ_{22}, and δ_{33}, are taken to be 223, 79 and 55 ppm, respectively. Shifts observed in oriented samples are functions of the angle between the magnetic field, B_0, and the principle shift tensor axes.

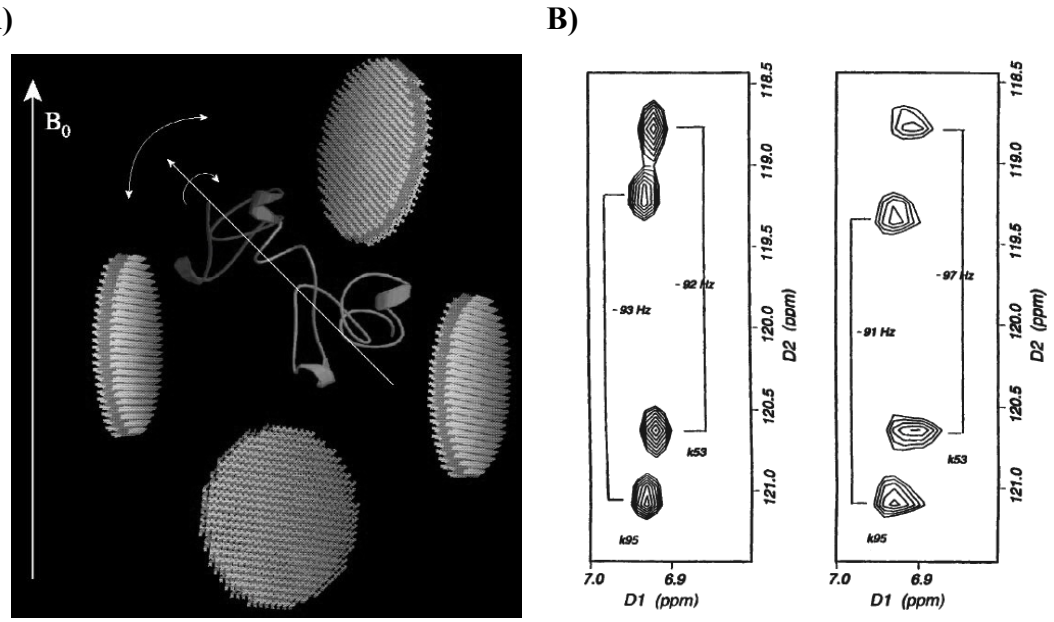

Figure 30. **(A)** Induced protein orientation by dilute phospholipid bicelles. The protein tumbles rapidly, but anisotropically, in large aqueous inter-bicelle spaces.
(**B)** Segments from a proton coupled, nitrogen decoupled, ^{15}N-^{1}H HSQC spectrum of a 0.4 mM solution of a barley lecithin fragment in a 5% DMPC/DHPC 3:1 bicelle (doped with a positively charged amphiphile). Left is an isotropic spectrum at 25 ºC, right is an oriented spectrum at 35 ºC. Both increases and decreases in couplings are observed. (Figures are adopted from *Nat. Struct. Biol.* **1998,** 517–522. [72])

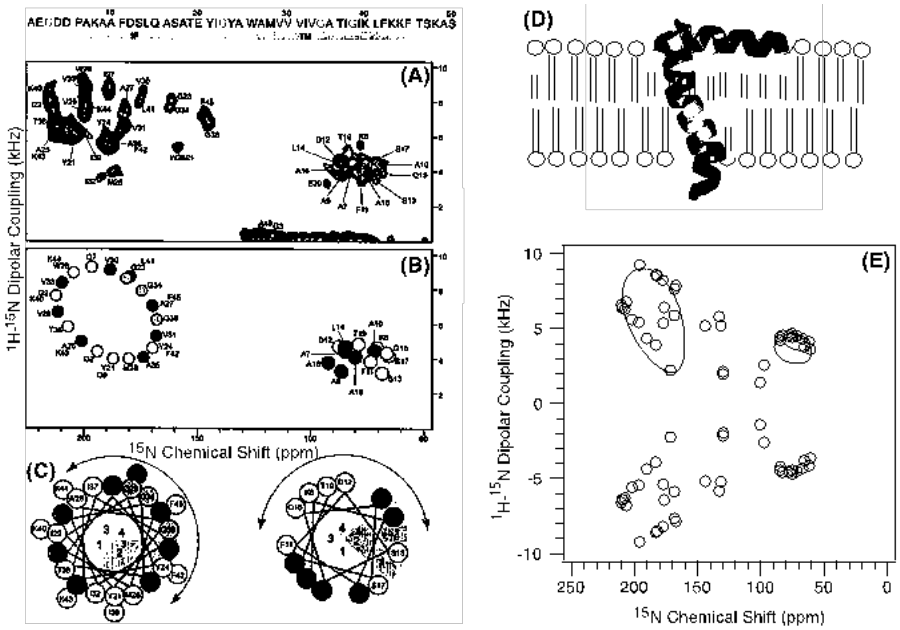

Figure 31. (A) Two-dimensional experimental ^{15}N chemical shift/^{1}H–^{15}N dipolar coupling PISEMA spectrum of a uniformly ^{15}N-labeled fd coat protein in aligned lipid bilayers. The amino acid sequence of the protein is shown at the top. The protein consists of two helices and the corresponding residues are indicated as IP (in-plane) and TM (transmembrane). (B) Pisa wheel PISEMA spectrum calculated from a protein model with the IP helix nearly parallel to the membrane surface (tilted by 87º from the bilayer normal or B_0), and the TM helix crossing the membrane with a 30º tilt from the bilayer normal. The PISA wheel (B) and helical wheel (C) rotations are set to match the resonances from Ala, Gly, Leu, and Val residues of the protein in the experimental PISEMA spectrum (A). (C) Helical wheel representations of the protein in-plane and transmembrane helices. (D) The structure of the fd coat protein determined using solid-state NMR studies (PDB ID: 1MZT). (E) Simulated 2D PISEMA spectrum of the protein from its structure given in (D). PISA wheel patterns (similar to (B)) for ideal a- helices with tilt angles of 30º and 87º are also shown in (E).

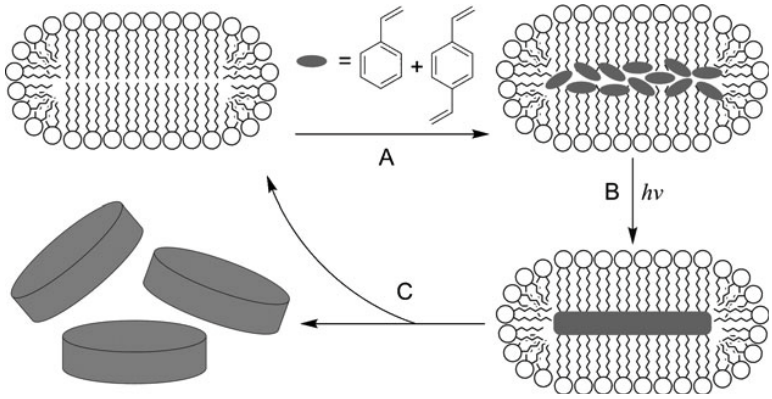

Figure 32. Directed assembly of nanodisks: (a) monomers are loaded into the hydrophobic interior of bicelles (discoidal lipid aggregates); (b) UV-induced free-radical polymerization produces nanodisks enclosed within the bicelle; (c) lipids are first separated from the nanodisks by methanol washing and then reused to template a new batch of nanodisks.

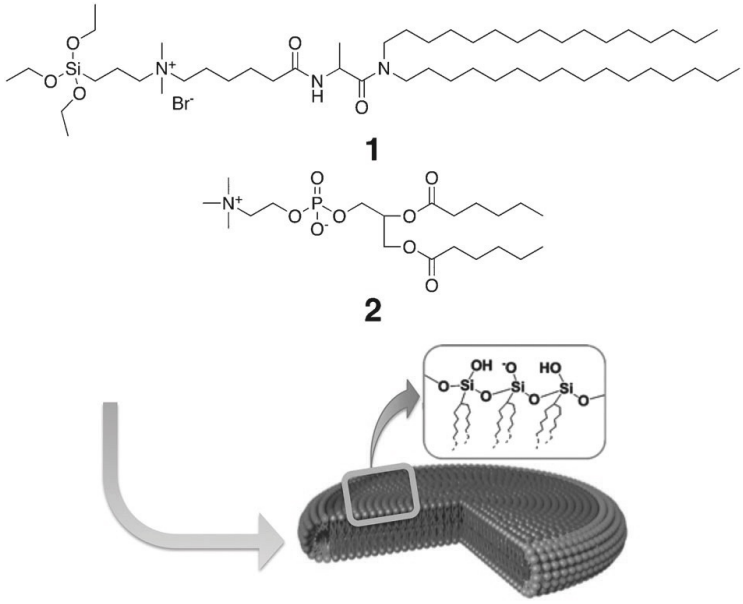

Figure 33. Schematic representation of organic–inorganic hybrid nanodiscs formed by the self-assembly of a binary lipid mixture.

1.4.3. Stabilization of Bicelle

Remaining problems of bicelle for application is mainly thermal instability. Especially, when we utilize magnetically oriented bicelle, we always face with problems of temperature in which systems form oriented bicelle.[54d] Temperature range in which systems form oriented bicelle is typically around 35~40 ºC, which limits capability of magnetically oriented bicelle for various measurements with various kind of methods.

Until now, few reports have succeeded in stabilization of magnetically oriented bicelle. Tachibana and coworkers reported introduction of cholesterol into lipid bilayer leads thermal stabilization of bicelles and upgraded duration against membrane-destabilizing small molecules.[114] They reported that cholesterol doping can enhance durability of magnetically oriented bicelle against mellitin, membrane destructive honey bee venom composed of 26 peptides, up to the degree of vesicles. Martin and coworkers realized RDC measurement at room temperature by stabilizing DMPC/DHPC magnetically oriented bicelle by incorporating cholesterol sulfate into lipid bilayer region (Figure 34).[115] Yamamoto and coworkers are succeeded in fabrication of stable bicelles by optimizing combination of lipids and surfactants.[116] They reports that stable bicelles can be achieved by enhancing miscibility of lipids and surfactant. Using particular combination of lipid/surfactant (diC10PC/diC7PC), the surfactant in bicelle is delocalized to some extent, and they are incorporated into the lipid bilayer. Long chain lipids also delocalizes from the plane of the bilayer into the edge of it. As a result of the delocalization of lipid/surfactant, the bicelle formed in this way is estimated to be partially like ellipsoidal mixed micelle. A little bit micelle-like assembly is hard to change their morphology due to temperature change, thus this system could acquire resistance from thermal disturbance. To summarize these studies, all these method mentioned here are based on the theory of “adding some materials into the lipid bilayers.”

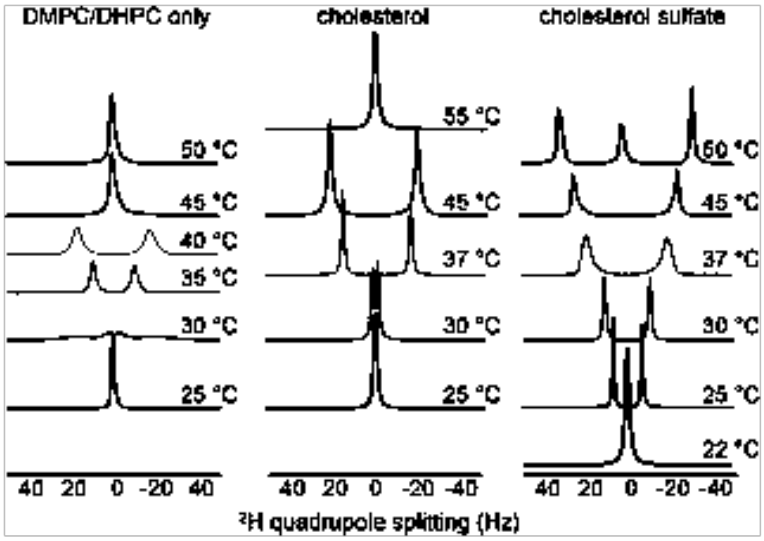

Figure 34. Comparison of deuterium quadrupole splitting in 10% D_2O/ 90% H_2O, *q* = 2.6 DMPC/DHPC bicelles of total lipid content 20% w/v using undoped bicelles and bicelles doped to 13.4% of the lipid content with either cholesterol (CH) or cholesterol sulfate (CS).

1.5. Objectives and Outline of this work

Although bicelles are prominent model membrane, some problems still remain mainly in their stability. There are some studies aimed for morphological stabilization of bicelles against heat, however, their aims can be accomplished only by modifying composition of lipid bilayers. This approach is reasonable in some regards, though, in the situation that some membrane proteins are incorporated into the bilayer of bicelles, changing membrane composition might lead unreasonable interactions to these proteins. In addition, this approach, in converse, may prevent us to step into fabrication of complicated membrane models, e.g. lipid rafts. On the other hand, there are only few reports about fabrication or optimization of surfactants that stabilize edge of lipid bilayers, maybe because demand for thermally stable bicelles is limited inside the fields of structural biologist at this moment, and quite few researchers with ability of organic synthesis notice this situation. So, only several existing derivatives of short chain phospholipids around DHPC are reported here. New-surfactant approach seems reasonable because suitable surfactants will stabilize bicelles without changing composition of lipid bilayer, however, there are almost no reports related to this approach. So if we get further into this field, new and large development is expected to be provided. Thus, the aim of the author on the thesis is following two; to build design method of surfactants for thermally stable bicelles, and to functionalization of bicelles by modification of designed surfactants. The author realized these two aims through several years of studies. In each chapter, the author will explain methods and results for the achievements of these aims.

References

[1] Wallin, E. von.; Heijne, G. *Protein science : publ. Protein. Soc.* **1998**, *7*, 1029–1038.

[2] (a) Nishikawa, T.; Murakami, M.; Kouyama, T. *J. Mol. Biol.* **2005**, *352*, 319–328. (b) Luecke, H.; Schobert, B.; Richter, H. T.; Cartailler, J. P.; Lanyi, J. K. *J. Mol. Biol.* **1999**, *291*, 899–911.

[3] Oshima, A.; Tani, K.; Hiroaki, Y.; Fujiyoshi, Y.; Sosinsky, GE. *Proc. Natl. Acad. Sci. USA,* **2007**, *104***,** 10034–10039.

[4] Savage. D. F.; Egea. P. F.; Robles–Colmenares. Y.; O'Connell. J. D.; Stroud. R. M. *PLOS Biology*, **2003**, *1*, 334–340.

[5] Dürr, U. H. N.; Gildenberg, M.; Ramamoorthy, A. *Chem. Rev.* **2012**, *112*, 6054–6074.

[6] Singer, S. J.; Nicolson, G. L. *Science* **1972**, *175*, 720–731.

[7] Lenaz, G. *Biosci. Rep.,* **1987**, *11*, 823–837.

[8] (a) Nishizuka, Y. *Science* **1984**, *225*, 1365–1370.

[9] (a) de Kruyff, B.; Demel, R. A.; Slotboom, A. J.; van Deenen, L. L.; Rosenthal, A. F. *Biochim. Biophys. Acta.* **1973**, *307*, 1–19. (b) Kruyff, B.; Demel, R. A.; Van Deenen, L. *Biochim. Biophys. Acta.* **1972**, *180*, 569–586. (c) Ladbrooke, B. D.; Chapman, D. *Chem. Phys. Lipids.* **1969**, *3*, 304–367. (d) Bunow, M. R.; Bunow, B. *Biophys. J.* **1979**, *27*, 325–337.

[10] Chen, S. C.; Sturtevant, J. M.; Gaffney, B. J. *Proc. Natl. Acad. Sci.* **1980**, *77*, 5060–5063.

[11] (a) Wang, Z. Q.; Lin, H. N.; Li, S.; Huang, C. H. *The J. biol. chem.,* **1995**, *270*, 2014–2023. (b) Marsh, D. *Biophys. J.* **1999**, *77*, 953–963.

[12] Mabrey, S.; Sturtevant, J.M. *Proc. Natl. Acad. Sci. U.S.A.*, **1976**, *73*, 3862–3866.

[13] Davis, P.J.; Coolbear, K.P.; Keough, K.M.W. *Can. J. Biochem.* **1980**, *58*, 851–858.

[14] Lin, H.; Huang, C. *Biochim. Biophys. Acta.* **1988***,* 946, 178–184.

[15] (a) Chapman, D.; Urbina, J.; Keough, K.M. *J. Biol. Chem.* **1974**, *249*, 2512–2518. (b) Blume, A.; Ackerman, T. *FEBS Lett.* **1974**, *43*, 71–74. (c) Lee, A.G. *Biochim. Biophys. Acta.* **1977**, 472, 285–344.

[16] Marsh, D. *Biochim. Biophys. Acta.,* **2009**, *1788*, 2114–2123.

[17] (a) Shaw, A. S. *Nature Immunology,* **2006**, *7*, 1139–1142. (b) Lingwood, D.; Simons, K. *Science,* **2010**, *327*, 46–50.

[18] Taylor, D. R.; Hooper, N. M. *Semin.Cell. Dev. Biol.* **2007**, *18*, 638–648.

[19] (a) Tokumasu, F.; Jin, A. J.; Feigenson, G. W.; Dvorak, J. A. *Biophys. J.* **2003**, *84*, 2609–2618. (b) Sheikh, K. H.; Jarvis, S. P. *J. Am. Chem. Soc.* **2011**, *133*, 18296–18303.

[20] Ishitsuka, R. *J. Biochem.* **2005**, *137*, 249–254.

[21] Risselada, H. J.; Marrink, S. J. *Proc. Nat. Acad. Sci.* **2008**, *105*, 17367–17372.

[22] Rajendran, L. *J. Cell Sci.* **2005**, *118*, 1099–1102.

[23] (a) Sahl, S. J.; Leutenegger, M.; Hilbert, M.; Hell, S. W.; Eggeling, C. *Proc. Nat. Acad. Sci.* **2010**, *107*, 6829–6834. (b) Eggeling, C.; Ringemann, C.; Medda, R.; Schwarzmann, G.; Sandhoff, K.; Polyakova, S.; Belov, V. N.; Hein, B.; von

Middendorff, C.; Schönle, A.; Hell, S. W. *Nature* **2009**, *457*, 1159–1162.
[24] Owen, D. M.; Williamson, D. J.; Magenau, A.; Gaus, K. *Nat. Commun.* **2012**, *3*, 1256.
[25] (a) Scott, H. L.; Coe, T. J.; *Biophys. J.* **1983**, *42*, 219–224. (b) YashRoy, R. C. *Methods* **1991**, *23*, 259–261. (c) Jahn, R.; Grubmuller, H. *Curr. Opinion. Cell. Biol.* **2002**, *14*, 488–495. (d) Lee, A. G. *Biochim. Biophys. Acta* **2003**, *1612*, 1–40.
[26] (a) Inomata, K.; Ohno, A.; Tochio, H.; Isogai, S.; Tenno, T.; Nakase, I.; Takeuchi, T.; Futaki, S.; Ito, Y.; Hiroaki, H.; Shirakawa, M. *Nature* **2009**, *458*, 106–109. (b) Zandomeneghi, G.; Ilg, K.; Aebi, M.; Meier, B. H. *J. Am. Chem. Soc.* **2012**, *134*, 17513–17519. (c) Bertini, I.; Felli, I. C.; Gonnelli, L.; Kumar M V, V.; Pierattelli, R. *Angew. Chem. Int. Ed.* **2011**, *50*, 2339–2341.
[27] Chan, Y. –H. M.; Boxer, S. G. *Curr. Opin. Chem. Biol.* **2007**, *11*, 581–587.
[28] (a) Warschawski, D. E.; Arnold, A. A.; Beaugrand, M.; Gravel, A.; Chartrand, É.; Marcotte, I. *Biochim. Biophys. Acta.* **2011**, *1808*, 1957–1974. (b) Seddon, A. M.; Curnow, P.; Booth, P. J. *Biochim. Biophys. Acta.***2004**, *1666*, 105–117.
[29] (a) Abdine, A.; Verhoeven, M. A.; Park, K.-H.; Ghazi, A.; Guittet, E.; Berrier, C.; Van Heijenoort, C.; Warschawski, D. E. *J. magn. reson* **2010**, *204*, 155–159. (b) Lakshmi, K. V.; Auger, M.; Raap, J.; Lugtenburg, J.; Griffin, R. G.; Herzfeld, J. *J. Am. Chem. Soc.* **1993**, *115*, 8515–8516.
[30] Perkins, W. R.; Minchey, S. R.; Ahl, P. L.; Janoff, A. S. *Chem. Phys. Lipids* **1993**, *64*, 197–217.
[31] Hirsh, D. J.; Hammer, J.; Maloy, W. L.; Blazyk, J.; Schaefer, J. *Biochemistry* **1996**, *35*, 12733–12741.
[32] Hu, J.; Qin, H.; Li, C.; Sharma, M.; Cross, T. A.; Gao, F. P. *Protein Sci.* **2007**, *16*, 2153–2165.
[33] Bloom, M.; Burnell, E. E.; MacKay, A. L.; Nichol, C. P.; Valic, M. I.; Weeks, G. *Biochemistry* **1978**, *17*, 5750–5762.
[34] Walde, P.; Cosentino, K.; Engel, H.; Stano, P. *ChemBioChem* **2010**, *11*, 848–865.
[35] (a) Clement, N. R.; Gould, J. M. *Biochemistry* **1981**, *20*, 1544–1548. (b) Chiu, H.-C.; Lin, Y.-W.; Huang, Y.-F.; Chuang, C.-K.; Chern, C.-S. *Angew. Chem. Int. E.* **2008**, *47*, 1875–1878. (c) Suzuki, Y.; Okuro, K.; Takeuchi, T.; Aida, T. *J. Am. Chem. Soc.* **2012**, *134*, 15273–15276.
[36] (a) Mansy, S. S.; Schrum, J. P.; Krishnamurthy, M.; Tobé, S.; Treco, D. A.; Szostak, J. W. *Nature* **2008**, *454*, 122–125. (b) Chen, I. A.; Salehi-Ashtiani, K.; Szostak, J. W. *J. Am. Chem. Soc.* **2005**, *127*, 13213–13219.
[37] (a) Toyota, T.; Takakura, K.; Kageyama, Y.; Kurihara, K.; Maru, N.; Ohnuma, K.; Kaneko, K.; Sugawara, T. *Langmuir* **2008**, *24*, 3037–3044. (b) Hatta, E. *J. Phys. Chem. B.* **2007**, *111*, 10155–10159. (c) Hanczyc, M. M.; Szostak, J. W. *Curr. Opin. Chem. Biol.* **2004**, *8*, 660–664. (d) Takakura, K.; Sugawara, T. *Langmuir* **2004**, *20*, 3832–3834. (e) Kurihara, K.; Okura, Y.; Matsuo, M.; Toyota, T.; Suzuki, K.; Sugawara, T. *Nat. Commun.*, **2015**, *6*, 9352.
[38] (a) Siu, H.; Duhamel, J.; Sasaki, D. Y.; Pincus, J. L. *Langmuir* **2010**, *26*, 10985–10994. (b) Litt, J.; Padala, C.; Asuri, P.; Vutukuru, S.; Athmakuri, K.; Kumar, S.; Dordick, J.; Kane, R. S. *J. Am. Chem. Soc.* **2009**, *131*, 7107–7111. (c) Marsh, D. *Biochim. Biophys. Acta.* **2010**, *1798*, 688–699. (d) Feigenson, G. W. *Biochim.*

Biophys. Acta. **2009**, *1788*, 47–52.
[39] Da Costa, G.; Mouret, L.; Chevance, S.; Le Rumeur, E.; Bondon, A. *Eur. Biophys. J.* **2007**, *36*, 933–942.
[40] Ong, R. L.; Marchesi, V. T.; Prestegard, J. H. *Biochemistry* **1981**, *20*, 4283–4292.
[41] Castellana, E. T.; Cremer, P. S. *Surface Science Reports* **2006**, *61*, 429–444.
[42] (a) Antather, D.; Smethazko, M.; Saba, M.; Alguel, Y.; Schalkhammer, T. *J. Nanosci. Nanotechnol.* **2004**, *4*, 1–22. (b) Reimhult, E.; Kumar, K. *Trends Biotechnol.* **2008**, *26*, 82–89.
[43] Richter, R. P.; Bérat, R.; Brisson, A. R. *Langmuir* **2006**, *22*, 3497–3505.
[44] Bamberg, E.; Hegemann, P.; Oesterhelt, D. *Prog. Clin. Biol. Res.* **1984**, *164*, 73–79.
[45] (a) Li, D.; Caffrey, M. *Proc. Natl. Acad. Sci.* **2011**, *108*, 8639–8644. (b) Landau, E. M.; Rosenbusch, J. P. *Proc. Natl. Acad. Sci.* **1996**, *93*, 14532–14535.
[46] Caffrey, M. *Annu. Rev. Biophys.*, **2009**, *38*, 29–51.
[47] Mazer, N. A.; Benedek, G. B.; Carey, M. C. *Biochemistry,* **1980**, *19*, 601–615.
[48] Müller, K. *Biochemistry,* **1981**, *20*, 404–414.
[49] Speyer, J. B.; Sripada, P. K.; Das Gupta, S. K.; Graham Shipley, G.; Griffin, R. G. *Biophys. J.* **1987**, *51*, 687–691.
[50] Sanders, C. R.; Schwonek, J. P. *Biochemistry* **1992**, *31*, 8898–8905.
[51] (a) Sanders, C. R.; Prestegard, J. H. *Biophys. J.* **1990**, *58*, 447–460. (b) Aubin, Y.; Ito, Y.; Paulson, J. C.; Prestegard, J. H. *Biochemistry* **1993**, *32*, 13405–13413.
[52] Sanders, C. R.; Landis, G. C. *Biochemistry* **1995**, *34*, 4030–4040.
[53] Tjandra, N. *Science* **1997**, *278*, 1111–1114.
[54] (a) Sanders, C. R.; Prosser, R. S. *Structure* **1998**, *6*, 1227–1234. (b) Sanders, C. R.; Oxenoid, K. *Biochim. Biophys. Acta* **2000**, *1508*, 129–145. (c) Marcotte, I.; Auger, M. l. *Concepts. Magn. Reson.* **2005**, *24A*, 17–37. (d) Prosser, R. S.; Evanics, F.; Kitevski, J. L.; Al-Abdul-Wahid, M. S. *Biochemistry* **2006**, *45*, 8453–8465. (e) Diller, A.; Loudet, C.; Aussenac, F.; Raffard, G.; Fournier, S.; Laguerre, M.; GrElard, A.; Opella, S. J.; Marassi, F. M.; Dufourc, E. J. *Biochimie* **2009**, *91*, 744–751. (f) Dürr, U. H. N.; Gildenberg, M.; Ramamoorthy, A. *Chem. Rev.* **2012**, *112*, 6054–6074.
[55] Wang, H.; Eberstadt, M.; Olejniczak, E. T.; Meadows, R. P.; Fesik, S. W. *Cell*, **1998**, *95*, 269–277.
[56] Triba, M. N.; Devaux, P. F.; Warschawski, D. E. *Biophys. J.* **2006**, *91*, 1357–1367.
[57] Aussenac, F.; Lavigne, B.; Dufourc, E. J. *Langmuir* **2005**, *21*, 7129–7135
[58] Yamaguchi, T.; Suzuki, T.; Yasuda, T.; Oishi, T.; Matsumori, N.; Murata, M. *Bioorg. Med. Chem.* **2012**, *20*, 270–278.
[59] (a) Park, S. H.; Loudet, C.; Marassi, F. M.; Dufourc, E. J.; Opella, S. J. *J. Magn. Reson.* **2008**, *193*, 133–138. (b) Loudet-Courreges, C. c.; Nallet, F. d. r.; Dufourc, E. J.; Oda, R. *Langmuir* **2011**, 9122–9130. (c) Loudet, C.; Diller, A.; GrElard, A.; Oda, R.; Dufourc, E. J. *Prog. Lipid Res.* **2010**, *49*, 289–297. (d) Loudet, C.; Manet, S.; Gineste, S.; Oda, R.; Achard, M.-F.; Dufourc, E. J. *Biophys. J.* **2007**, *92*, 3949–3959.
[60] Park, S. H.; Opella, S. J. *J. Am. Chem. Soc.* **2010**, *132*, 12552–12553.
[61] Raffard, G.; Steinbruckner, S.; Arnold, A.; Davis, J. H.; Dufourc, E. J. *Langmuir*

2000, *16*, 7655–7662.
[62] (a) Yang, P. W.; Lin, T. L.; Hu, Y.; Jeng, U. S. *Chinese Journal of Physics* **2012**, *50*, 349–356. (b) Nieh, M.-P.; Dolinar, P.; Kučerka, N.; Kline, S. R.; Debeer-Schmitt, L. M.; Littrell, K. C.; Katsaras, J. *Langmuir* **2011**, *27*, 14308–14316.
[63] Thompson, A. A.; Liu, J. J.; Chun, E.; Wacker, D.; Wu, H.; Cherezov, V.; Stevens, R. C. *Methods* **2011**, *55*, 310–317.
[64] Andersson, A.; Mäler, L. *Langmuir* **2006**, *22*, 2447–2449.
[65] Soong, R.; Majonis, D.; Macdonald, P. M. *Biophys. J.* **1999**, *77*, 888–902.
[66] van Dam, L.; Karlsson, G.; Edwards, K. *Biochim. Biophys. Acta.* **2004**, *1664*, 241–256.
[67] Bolze, J.; Fujisawa, T.; Nagao, T.; Norisada, K.; Saito, H.; Naito, A. *Chem. Phys. Lett.* **2000**, *329*, 215–220.
[68] Nieh, M.-P.; Raghunathan, V. A.; Glinka, C. J.; Harroun, T. A.; Pabst, G.; Katsaras, J. *Langmuir* **2004**, *20*, 7893–7897.
[69] Sasaki, R.; Sasaki, H.; Fukuzawa, S.; Kikuchi, J.; Hirota, H., Tachibana, K. *Bull. Chem. Soc. Jpn.* **2007**, *80*, 1208–1216.
[70] Rowe, B. A.; Neal, S. L. *Langmuir* **2003**, *19*, 2039–2048.
[71] Sternin, E.; Nizza, D.; Gawrisch, K. *Langmuir* **2001**, *17*, 2610–2616.
[72] (a) Nieh, M.-P.; Raghunathan, V. A.; Pabst, G.; Harroun, T.; Nagashima, K.; Morales, H.; Katsaras, J.; Macdonald, P. *Langmuir* **2011**, *27*, 4838–4847. (b) Cho, H. S.; Dominick, J. L.; Spence, M. M. *J. Phys. Chem. B.* **2010**, *114*, 9238–9245.
[73] (a) Wu, E. S.; Jacobson, K.; Papahadjopoulos, D. *Biochemistry* **1977**, *16*, 3936–3941. (b) Ellena, J. F.; Lepore, L. S.; Cafiso, D. S. *J. Phys. Chem.* **1993**, *97*, 2952–2957.
[74] Matsumori, N.; Murata, M. *Nat. Prod. Rep.* **2010**, *27*, 1480–1492.
[75] Vold, R. R.; Prosser, R. S.; Deese, A. J. *J. Biomol. NMR* **1997**, *9*, 329–335.
[76] (a) Glover, K. J.; Whiles, J. A.; Wood, M. J.; Melacini, G.; Komives, E. A.; Vold, R. R. *Biochemistry* **2001**, *40*, 13137–13142. (b) Whiles, J. A.; Brasseur, R.; Glover, K. J.; Melacini, G.; Komives, E. A.; Vold, R. R. *Biophys. J.* **2001**, *80*, 280–293.
[77] Andersson, A.; Mäler, L. *J. Biomol. NMR* **2002**, *24*, 103–112.
[78] Dittmer, J.; Thøgersen, L.; Underhaug, J.; Bertelsen, K.; Vosegaard, T.; Pedersen, J. M.; Schiøtt, B.; Tajkhorshid, E.; Skrydstrup, T.; Nielsen, N. C. *J. Phys. Chem. B.* **2009**, *113*, 6928–6937.
[79] (a) Matsumori, N.; Morooka, A.; Murata, M. *J. Med. Chem.* **2006**, *49*, 3501–3508. (b) Matsumori, N.; Morooka, A.; Murata, M. *J. Am. Chem. Soc.* **2007**, *129*, 14989–14995. (c) Houdai, T.; Matsumori, N.; Murata, M. *Org. Lett.* **2008**, *10*, 4191–4194.
[80] Poget, S. F.; Cahill, S. M.; Girvin, M. E. *J. Am. Chem. Soc.* **2007**, *129*, 2432–2433.
[81] Lührs, T.; Zahn, R.; Wüthrich, K. *J. Mol. Biol.* **2006**, *357*, 833–841.
[82] Prestegard, J. H. *Nat. Struct. Biol.* **1998**, *5 Suppl*, 517–522.
[83] (a) Bax, A.; Tjandra, N. *J. Biomol. NMR* **1997**, *10*, 289-292. (b) Cornilescu, G.; Marquardt, J. L.; Ottiger, M.; Bax, A. *J. Am. Chem. Soc.* **1998**, *120*, 6836–6837.

(c) Ottiger, M.; Bax, A. *J. Am. Chem. Soc.* **1998**, *120*, 12334–12341.
[84] Yan, J.; Delaglio, F.; Kaerner, A.; Kline, A. D.; Mo, H.; Shapiro, M. J.; Smitka, T. A.; Stephenson, G. A.; Zartler, E. R. *J. Am. Chem. Soc.* **2004**, *126*, 5008–5017.
[85] (a) Moll, F.III.; Cross, T. A. *Biophys. J.* **1990**, *57*, 351–362. (b) Hallock, K. J.; Wildman, K. H.; Lee, D.-K.; Ramamoorthy, A. *Biophys. J.* **2002**, *82*, 2499–2503.
[86] Yamamoto, K.; Soong, R.; Ramamoorthy, A. *Langmuir* **2009**, *25*, 7010–7018.
[87] (a) Cook, G. A.; Stefer, S.; Opella, S. J. *Biopolymers* **2011**, *96*, 32–40. (b) Schmidt, P.; Berger, C.; Scheidt, H. A.; Berndt, S.; Bunge, A.; Beck-Sickinger, A. G.; Huster, D. *Biophys. Chem.* **2010**, *150*, 29–36.
[88] (a) Park, S. H.; Casagrande, F.; Das, B. B.; Albrecht, L.; Chu, M.; Opella, S. J. *Biochemistry* **2011**, *50*, 2371–2380. (b) Park, S. H.; Prytulla, S.; De Angelis, A. A.; Brown, J. M.; Kiefer, H.; Opella, S. J. *J. Am. Chem. Soc.* **2006**, *128*, 7402–7403.
[89] Park, S. H.; Casagrande, F.; Cho, L.; Albrecht, L.; Opella, S. J. *J. Mol. Biol.* **2011**, *414*, 194–203.
[90] Cui, T.; Canlas, C. G.; Xu, Y.; Tang, P. *Biochim. Biophys. Acta.* **2010**, *1798*, 161–166.
[91] Cook, G. A.; Opella, S. J. *Eur. Biophys. J.* **2010**, *39*, 1097–1104.
[92] Park, S. H.; Opella, S. J. *Protein Sci.* **2007**, *16*, 2205–2215.
[93] De Angelis, A. A.; Howell, S. C.; Nevzorov, A. A.; Opella, S. J. *J. Am. Chem. Soc.* **2006**, *128*, 12256–12267.
[94] Cho, M-K.; Gayen, A.; Banigan, J. R.; Leninger, M.; Traaseth, N. J. *J. Am. Chem. Soc.* **2014**, *136*, 8072–8080.
[95] Dürr, U. H. N.; Yamamoto, K.; Im, S.-C.; Waskell, L.; Ramamoorthy, A. *J. Am. Chem. Soc.* **2007**, *129*, 6670–6671.
[96] Marcotte, I.; Dufourc, E. J.; Ouellet, M.; Auger, M. *Biophys. J.* **2003**, *85*, 328–339.
[97] Rinaldi, F.; Lin, M.; Shapiro, M. J.; Petersheim, M. *Biophys. J.* **1997**, *73*, 3337–3348.
[98] Smith, P. E. S.; Brender, J. R.; Ramamoorthy, A. *J. Am. Chem. Soc.* **2009**, *131*, 4470–4478.
[99] Park, T.-J.; Kim, J.-S.; Ahn, H.-C.; Kim, Y. *Biophys. J.* **2011**, *101*, 1193–1201.
[100] Marcotte, I.; Wegener, K. L.; Lam, Y.-H.; Chia, B. C. S.; de Planque, M. R. R.; Bowie, J. H.; Auger, M.; Separovic, F. *Chem. Phys. Lipids* **2003**, *122*, 107–120.
[101] Chartrand, É.; Arnold, A. A.; Gravel, A.; Jenna, S.; Marcotte, I. *Biochim. Biophys. Acta.* **2010**, *1798*, 1651–1662.
[102] (a) Ouellet, M.; Bernard, G.; Voyer, N.; Auger, M. *Biophys. J.* **2006**, *90*, 4071–4084. (b) Ouellet, M.; Voyer, N.; Auger, M. *Biochim. Biophys. Acta.* **2010**, *1798*, 235–243.
[103] (a) Wu, C. H.; Ramamoorthy, A.; Opella, S. J. *J. Magn. Reson. A.* **1994**, *109*, 270–272. (b) Ramamoorthy, A.; Wu, C. H.; Opella, S. J. *J. magn. reson.* **1999**, *140*, 131–140. (c) Ramamoorthy, A.; Wei, Y.; Lee, D.-K. In *Annual Reports on NMR Spectroscopy*; Elsevier: 2004; Vol. 52, p 1–52.
[104] Yamamoto, K.; Lee, D. K.; Ramamoorthy, A. *Chem. Phys. Lett.* **2005**, *407*, 289–293.
[105] Dvinskikh, S. V.; Yamamoto, K.; Ramamoorthy, A. *J. Chem. Phys.* **2006**, *125*,

034507.
[106] Nevzorov, A. A.; Opella, S. J. *J. Magn. Reson.* **2003**, *164*, 182–186.
[107] (a) Gopinath, T.; Traaseth, N. J.; Mote, K.; Veglia, G. *J. Am. Chem. Soc.* **2010**, *132*, 5357–5363. (b) Gopinath, T.; Verardi, R.; Traaseth, N. J.; Veglia, G. *J. Phys. Chem. B.* **2010**, *114*, 5089–5095. (c) Gopinath, T.; Mote, K. R.; Veglia, G. *J. Chem. Phys.* **2011**, *135*, 074503.
[108] Xu, J.; Dürr, U. H. N.; Im, S.-C.; Gan, Z.; Waskell, L.; Ramamoorthy, A. *Angew. Chem. Int. Ed.* **2008**, *47*, 7864–7867.
[109] Sasaki, H.; Araki, M.; Fukuzawa, S.; Tachibana, K. *Bioorg. Med. Chem. Lett.* **2003**, *13*, 3583–3585.
[110] Bonderer, L. J.; Studart, A. R.; Gauckler, L. J.; *Science* **2008**, *319*, 1069–1073.
[111] Sheng, K.; Shi, G. *Synt. Metals.* **2010**, *160*, 1354–1358.
[112] Tekobo, S.; Pinkhassik, E. *Chem. Commun.* **2009**, 1112–1114.
[113] Yasuhara, K.; Miki, S.; Nakazono, H.; Ohta, A.; Kikuchi, J.-i. *Chem. Commun.* **2011**, *47*, 4691–4693.
[114] Sasaki, H.; Fukuzawa, S.; Kikuchi, J.; Yokoyama, S.; Hirota, H.; Tachibana, K. *Langmuir* **2003**, *19*, 9841–9844.
[115] Shapiro, R. A.; Brindley, A. J.; Martin, R. W. *J. Am. Chem. Soc.* **2010**, *132*, 11406–11407.
[116] (a) Yamamoto, K.; Pearcy, K.; Ramamoorthy, A. *Langmuir*, **2014**, *30*, 1622–1629. (b) Yamamoto, K.; Pearcy, K.; Lee, D-K.; Yu, C.; Im, S-C.; Waskell, L.; Ramamoorthy, A. *Langmuir*, **2015**, *31*, 1496–1504.

Chapter 1

Magnetically Orientable Bicelles with Unprecedented Stability by Novel Surfactants Derived from Sodium Cholate

Abstract

Five novel surfactants were prepared by modifying the three hydroxy groups of sodium cholate with triethylene glycol chains endcapped with an amide (**SC-C$_1$**, **SC-^{n}C$_4$**, and **SC-^{n}C$_5$**) or a carbamoyl group (**SC-O^{n}C$_4$** and **SC-O^{t}C$_4$**). The phase behavior of aqueous mixtures of these surfactants with 1,2-dimyristoyl-*sn*-glycero-3-phosphatidylcholine (DMPC) was systematically studied by ^{31}P NMR spectroscopy. The surfactants endcapped with carbamate groups (**SC-O^{n}C$_4$** and **SC-O^{t}C$_4$**) formed magnetically alignable bicelles over unprecedentedly wide ranges of conditions, in terms of temperature (from 21–23 to >90 °C), lipid/surfactant ratio (from 5 to 8), total lipid content (5–20 wt%), and lipid type [DMPC, 1,2-dilauroyl-*sn*-glycero-3-phosphatidylcholine (DLPC), or 1-palmitoyl-2-oleoyl-*sn*-glycero-3-phosphatidylcholine (POPC)]. In conjunction with appropriate phospholipids, the carbamate-endcapped surfactants afforded unique bicelles, characterized by exceptional thermal stabilities (from 0 to >90 °C), biomimetic lipid compositions (DMPC/POPC = 25:75 to 50:50), and extremely large ^{2}H quadrupole splittings (up to 71 Hz).

Introduction

Bicelles (bilayered micelles) are aqueous lipid–surfactant assemblies in which lipid bilayer fragments are edge-stabilized by certain surfactants.[1] Because bicelles adopt morphologies that are intermediate between those of lipid vesicles and lipid–surfactant mixed micelles, they form a new class of biomembrane models that simultaneously realize a fluidity comparable to that of natural membranes and a structural simplicity similar to lipid–surfactant mixed micelles.[1a,2] In addition, bicelles with sufficient lateral size can spontaneously align in a magnetic field, and are therefore useful as aligned media for modern NMR techniques that provide three-dimensional structural information on biomolecules.[3] Indeed, in recent NMR studies, bicelles have been successfully used for clarifying the atomic-resolution structures and dynamic profiles of proteins.[4]

Although various bicellar systems have been developed, their application has been limited due to insufficient stability of their magnetically alignable phases. Most reported bicelles show optimal alignment in a limited range of conditions of temperature, lipid content, pH, ionic strength, etc.[3e,5] For example, the most widely used bicellar mixtures, which consist of 1,2-dimyristoyl-*sn*-glycero-3-phosphatidylcholine (DMPC) and 1,2-dihexanoyl-*sn*-glycero-3-phosphatidylcholine (DHPC), exhibit an alignable phase only within 32–40 °C.[3a] As a result, NMR studies using these bicelles are commonly carried out within this narrow range of temperatures, which precludes many cutting-edge multidimensional NMR experiments on proteins at their biologically relevant temperatures. Furthermore, the radio-frequency pulses used in NMR experiments can cause heating of samples and thereby inducing deterioration of the bicelles during repetitive aquation, which further limits the range of application of conventional bicelles.

Consequently, there is a longstanding demand for thermally tolerant bicellar systems. Several strategies have been proposed for stabilizing the alignable phases of bicelles; these include (i) optimization of the lipids,[6] (ii) chemical modification of the lipids,[7] (iii) doping of the lipid bilayers with cholesterols or charged surfactants,[6a,8] and (iv) optimization or development of surfactants.[6,9] Among them, strategy (iv) is of particular importance, because (i)–(iii) inevitably result in changes in the interior

environment of the lipid bilayers. Also in terms of compatibility with target proteins, further exploration of (iv) is demanded; it has been reported that some membrane proteins, such as cytochrome P450, can be destabilized by the presence of surfactants in bicelles.[10] In developing novel surfactants capable of forming thermally stable bicelles, the main difficulty is that the surfactants need to meet two seemingly contradictory requirements. If the miscibility of the surfactant with the phospholipid is too high, their mixture tends to form isotropic mixed micelles rather than bicelles (Figure 1c, lower). Insufficient miscibility, on the other hand, results in separation of bicelles into vesicles and surfactant–phospholipid mixed micelles (Figure 1c, upper). Moreover, phospholipids generally show thermotropic transitions that are accompanied by drastic changes in their miscibility with surfactants,[11] which also increases the difficulty of surfactant design.

To develop surfactants with improved bicelle-formation abilities, the author focused on sodium cholate (**SC**; Figure 1b, upper), which has a rigid and amphiphilic steroid plane with hydrophilic and hydrophobic faces residing back-to-back.[12] This characteristic structure provides **SC** with surface-active properties and permits its use in the efficient dispersion of various hydrophobic materials in aqueous media. When mixed with phospholipids, **SC** and its derivatives can form bicelles that are more stable than those of DHPC.[9] In these bicelles, **SC** and the phospholipid assemble in such way that the hydrophobic face of **SC** stacks on the edge of the lipid bilayer while the hydrophilic face of **SC** is oriented toward the solvent water. Because **SC** has a rigid quasiplanar skeleton with several modifiable functional groups (CO_2H × 1; OH × 3), chemical derivatization of **SC** would seem a promising approach to the design of surfactants capable of forming stable bicelles. Indeed, several **SC**-based surfactants produced by modification of the carboxy group have been reported to afford magnetically alignable bicelles with improved stabilities.[9] Modification of the hydroxy groups would also be expected to afford surfactants with improved bicelle-formation abilities.[13]

Here, the author report a series of novel **SC**-based surfactants with excellent structural tunabilities (Figure 1b, lower). Among these surfactants, those containing carbamate groups formed unprecedentedly stable bicelles over wide ranges of temperature, lipid/surfactant ratio, total lipid content, and lipid type. These achievements should expand the range of utility of bicelles as biomembrane models

and aligned media for NMR studies. The author also found that subtle modifications of the molecular structure of the surfactants had critical effects on their bicelle-formation abilities. This observation should yield a simple guideline for the rational design of bicelles with desired structures and properties.

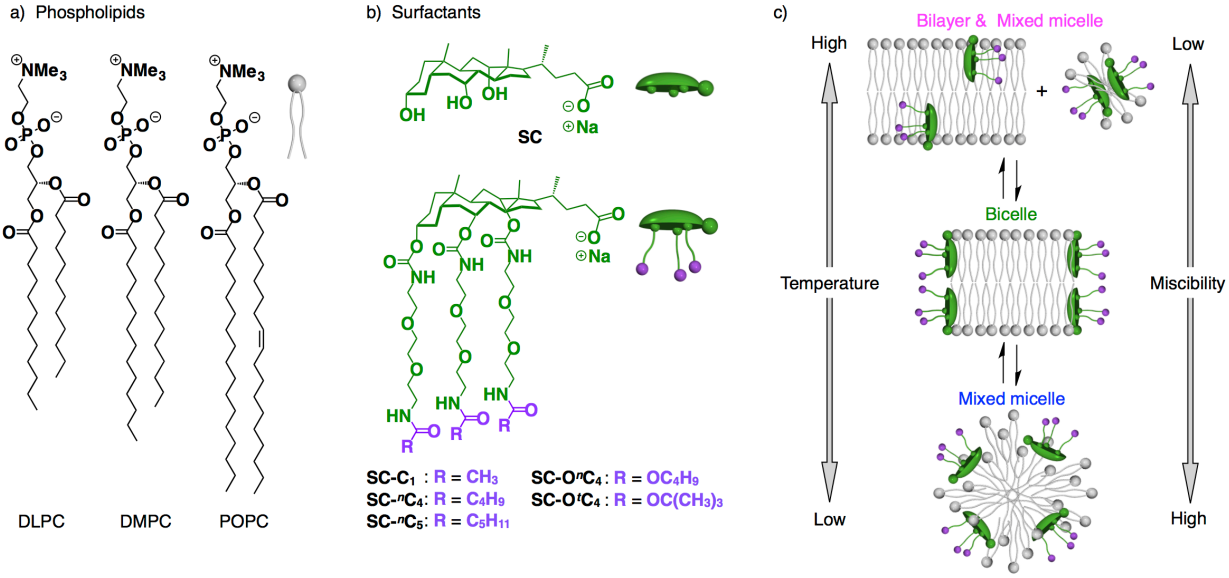

Figure 1. Chemical structures of a) phospholipids and b) surfactants based on sodium cholate (**SC**). c) Schematic representation of the phase behavior of a bicellar mixture composed of a phospholipid and a **SC**-based surfactant.

Results and discussion

Design and Synthesis of SC-Based Surfactants

The author designed and synthesized two series of novel surfactants by modifying the three hydroxy groups of **SC** with triethylene glycol chains. A series of surfactants was designed by endcapping one terminus of the triethylene glycol chains with an aliphatic amide group. The amide connection permitted the ready introduction of various endcapping groups, so that hydrophobicity of the surfactants could be systematically tuned (**SC-C_1**, **SC-$^nC_4$**, and **SC-$^nC_5$**; Figure 1b, lower). As described later, the author's study showed that simple tuning of the hydrophobicity did not lead to ideal bicelle-forming surfactants. Consequently, the author designed a second series of surfactants in which the amide endcapping groups were replaced by carbamate groups (**SC-$^nOC_4$** and **SC-$^tOC_4$**; Figure 1b, lower).

These surfactants were successfully synthesized according to the reported method with some modifications (see experimental section). Hereafter, the surfactants are denoted according to the substituents on the endcapping carbonyl groups (R in Figure 1b, lower): **SC-C_1** (methyl), **SC-$^nC_4$** (butyl), **SC-$^nC_5$** (pentyl), **SC-O$^nC_4$** (butoxy), and **SC-O$^tC_4$** (*tert*-butoxy).

Phase behavior of Mixtures of DMPC with Amide-Endcapped SC-Based Surfactants

For each of the **SC**-based surfactants prepared as described above, the author prepared a bicellar mixture with DMPC (Figure 1a) according to the general method with a DMPC/surfactant ratio of 83.3:16.7 (mol/mol) and a total lipid content (DMPC + surfactant) of 20% w/v in D_2O containing 100 mM KCl (see Supporting Information). **SC** was used as a reference surfactant. The phase behavior of these mixtures was investigated by ^{31}P NMR spectroscopy.

As shown in Figure 2a, the mixture of DMPC and **SC** showed a magnetically alignable phase within a certain range of temperature. Below 24 °C, DMPC was highly miscible with **SC**. Because **SC** molecules tend to form face-to-face dimers in hydrophobic environments, the mixture formed mixed bilayers (Figure S1, lower), resulting in a broad ^{31}P NMR signal at around –5 ppm (Figure 2a, blue). Upon heating, DMPC underwent a gel-to-fluid transition at 24 °C, where the miscibility with **SC** fell to a moderate level suitable for bicelle formation (Figure S1, middle). Consequently, the signal at 0 ppm disappeared at 20 °C, and a new signal assignable to magnetically aligned bicelles at –9 ppm emerged between 30 and 50 °C (Figure 2a, green). However, upon further heating to >55 °C, where the lipid–surfactant miscibility became insufficient to maintain homogeneity, the mixture separated into large bilayers and isotropic mixed micelles (Figure S1, upper), which gave ^{31}P NMR signals at 0 and –15 ppm, respectively (Figure 2a, magenta).

Unlike the case of **SC**, the mixture of **SC-C$_1$** with DMPC segregated into isotropic micelles and large bilayers at all temperatures, because **SC-C$_1$** is too hydrophilic to associate with DMPC. Consequently, throughout the temperature region 15–90 °C, the bilayers of DMPC remained insoluble, and only a broad signal was observed in the ^{31}P NMR spectra (Figure 2b). Although hydrophilic endcapping groups such as acetyl groups apparently seem to stabilize the rim regions of the bicelles, this design also suppressed the bilayer lysis process, a key intermediate step in the formation of bicelles, which exist in a rapid equilibrium between fission and fusion.

Taking account of the above observations, the author decided to use **SC-^{n}C$_4$**, bearing more hydrophobic endcapping groups as a new surfactant. Owing to the

improved lipid–surfactant miscibility, the mixture of **SC-^{n}C$_4$** with DMPC did not segregate but, instead, formed mixed micelles from 15 to 21 °C (Figure 1c, lower), giving rise to a sharp ^{31}P NMR signal at 0 ppm (Figure 2c, blue). When the temperature was increased, appropriate lipid–surfactant miscibility for bicelle formation occurred (Figure 1c, mid) and a characteristic ^{31}P NMR signal at –9 ppm emerged from 25 to 30 °C (Figure 2c, green). However, the lipid–surfactant miscibility decreased as the temperature was increased further, and the mixture segregated into large bilayers and mixed micelles at >40 °C (Figure 1c, upper), as confirmed by ^{31}P NMR measurements (Figure 2c, magenta). With the aim of expanding the temperature range of an alignable phase into the high-temperature region, the author tested **SC-^{n}C$_5$** as a surfactant. However, the miscibility of the mixture of **SC-^{n}C$_5$** with DMPC was too high and it formed isotropic mixed micelles over a wide temperature region up to 50 °C (Figure 2d, blue), and an alignable phase appeared only at temperatures above 70 °C (Figure 2d, green).

Phase Behavior of Mixtures of DMPC with Carbamate-Endcapped SC-Based Surfactants

The above observations indicated that the hydrophobicity of the endcapping group is critical for the stability of alignable bicelles. The results suggested that simple tuning of the hydrophobicity would not lead to ideal surfactants that would afford alignable bicelles at both low and high temperatures; because lipid–surfactant miscibility is highly temperature dependent, surfactants designed for bicelle formation at low temperatures do not work at high temperatures, and vice versa.

To address this issue, the author turned his attention to the peculiar conformational profiles of carbamates. Although amides and carbamates share common features, the additional oxygen in the carbamate functionality exerts unique steric and electronic effects. Consequently, the conformation of carbamates is not largely biased to the *trans* form, unlike that of the corresponding amides. In addition, the barrier to C–N-bond rotation in carbamate is 3–4 kcal mol^{-1} lower than that in the corresponding amide.[14] These conformational characteristics of carbamates, from the thermotropic and kinetic viewpoints, might affect their miscibility with phospholipids. With this expectation in mind, the author designed **SC-O^{n}C$_4$** as a carbamate analogue of **SC-^{n}C$_4$**.

As shown in Figure 2e, **SC-O^{n}C$_4$** exhibited surprisingly good bicelle-forming ability, and the mixture of **SC-O^{n}C$_4$** and DMPC formed an alignable phase over a quite wide range of temperatures from 21 to >90 °C, unlike the case of amide-endcapped surfactants. Note that subtle differences in the molecular structure of the surfactants (**SC-O^{n}C$_4$** versus **SC-^{n}C$_4$** and **SC-^{n}C$_5$**) have marked effects on their bicelle-formation performance. When the substituent in the carbamate unit was changed from butoxy (**SC-O^{n}C$_4$**) to *tert*-butoxy (**SC-O^{t}C$_4$**), the resulting mixture with DMPC again exhibited an alignable phase over a wide temperature range from 25 to >90 °C (Figure 2f), indicating that carbamate endcapping is generally effective for designing surfactants that can form thermally stable bicelles. For more detailed analysis, the ^{31}P NMR spectra of the mixture with **SC-O^{t}C$_4$** were remeasured at a higher ^{1}H decoupling power (70 kHz), suitable for estimating the order parameter of bicelles. Accordingly, the order parameter of the present bicelles was estimated to be 0.83–0.85 at 40–90 °C (Figure S2).[15]

Among the DMPC-based bicellar systems reported so far, the present systems consisting of DMPC and the carbamate-endcapped surfactants **SC-O^{n}C$_4$** and **SC-O^{i}C$_4$** exhibit the widest thermal ranges of magnetically alignable phases. The author also found that the present bicellar system exhibited a thermally stable alignable phase even when the molar ratio of phospholipid to surfactant (= *q* value) was changed from 5 to 8 (Figure 3). Of further interest, the present bicellar system showed an excellent temporal stability, which is favorable for NMR measurements taking long data-accumulation time. When the bicellar mixture of **SC-O^{i}C$_4$** and DMPC was left to stand at 40 °C for 8 days, the mixture kept on showing a ^{31}P NMR signal at –11.5 ppm characteristic of magnetically alignable bicelles, where the signal hardly changed its shape over time (Figure S3a). This feature most likely originated from the cholate skeleton of **SC-O^{i}C$_4$**, because the analogous bicellar mixture of **SC** also showed similar temporal stability (Figure S3b).

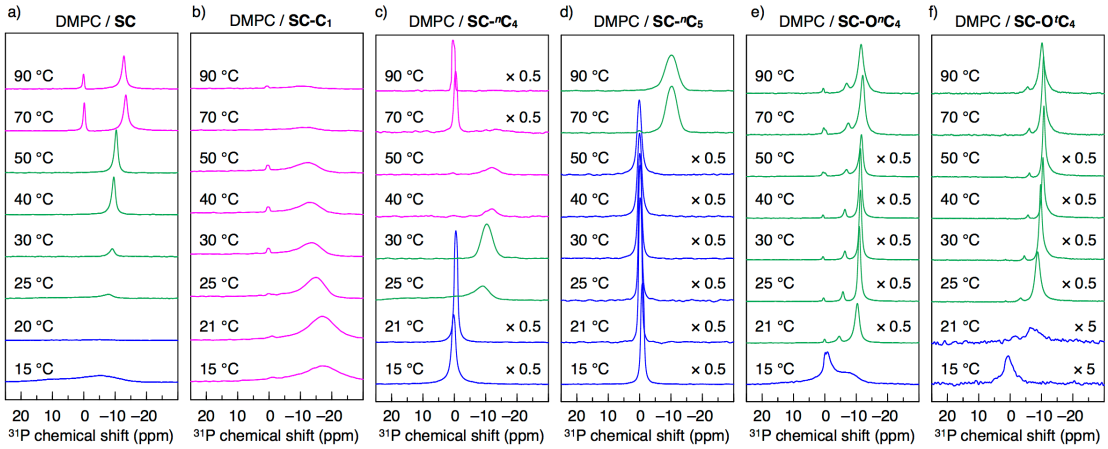

Figure 2. Variable-temperature ^{31}P NMR spectra with a ^{1}H decoupling of 6 kHz for bicellar mixtures of DMPC and **SC**-based surfactants: a) **SC**, b) **SC-C$_1$**, c) **SC-^{n}C$_4$**, d) **SC-^{n}C$_5$**, e) **SC-O^{n}C$_4$**, and f) **SC-O^{t}C$_4$**. DMPC/surfactant = 83:17 (mol/mol). Total lipid content (DMPC + surfactant) = 20% w/v. Medium = 100 mM KCl in D_2O.

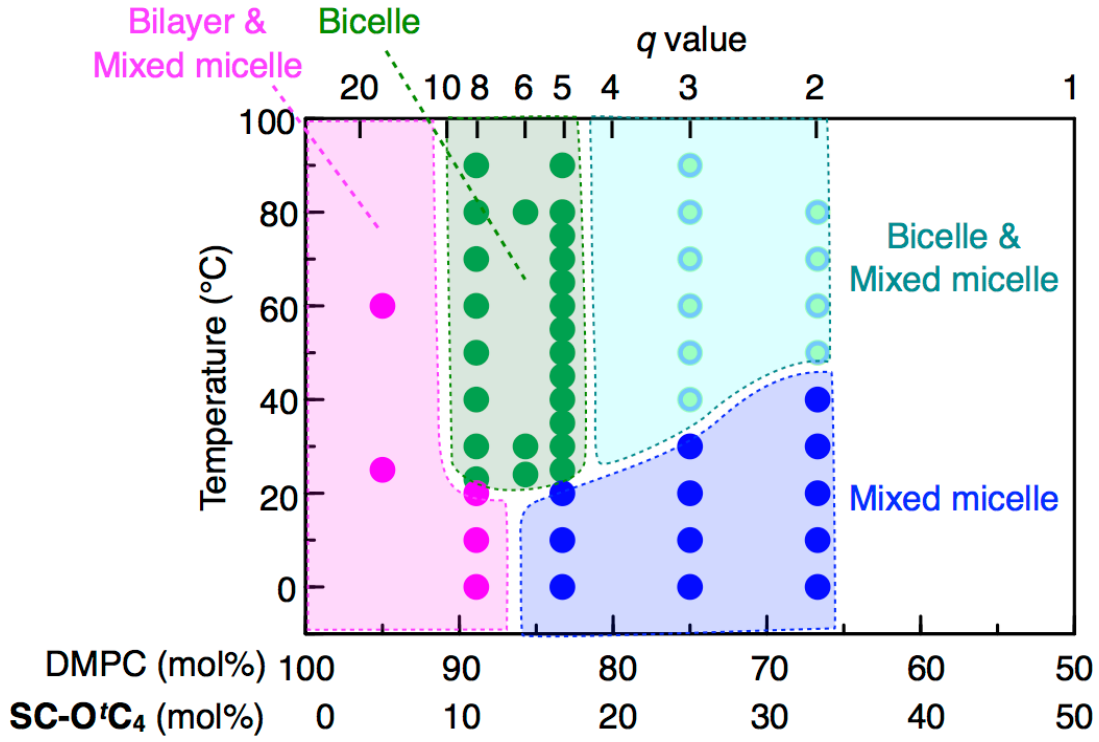

Figure 3. Phase diagram of the bicellar mixtures of DMPC and **SC-O^{t}C$_4$** at various temperatures (from 0 to 90 °C) and DMPC/**SC-O^{t}C$_4$** ratios (from 67:33 to 95:5, mol/mol). Total lipid content (DMPC + surfactant) = 20% w/v. Medium: 100 mM KCl in D_2O.

Alignment-Induction Ability of Bicelles of SC-O^{t}C$_4$ and DMPC

Having prepared novel surfactants with excellent bicelle-forming abilities (**SC-O^{n}C$_4$** and **SC-O^{t}C$_4$**), the author next evaluated their utility and scope by using **SC-O^{t}C$_4$** as a typical representative of the carbamate-endcapped surfactants.

The ^{2}H quadrupole splitting of the solvent signal is a reliable probe for evaluating the ability of bicelles to align surrounding molecules, which is crucial for NMR studies on biomolecules by observing residual dipole couplings (RDC) and chemical-shift anisotropies.[1,16] The ^{2}H quadrupole splitting of common bicellar mixtures is highly temperature dependent, and a satisfactory splitting (>15 Hz) is realized only within a narrow temperature range (e.g., 35–50 °C for a bicellar mixtures of DMPC and DHPC).[17]

When a mixture of **SC** and DMPC was heated from 25 °C to 60 °C, splitting emerged at 30 °C and enlarged with increasing temperature up to 50 °C, but then fell drastically to a zero value between 55 and 60 °C (Figure 4a). In sharp contrast, a bicellar mixture of **SC-O^{t}C$_4$** and DMPC showed a 15-Hz splitting even at 25 °C. Moreover, this splitting increased up to 71 Hz as the temperature was raised to 90 °C (Figure 4b). Thus, the bicellar mixture containing **SC-O^{t}C$_4$** serves as a useful alignable medium from 25 to >90 °C, which implies that it is potentially useful for investigating the structure and dynamics of various proteins, from thermally unstable proteins to thermophilic proteins, at their biologically relevant temperatures. To the best of the author's knowledge, the splitting value of 71 Hz is the largest reported ^{2}H quadrupole splitting of the D_2O signal induced by bicelles.

Upon extensive dilution, bicelles generally lose their alignment ability or they become incapable of maintaining the bicellar phase. However, the alignment-induction ability of the **SC-O^{t}C$_4$**-based bicelles was so excellent that meaningful ^{2}H quadrupole splitting was realized even when the bicellar mixture was diluted up to a D_2O content of 95% (Figure 4c and 4d). Such tolerance toward dilution is particularly useful in RDC measurements on proteins in solutions.

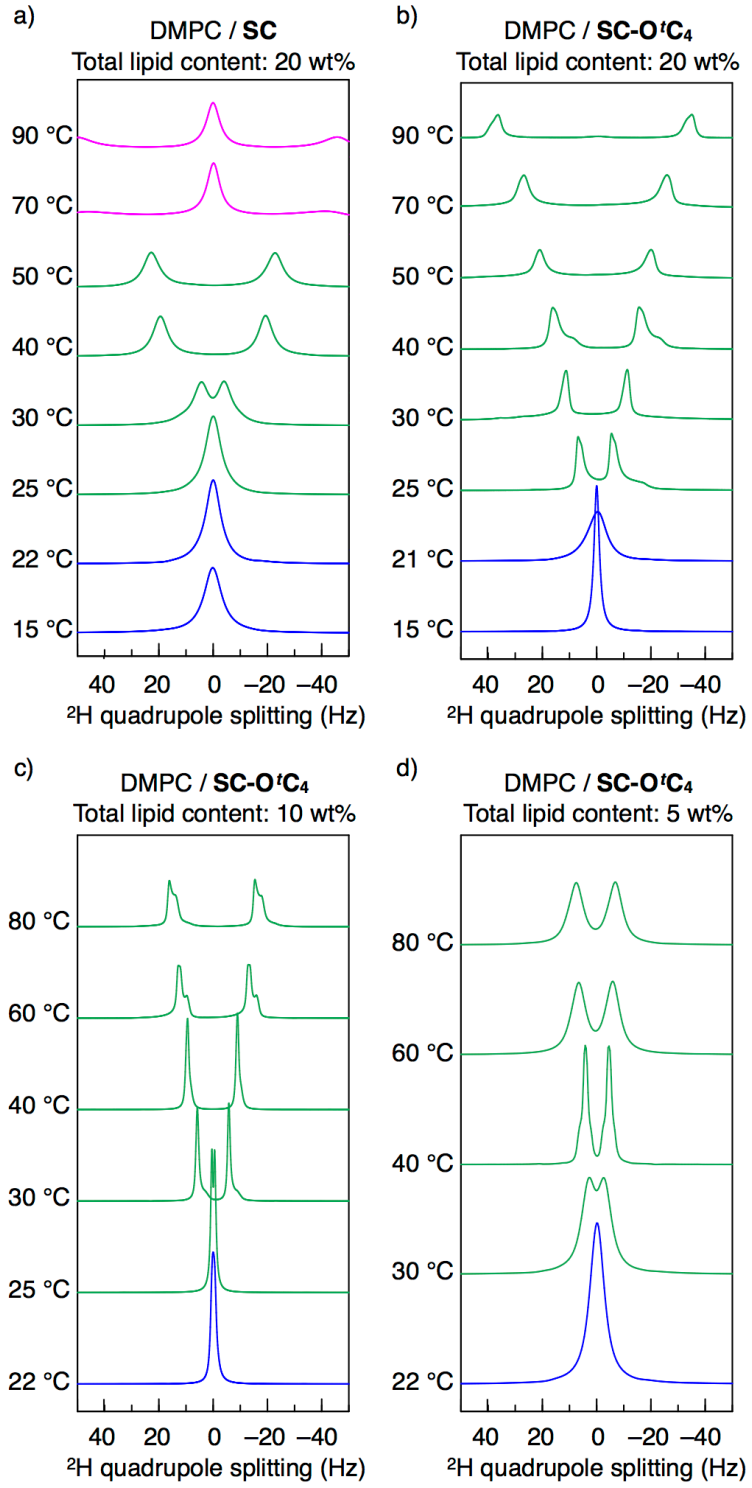

Figure 4. Variable-temperature ^{2}H quadrupole splitting of the bicellar mixtures of DMPC with a) **SC** and b–d) **SC-O^{t}C$_4$**. Total lipid content (DMPC + surfactant) = a) 20%, b) 20%, c) 10%, and d) 5% w/v. DMPC/surfactant = 83:17 (mol/mol). Medium: 100 mM KCl in D_2O.

Scope of SC-O′C_4 as a Bicelle-Forming Surfactant with Various Phospholipids

In the studies discussed above, DMPC was always used as the phospholipid component of the bicellar mixtures. The author therefore investigated the scope of **SC-O′C_4** as a bicelle-forming surfactant with various phospholipids.

To expand the thermal range of magnetically alignable phase, the author used 1,2-dilauroyl-*sn*-glycero-3-phosphatidylcholine (DLPC), which contains 11 carbons in the saturated acyl chains (Figure 1a) instead of DMPC, which has 13 carbons in its saturated acyl chains (Figure 1a). The gel-to-fluid transition temperature of DLPC (–1 °C) is notably lower than that of DMPC (24 °C), which is advantageous in terms of the formation of a magnetically alignable phase at low temperatures. When **SC-O′C_4** was mixed with DLPC, the bicellar mixture exhibited a magnetically alignable phase from 0 to 90 °C (Figure 5a). To the best of the author's knowledge, this is the third reported example of bicellar mixtures that form alignable phases over the entire temperature range of liquid water.[6]

The author also examined 1-palmitoyl-2-oleoyl-*sn*-glycero-3-phosphatidyl-choline (POPC) as a phospholipid component for forming bicelles. POPC has 16 carbon atoms in saturated acyl chain and 18 carbons in the unsaturated acyl chain (Figure 1a). Various mixed membranes composed of saturated phospholipids and POPC are found in nature. In these membranes, POPC, which has a moiety with a *cis*-configuration and, consequently, a low packing efficiency, ensures the fluidity of the system and lowers the gel-to-fluid transition temperature. Although studies on these biomimetic mixed membranes are of particular importance, such mixed membranes have rarely been used in forming bicelles; only one example involving the use of DMPC/POPC as a mixed membrane and DHPC as a surfactant has been reported.[18] This system showed a magnetically alignable phase only within a narrow temperature range (10 to 15 °C). However, when **SC-O′C_4** was used as a surfactant for a 50:50 molar mixture of DMPC and POPC, an alignable phase was observed over an extended temperature range up to room temperature (10–25 °C; Figure 5c and 5d). Furthermore, temperature range of the alignable phase could be readily tuned by changing the phospholipid composition (Figure 5e). For example, when the molar ratio of DMPC/POPC was 30:70, the lower temperature limit of the alignable phase became 1 °C.

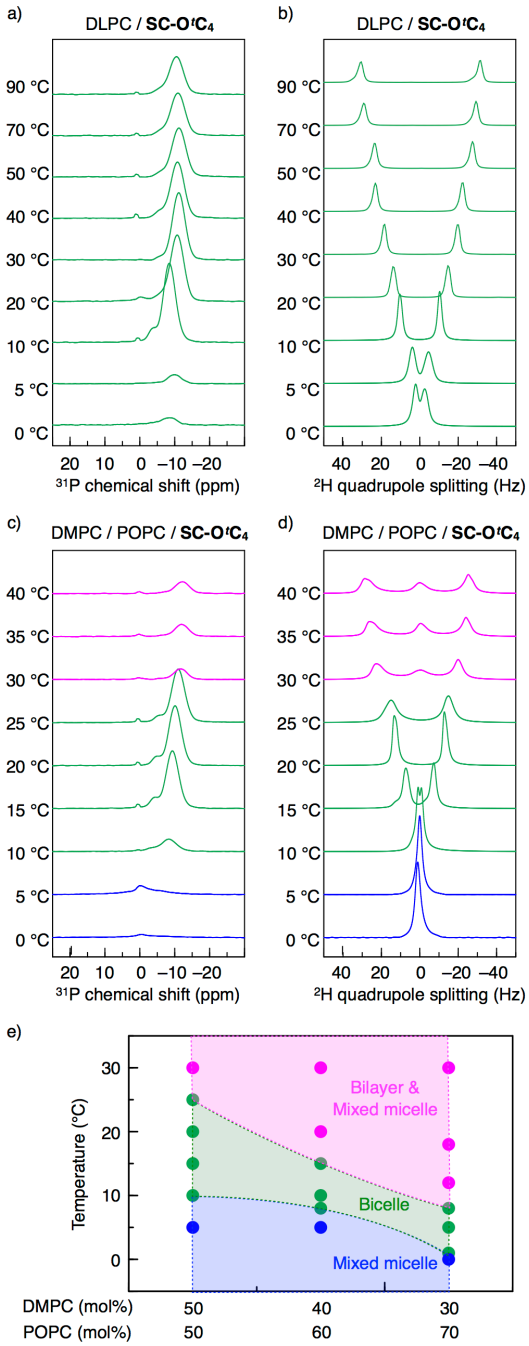

Figure 5. Variable-temperature NMR spectra of the bicellar mixtures. a, b) DLPC and **SC-O'C4**. c, d) DMPC, POPC, and **SC-O'C4**. Total lipid content (phospholipid + surfactant) = 20 wt%. Medium: D_2O containing 100 mM KCl. ^{31}P NMR spectra with a ^{1}H decoupling of 6 kHz (a, c) and ^{2}H quadrupole splitting (b, d) were measured. e) Phase diagram of the bicellar mixtures of DMPC, POPC, and **SC-O'C4** with various temperatures and DMPC/POPC ratios.

Conclusions

The author succeeded in developing novel surfactants (**SC-O^{n}C$_4$** and **SC-O^{t}C$_4$**) that are capable of forming unprecedentedly stable bicelles. These surfactants were derived from sodium cholate (**SC**) by modifying its three hydroxy groups with triethylene glycol chains endcapped with a carbamate group. The important achievements of this work are as follows.

(i) **SC-O^{t}C$_4$** affords magnetically alignable bicelles over an unprecedentedly wide range of conditions of temperature, lipid/surfactant ratio, total lipid content, and lipid type.

(ii) **SC-O^{t}C$_4$**, in conjunction with DLPC, affords bicelles that are magnetically alignable over the whole temperature region of liquid water.

(iii) **SC-O^{t}C$_4$**, in conjunction with DMPC and POPC, affords the first biomimetic bicelles that can exist at room temperature.

(iv) **SC-O^{t}C$_4$** affords bicelles that show an excellent ability to align surrounding molecules, as established by the largest ^{2}H quadruple splitting (71 Hz) ever reported for bicelles.

(v) A simple guideline is revealed for the molecular design of **SC**-based surfactants that can realize the above features. Carbamate endcapping is essential. Even subtle modifications of the carbamates, such as replacement with similar amides (**SC-^{n}C$_4$** and **SC-^{n}C$_5$**), produces critically unfavorable effects.

These achievements not only expand the range of possibilities for bicelles, but also lead to rational design of bicelles with desired structures and properties, as well as permitting the introduction of functional groups on the rims of bicelles.

Experinmental Section

1. Materials and General Methods

All the reagents and chemicals used were obtained from commercial sources and used as received, unless otherwise noted. Dichloromethane (CH_2Cl_2) and diethyl ether (Et_2O) were dried by activated alumina column in an Innovative Technology, Inc., PureSolv system. 1,2-Dimyristoyl-*sn*-glycero-3-phosphatidylcholine (DMPC) and 1,2-lauroyl-*sn*-glycero-3- phosphatidylcholine (DLPC) were purchased from Wako Chemicals and used as received. 1-Palmitoyl-2-oleoyl-*sn*-glycero-3-phosphatidylcholine (POPC) was purchased from Avanti Polar Lipids and used as received. Butyl 2-[2-(2-aminoethoxy)ethoxy] ethylcarbamate (**H_2N-TEG-O^{t}C$_4$**),[19] and *N*-{2-[2-(2-aminoethoxy)ethoxy]ethyl}acetamide (**H_2N-TEG-C$_1$**)[20] were prepared from a diamine derived from triethylene glycol, 2-[2-(2-aminoethoxy)ethoxy]ethylamine (**H_2N-TEG-NH_2**), according to literature (Scheme S1). Benzyl cholate (**2**)[21] was prepared from cholic acid (**1**) according to literature (Scheme S2).

Solution state ^1H, ^2H, ^{13}C, and ^{31}P NMR spectra were recorded on a JEOL model EXcalibur 500 or ECA-500 spectrometer, operating at 500, 75, 125, and 202 MHz, respectively. Chemical shifts are given with respect to an internal (^1H and ^{13}C, tetramethylsilane) or external (^{31}P, 85% aqueous H_3PO_4) standard. For ^{31}P NMR measurement, WALTZ proton decoupling was used during a signal acquisition, with the proton decoupler field strength of 6.0 kHz, 90° pulse width of 9.8 μs, and recycle delay of 2.0 s (Figures 2 and 5). For ^{31}P NMR experiment with high power two-pulse phase modulation (TPPM) proton decoupling,[22] a Bruker Avance III 600 spectrometer operating at 242.9 MHz was used, with the proton decoupling field strength of 70.0 kHz, 30° pulse width of 2.6 μs, and recycle delay of 15 s (Figure S2). To the FID data of ^{31}P NMR thus obtained, an exponential line broadening of 50 Hz was applied prior to Fourier transformation. Matrix-assisted laser desorption ionization time-of-flight (MALDI-TOF) mass spectrometry was performed in the reflector mode on a Brucker model autoflex TM speed spectrometer using α-cyano-4-hydroxycinnamic acid or dithranol as a matrix.

2. Synthesis of Side Chain Units with an Amide or Carbamate Terminus

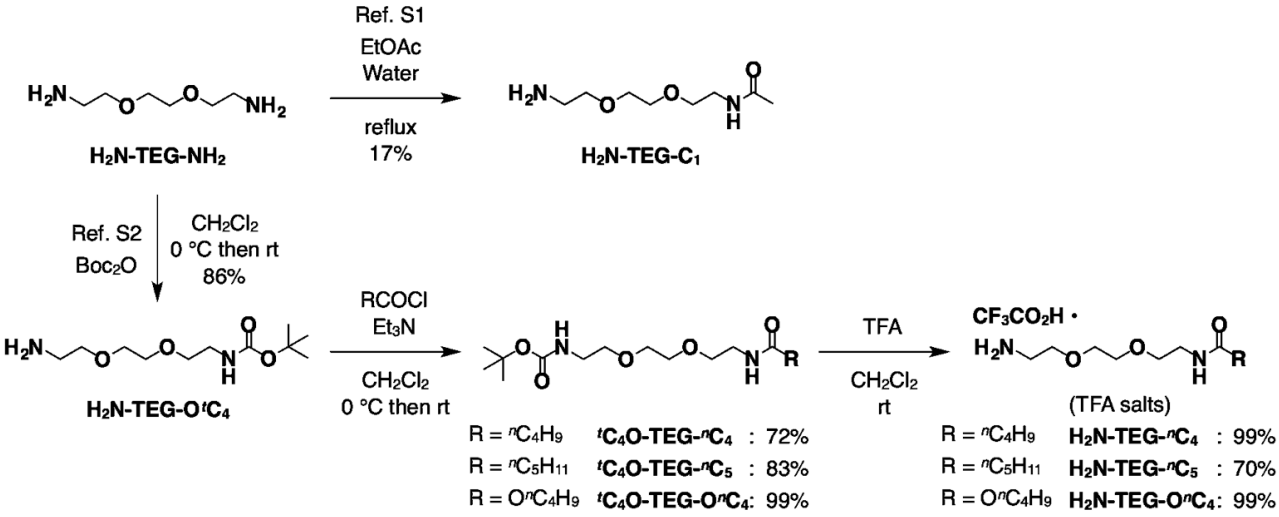

Scheme S1. Synthesis of Side Chain Units with an Amide or Carbamate Terminus

^{t}C$_4$O-TEG-^{n}C$_4$:

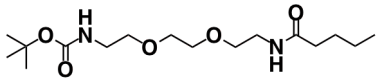

To a CH_2Cl_2 solution (20 mL) of **H$_2$N-TEG-O^{t}C$_4$** (2.00 g, 8.05 mmol) and NEt_3 (1.50 mL, 10.8 mmol) was added pentanoyl chloride (1.20 g, 9.95 mmol) dropwise at 0 °C. After being stirred at room temperature for 14 h, the reaction mixture was diluted with CH_2Cl_2 (30 mL), successively washed with water (3 × 30 mL) and brine (30 mL), dried over Na_2SO_4, and concentrated to dryness under reduced pressure. The resultant residue was subjected to silica gel column chromatography eluted with EtOAc to give **^{t}C$_4$O-TEG-^{n}C$_4$** as colorless oil (1.94 g, 5.83 mmol, 72%).

^{1}H NMR ($CDCl_3$): δ 0.88 (t, 3H, J = 6.9 Hz), 1.30 (m, 2H), 1.44 (s, 9H), 1.63 (m, 2H), 2.17 (t, 2H, J = 7.4 Hz), 3.32 (m, 2H), 3.45 (m, 2H), 3.55 (4H, t, J = 5.0 Hz), 3.60 (m, 4H), 4.99 (s, 1H), 5.99 (s, 1H).

^{13}C NMR ($CDCl_3$): δ 13.9, 22.5, 27.9, 28.45, 28.49, 36.6, 39.2, 40.4, 70.1, 70.2, 70.3, 79.5, 156.0, 173.3.

MALDI-TOF MS: *m/z* calcd. for $C_{16}H_{32}N_2NaO_5$ ([M + Na]$^+$) 355.2209, found 355.2655.

^{t}C$_4$O-TEG-^{n}C$_5$:

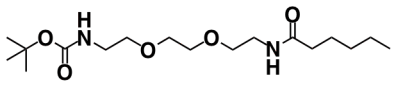

The title compound was synthesized from **H$_2$N-TEG-O^{t}C$_4$** in the same procedure, using

hexanoyl chloride in place of pentanoyl chloride (colorless oil, 83%).

^{1}H NMR ($CDCl_3$): δ 0.86 (t, 3H, J = 6.9 Hz), 1.30 (m, 2H), 1.43 (s, 9H), 1.62 (m, 2H), 1.76 (m, 2H), 2.16 (t, 2H, J = 7.5 Hz), 3.32 (m, 2H), 3.45 (m, 2H), 3.54 (4H, t, J = 5.0 Hz), 3.60 (m, 4H), 4.99 (s, 1H), 5.99 (s, 1H).

^{13}C NMR ($CDCl_3$): δ 14.0, 22.5, 25.5, 28.5, 31.5, 36.8, 39.2, 40.4, 70.1, 70.2, 70.3, 79.4, 156.0, 173.3.

MALDI-TOF MS: *m/z* calcd. for $C_{17}H_{34}N_2NaO_5$([M + Na]$^+$) 369.2365, found 369.2491.

^{t}C$_4$O-TEG-O^{n}C$_4$

The title compound was synthesized from **H$_2$N-TEG-O^{t}C$_4$** in the same procedure, using butyl chloroformate in place of pentanoyl chloride (colorless oil, 99%).

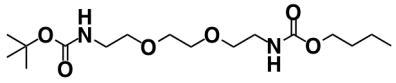

^{1}H NMR ($CDCl_3$): δ 0.93 (t, 3H, J = 7.5 Hz), 1.36 (m, 2H), 1.45 (s, 9H), 1.59 (m, 2H), 3.33 (m, 2H), 3.38 (m, 2H), 3.56 (m, 4H), 3.61 (m, 4H), 4.06 (t, 2H, J = 7.0 Hz), 5.06 (s, 1H), 5.21 (s, 1H).

^{13}C NMR ($CDCl_3$): δ 13.8, 19.1, 28.4, 31.1, 40.3, 40.8, 64.8, 70.2, 70.3, 79.3, 156.0, 156.8.

MALDI-TOF MS: *m/z* calcd. for $C_{16}H_{32}N_2NaO_6$ ([M + Na]$^+$) 371.2158, found 371.1628.

H$_2$N-TEG-^{n}C$_4$:

To a CH_2Cl_2 solution (10 mL) of **^{t}C$_4$O-TEG-^{n}C$_4$** (1.47 g, 4.43 mmol) was added trifluoroacetic acid (TFA, 2 mL) at room temperature. The mixture was stirred for 12 h and then concentrated to dryness under reduced pressure to give the TFA salt of **H$_2$N-TEG-^{n}C$_4$** as colorless oil (1.53 g, 4.42 mmol, quant).

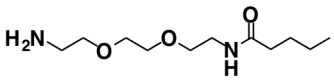

^{1}H NMR ($CDCl_3$): δ 0.89(t, 3H, J = 7.2 Hz), 1.32 (m, 2H), 1.56 (m, 2H), 2.25 (t, 2H, J = 7.4 Hz), 3.20 (2H, m), 3.45 (2H,m), 3.56–3.68 (4H, overlapped), 3.74 (m, 4H), 6.91 (s, 1H), 7.78 (s, 2H).

^{13}C NMR ($CDCl_3$): δ 13.5, 22.2, 27.9, 35.9, 39.7, 39.9, 66.5, 69.7, 70.1, 70.2, 114.6, 116.8, 160.9, 176.7.

MALDI-TOF MS: *m/z* calcd. for $C_{11}H_{24}N_2NaO_3$ ([M + Na]$^+$) 255.1685, found 255.1584.

H_2N-TEG-$^nC_5$:

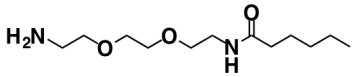

The TFA salt of the title compound was synthesized in the same procedure to the TFA salt of **H_2N-TEG-$^nC_4$**, using from **^tC_4O-TEG-$^nC_5$** in place of **^tC_4O-TEG-$^nC_4$** (colorless oil, quant).

^{1}H NMR ($CDCl_3$): δ 0.87 (t, 3H, J = 7.0 Hz), 1.20–1.36 (overlapped, 6H), 1.59 (m, 2H), 2.25 (t, 2H, J = 7.5 Hz), 3.22 (2H, m), 3.48 (2H,m), 3.56–3.72 (overlapped, 4H), 3.76 (m, 4H), 6.80 (s, 1H), 7.69 (s, 2H).

^{13}C NMR ($CDCl_3$): δ 13.5, 22.2, 25.7, 31.2, 35.9, 39.7, 39.9, 66.4, 69.7, 70.0, 70.2, 114.3, 116.7, 160.9, 177.3.

MALDI-TOF MS: *m/z* calcd. for $C_{12}H_{26}N_2NaO_3$ ($[M + Na]^+$) 269.1841, found 269.1894.

H_2N-TEG-O$^nC_4$:

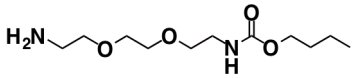

The TFA salt of the title compound was synthesized in the same procedure to the TFA salt of **H_2N-TEG-$^nC_4$**, using from **^tC_4O-TEG-O$^nC_4$** in place of **^tC_4O-TEG-$^nC_4$** (colorless oil, quant).

^{1}H NMR ($CDCl_3$): δ 0.93 (t, 3H, J = 7.5 Hz), 1.36 (m, 2H), 1.58 (m, 2H), 3.20 (m, 2H), 3.34 (m, 2H), 3.56 (t, 4H, J = 5.5Hz), 3.63 (m, 2H), 3.75 (m, 2H), 4.04 (m, 2H), 7.94 (s, 2H).

^{13}C NMR ($CDCl_3$): δ 13.6, 19.0, 30.9, 39.7, 66.5, 70.1, 114.6, 116.8, 161.1, 161.4.

MALDI-TOF MS: *m/z* calcd. for $C_{11}H_{24}N_2NaO_4$ ($[M + Na]^+$) 271.1634, found 271.1403.

3. Synthesis of Cholate-based Surfactants

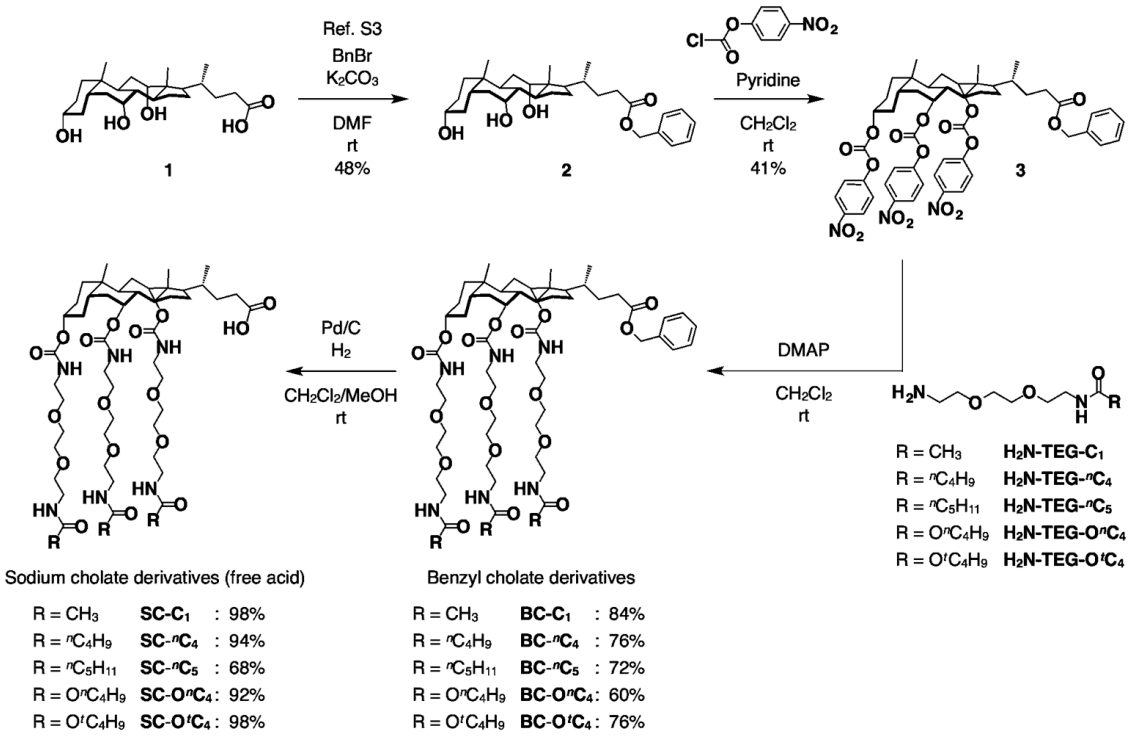

Scheme S2. Synthesis of cholate-based surfactants.

Compound 3:

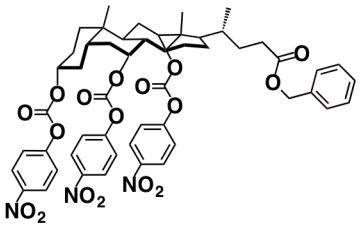

To a CH_2Cl_2 solution (100 mL) of benzyl cholate[S3] (**2**, 5.00 g, 10.0 mmol) and 4-nitrophenyl chloroformate (10.0 g, 49.6 mmol) was added pyridine (20 mL, 250 mmol) at room temperature. After being stirred for 16 h, the reaction mixture was diluted with CH_2Cl_2 (200 mL), successively washed with 1 M aqueous $NaHSO_4$ (3 × 150 mL) and brine (100 mL), dried over Na_2SO_4, and concentrated to dryness under reduced pressure. The resultant residue was subjected to silica gel column chromatography eluted with dichloromethane to give **3** as a white solid (4.08 g, 4.10 mmol, 41%).

^{1}H NMR ($CDCl_3$): δ 0.78 (s, 3H), 0.93 (d, 3H, J = 6.1 Hz), 0.99 (s, 3H), 1.0–2.48 (overlapped, 24H), 4.60 (m, 1H), 4.96 (m, 1H), 5.10 (d, 2H, J = 4.6 Hz), 5.14 (m, 1H), 7.30–7.38 (m, 5H), 7.39–7.45 (d + d + d, overlapped, 2H + 2H + 2H), 8.26–8.35 (d + d + d, overlapped, 2H + 2H + 2H).

^{13}C NMR ($CDCl_3$): δ 12.2, 17.7, 22.2, 22.9, 25.4, 26.4, 27.0, 28.7, 30.6, 31.2, 31.3, 34.0, 34.3, 34.5, 38.0, 40.4, 43.0, 45.4, 47.6, 66.3, 79.2, 81.2, 121.7, 121.9, 122.0,

125.3, 125.4, 128.3, 128.6, 135.9, 145.4, 145.5, 151.4, 151.8, 151.9, 155.4, 155.47, 155.53, 173.6.

MALDI-TOF MS: *m/z* calcd. for $C_{52}H_{55}N_3NaO_{17}$ ($[M + Na]^+$) 1016.3429, found. 1016.3283.

BC-C_1:

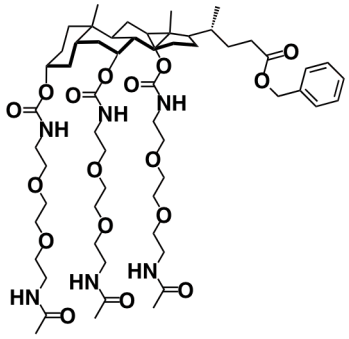

To a CH_2Cl_2 solution (25 mL) of **3** (500 mg, 0.50 mmol) and **H_2N-TEG-C_1** (486 mg 2.48 mmol) was added DMAP (304 mg, 2.48 mmol) at room temperature. After being stirred for 24 h, the reaction mixture was diluted with CH_2Cl_2 (25 mL), successively washed with water (6 × 50 mL) and brine (50 mL), dried over Na_2SO_4, and concentrated to dryness under reduced pressure. The resultant residue was subjected to silica gel column chromatography eluted with $CHCl_3$/MeOH (30:1 to 10:1, v/v) to give **BC-C_1** as a white solid (479 mg, 0.42 mmol, 84%).

^{1}H NMR ($CDCl_3$): δ 0.70 (s, 3H), 0.86 (s, 3H), 0.91 (d, 3H, J = 6.1 Hz), 1.02–2.41 (overlapped, 33H), 3.34–3.62 (overlapped, 36H), 4.48 (m, 1H), 4.81 (m, 1H), 4.96 (m, 1H), 5.11 (s, 2H, J = 4.6 Hz), 5.60–5.72 (s + s + s, overlapped, 1H + 1H +1H), 6.40–6.52 (s + s + s, overlapped, 1H + 1H +1H), 7.30–7.38 (m, 5H).

^{13}C NMR ($CDCl_3$): δ 12.3, 17.4, 18.4, 22.5, 23.1, 23.2, 27.2, 28.9, 30.8, 30.9, 31.2, 31.5, 34.2, 34.6, 35.0, 37.8, 39.2, 39.3, 40.6, 40.7, 40.8, 43.5, 45.3, 47.4, 58.3, 66.1, 69.7, 69.8, 70.0, 70.1, 70.2, 70.3, 128.2, 128.5, 136.0, 156.4, 170.5, 173.9.

MALDI-TOF MS: *m/z* calcd. for $C_{58}H_{94}N_6NaO_{17}$ ($[M + Na]^+$) 1169.6573, found 1169.6139.

BC-^{n}C_4:

The title compound was synthesized fin the same method as **BC-C_1**, using **H_2N-TEG-^{n}C_4** in place of **H_2N-TEG-C_1** (colorless viscous oil, 76%).

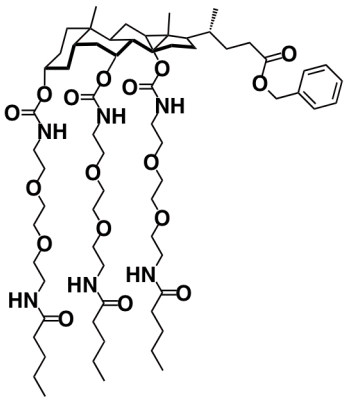

^{1}H NMR ($CDCl_3$): δ 0.69 (s, 3H), 0.84 (d, 3H, J = 6.5 Hz), 0.89–0.92 (overlapped, 12H), 1.01–2.41 (overlapped, 42H), 3.26–3.76 (overlapped, 36H), 4.46 (m, 1H), 4.79 (m, 1H), 4.95 (m, 1H), 5.10 (d, 2H, J = 4.6 Hz), 5.45 (s, 1H), 5.50 (s, 1H), 5.71 (s, 1H), 6.26 (s, 1H,), 6.33 (s, 1H), 6.36 (s, 1H), 7.30–7.38 (m, 5H)

^{13}C NMR ($CDCl_3$): δ 12.4, 13.9, 17.5, 22.5, 22.6, 22.9, 26.1, 27.3, 27.4, 27.9, 29.0, 30.9, 31.3, 31.7, 34.4, 34.7, 35.2, 38.0, 39.2, 40.76, 40.82, 40.9, 41.0, 43.7, 45.4, 47.4, 66.3, 70.1, 70.15, 70.20, 70.3, 70.4, 70.5, 71.40, 74.7, 75.8, 128.3, 128.6, 136.1, 156.4, 173.6, 174.0.

MALDI-TOF MS: *m/z* calcd. for $C_{67}H_{112}N_6NaO_{17}$ ($[M + Na]^+$) 1295.7982, found 1295.8285.

BC-^{n}C$_5$:

The title compound was synthesized in the same method as **BC-C$_1$**, using **H$_2$N-TEG-^{n}C$_5$** in place of **H$_2$N-TEG-C$_1$** (colorless viscous oil, 72%).

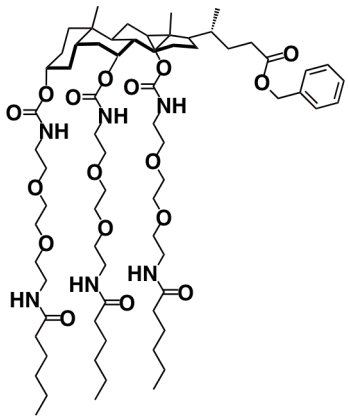

^{1}H NMR ($CDCl_3$): δ 0.69 (s, 3H), 0.80–0.96 (overlapped, 15H), 1.02–2.42 (overlapped, 48H), 3.28–3.76 (overlapped, 36H), 4.47 (m, 1H), 4.79 (m, 1H), 4.95 (m, 1H), 5.10 (d, 2H, J = 4.6 Hz), 5.44 (s, 1H), 5.50 (s, 1H), 5.69 (s, 1H), 6.26 (s, 1H,), 6.34 (s, 1H), 6.36 (s, 1H), 7.30–7.38 (m, 5H).

^{13}C NMR ($CDCl_3$): δ 12.4, 14.1, 17.6, 22.5, 22.6, 22.9, 25.5, 27.3, 27.4, 29.1, 30.9, 31.3, 31.6, 34.4, 34.8, 35.3, 36.7, 38.0, 39.2, 40.9, 41.0, 43.7, 45.4, 47.5, 66.3, 70.07, 70.12, 70.2, 70.35, 70.42, 70.5, 71.4, 74.7, 75.8, 128.3, 128.7, 136.1 156.4,173.6, 174.0.

MALDI-TOF MS: *m/z* calcd. for $C_{70}H_{118}N_6NaO_{17}$ ($[M + Na]^+$) 1337.8451, found 1337.8425.

BC-O^{n}C$_4$:

The title compound was synthesized in the same method as **BC-C$_1$**, using **H$_2$N-TEG-^{n}C$_5$** in place of **H$_2$N-TEG-C$_1$** (colorless viscous oil, 60%).

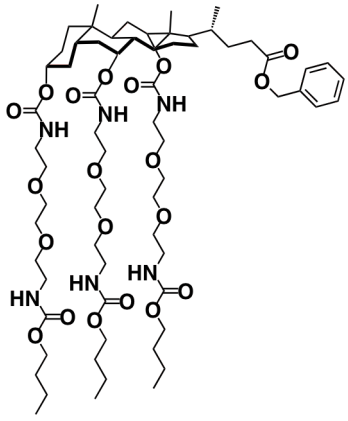

^{1}H NMR ($CDCl_3$): δ 0.69 (s, 3H), 0.80–0.97 (overlapped, 15H), 1.02–2.43 (overlapped, 36H), 3.20-3.76 (overlapped, 36H), 4.06 (t, 6H, J = 6.0 Hz), 4.47 (m, 1H), 4.76 (m, 1H), 4.96 (m, 1H), 5.10 (d, 2H, J = 4.6 Hz), 5.41 (s, 1H), 5.48 (s, 1H), 5.60 (s + s, overlapped, 1H + 1H), 5.72 (s, 1H), 5.91 (s, 1H), 7.29–7.39 (m, 5H)

^{13}C NMR ($CDCl_3$): δ 12.4, 13.8, 17.6, 19.1, 22.7, 22.9, 26.1, 27.3, 27.4, 28.0, 29.0, 30.9, 31.2, 31.4, 31.6, 32.7,

34.3, 34.8, 35.2, 38.0, 40.7, 40.8, 40.9, 41.1, 43.6, 45.4, 47.5, 64.9, 66.2, 70.1, 70.2, 70.3, 70.4, 70.5, 70.6, 71.4, 74.6, 75.6, 79.9, 128.3, 128.4, 128.6, 136.1, 156.5, 157.0, 174.0.

MALDI-TOF MS: *m/z* calcd. for $C_{67}H_{112}N_6NaO_{20}$ ($[M + Na]^+$) 1343.7829, found 1343.8143.

BC-O^{t}C$_4$:

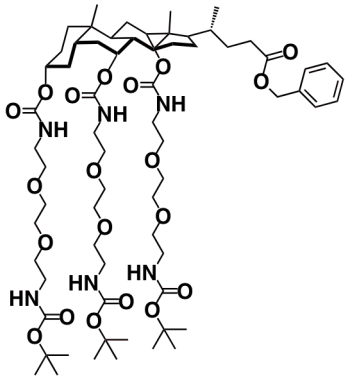

The title compound was synthesized in the same method as **BC-C$_1$**, using **H$_2$N-TEG-O^{t}C$_4$** in place of **H$_2$N-TEG-C$_1$** (white solid, 76%).

^{1}H NMR ($CDCl_3$): δ 0.69 (s, 3H), 0.85 (d, 3H, J = 6.1 Hz), 0.90(s, 3H), 1.02–2.41 (overlapped, 51H), 3.34–3.60 (overlapped, 36H), 4.48 (m, 1H), 4.73 (m, 1H), 4.96 (m, 1H), 5.10 (d, 2H, J = 4.6 Hz), 5.20–5.32 (s + s, overlapped, 2H), 5.47 (s, 1H), 5.60 (s, 1H), 5.66 (s, 1H), 6.00 (s, 1H), 7.30–7.38 (m, 5H).

^{13}C NMR ($CDCl_3$): δ 12.5, 17.3, 18.6, 22.5, 23.1, 26.5, 26.9, 27.4, 28.1, 28.3, 30.9, 32.6, 34.3, 34.6, 34.9, 35.1, 35.6, 39.6, 40.5, 41.1, 41.8, 46.5, 47.2, 68.2, 69.6, 69.8, 70.1, 72.9, 74.5, 77.2, 79.9, 127.9, 128.0, 128.2, 135.8, 155.7, 155.8, 156.0, 156.1, 156.2, 173.7.

MALDI-TOF MS: *m/z* calcd. for $C_{67}H_{112}NaN_6O_{20}$ ($[M + Na]^+$) 1343.7829, found 1343.9523.

SC-C$_1$:

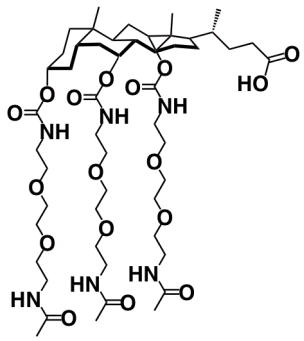

A solution of **BC-C$_1$** (182 mg, 0.16 mmol) in CH_2Cl_2/MeOH (50:50, v/v, 20 mL) was degassed and purged with N_2. To the mixture was added Pd/C (10 wt%, 30 mg) at room temperature under N_2 atmosphere. The mixture was degassed, purged with H_2, and stirred at room temperature 12 h. From the resultant mixture, the catalyst was filtered off through celite. The filtrate was concentrated to dryness under reduced pressure to give the free acid of **SC-C$_1$** as a white solid (164 mg, 0.16 mmol, 98%).

^{1}H NMR ($CDCl_3$): δ 0.73 (s, 3H), 0.85–0.95 (overlapped, 3H + 3H), 1.02–2.40 (overlapped, 33H), 3.30–3.79 (overlapped, 36H), 4.48 (m, 1H), 4.80 (m, 1H), 4.95 (m, 1H), 5.40–5.95 (s + s + s, overlapped, 1H + 1H + 1H), 6.53–7.00 (s + s + s, overlapped, 1H + 1H + 1H).
^{13}C NMR ($CDCl_3$): δ 12.1, 14.0, 17.4, 22.4, 22.9, 23.2, 25.9, 27.3, 28.9, 29.6, 30.5, 30.7, 31.5, 34.2, 34.6, 35.0, 37.9, 39.3, 40.7, 40.8, 43.6, 45.3, 46.7, 69.7, 70.1, 70.2, 71.3, 74.5, 75.7, 156.4, 170.7, 170.9, 176.8.
MALDI-TOF MS: *m/z* calcd. for $C_{51}H_{88}N_6NaO_{17}$ ($[M + Na]^+$) 1079.6104, found 1079.6591.

SC-^{n}C$_4$:

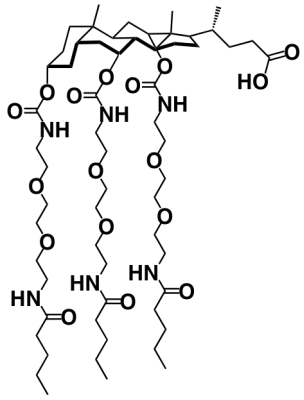

The free acid of the title compound was synthesized in the same method as **CA-C$_1$**, using **BC-^{n}C$_4$** in place of **BC-C$_1$** (white solid, 94%).
^{1}H NMR ($CDCl_3$): δ 0.72 (s, 3H), 0.86–0.94 (overlapped, 15H), 1.01–2.36 (overlapped, 42H), 3.23–3.72 (overlapped, 36H), 4.46 (m, 1H), 4.79 (m, 1H), 4.91 (m, 1H), 5.37–5.50 (s + s, overlapped, 1H + 1H), 5.77 (s, 1H), 6.26 (s, 1H,), 6.38–6.52 (s + s, overlapped, 1H + 1H).
^{13}C-NMR ($CDCl_3$): δ 12.3, 13.9, 17.5, 22.5, 22.6, 22.9, 26.1, 27.4, 27.9, 29.1, 30.5, 30.8, 31.7, 34.4, 34.7, 35.2, 36.4, 37.9, 39.2, 39.26, 39.32, 40.78, 40.80, 40.9, 41.0, 43.7, 45.4, 46.8, 66.3, 70.0, 70.1, 70.2, 70.3, 70.4, 70.5, 71.5, 74.7, 75.9, 156.4, 156.6, 173.7, 174.0, 177.0.
MALDI-TOF MS: *m/z* calcd. for $C_{60}H_{106}N_6NaO_{17}$ ($[M + Na]^+$) 1205.7512, found 1205.7971.

SC-^{n}C$_5$:

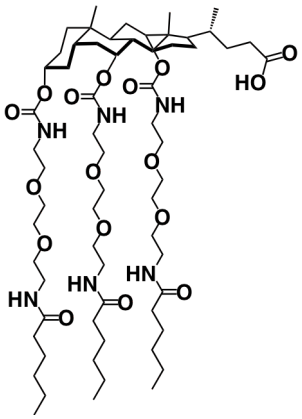

The free acid of the title compound was synthesized in the same method as **CA-C$_1$**, using **BC-^{n}C$_5$** in place of **BC-C$_1$** (colorless viscous oil, 68%).
^{1}H NMR ($CDCl_3$): δ 0.73 (s, 3H), 0.84–0.97 (overlapped, 15H), 1.01–2.39 (overlapped, 48H), 3.24–3.76 (overlapped, 36H), 4.48 (m, 1H), 4.80 (m, 1H), 4.92 (m, 1H), 5.38–5.54 (s + s, overlapped, 1H + 1H), 5.77 (s, 1H), 6.28 (s, 1H), 6.40–6.55 (s + s, overlapped, 1H + 1H).
^{13}C NMR ($CDCl_3$): δ 12.3, 14.1, 17.5, 22.5, 22.6, 22.9,

25.5, 26.1, 27.4, 29.1, 29.8, 30.5, 30.8, 31.6, 31.7, 34.4, 34.7, 35.2, 36.7, 37.9, 39.26, 39.33, 40.5, 40.8, 40.90, 40.93, 41.0, 43.7, 45.4, 46.7, 70.05, 70.13, 70.2, 70.3, 70.4, 70.5, 71.5, 74.7, 75.9, 156.4, 156.6, 173.8, 174.0, 177.0.

MALDI-TOF MS: *m/z* calcd. for $C_{63}H_{112}N_6NaO_{17}$ ($[M + Na]^+$) 1247.7982, found 1247.8519.

SC-O^{n}C$_4$:

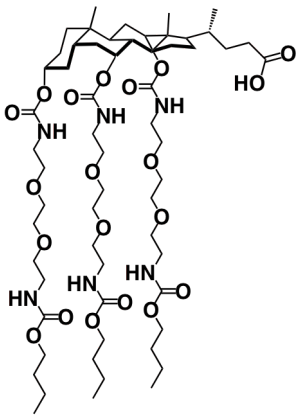

The free acid of the title compound was synthesized in the same method as **CA-C$_1$**, using **BC-^{n}C$_5$** in place of **BC-C$_1$** (white solid, 92%).

^{1}H NMR ($CDCl_3$): δ 0.73 (s, 3H), 0.85–0.97 (overlapped, 15H), 0.98–2.40 (overlapped, 36H) 3.28–3.76 (overlapped, 36H), 4.06 (m, 6H), 4.47 (m, 1H), 4.76 (m, 1H), 4.96 (m, 1H), 5.41 (s, 1H), 5.54 (s, 1H), 5.57 (s, 1H), 5.63 (s, 1H), 5.71 (s, 1H), 5.92 (s, 1H).

^{13}C NMR ($CDCl_3$): δ. 12.3, 13.8, 17.6, 19.1, 22.6, 22.9, 26.1, 27.4, 28.0, 29.0, 30.8, 31.2, 31.6, 34.3, 34.8, 35.2, 38.0, 40.8, 40.9, 41.0, 43.7, 45.4, 47.1, 64.9, 70.2, 70.4, 70.5, 70.6, 71.4, 75.7, 79.9, 156.5, 157.0, 174.0.

MALDI-TOF MS: *m/z* calcd. for $C_{60}H_{106}NaN_6O_{20}$ ($[M + Na]^+$) 1253.7360, found 1253.7885.

SC-O^{t}C$_4$:

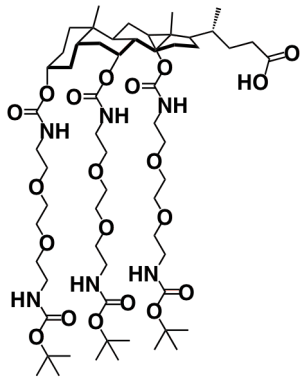

The free acid of the title compound was synthesized in the same method as **CA-C$_1$**, using **BC-O^{t}C$_4$** in place of **BC-C$_1$** (white solid, 98%).

^{1}H NMR ($CDCl_3$): δ 0.72 (s, 3H), 0.85–0.93 (s + d, overlapped, 3H + 3H), 1.02–2.40 (overlapped 51H), 3.30–3.79 (overlapped, 36H), 4.48 (m, 1H), 4.73 (m, 1H), 4.96 (m, 1H), 5.23 (s, 1H), 5.30 (s, 1H), 5.48 (s, 1H), 5.54 (s, 1H), 5.95 (s, 1H), 6.53 (s, 1H).

^{13}C NMR ($CDCl_3$): δ 12.1, 17.3, 22.3, 22.6, 25.7, 27.1, 27.2, 28.2, 28.6, 30.5, 30.6, 31.3, 34.1, 34.5, 34.9, 37.8, 40.1, 40.4, 40.6, 40.7, 41.4, 43.1, 45.0, 46.9, 69.8, 69.9, 70.1, 70.2, 71.1, 74.3, 75.3, 79.0, 79.3, 155.9, 156.1, 156.2, 156.3 177.3.

MALDI-TOF MS: *m/z* calcd. for $C_{60}H_{106}NaN_6O_{20}$ ($[M + Na]^+$) 1253.7360, found 1253.7651.

4. Typical Procedure for Preparation of Bicellar Mixtures

1,2-Dimyristoyl-*sn*-glycero-3-phosphatidylcholine (DMPC: 41.3 mg, 60 μmol) and the free acid of **SC-O^{t}C$_4$** (15.0 mg, 12 μmol) were dissolved in CH_2Cl_2 (1.0 mL). The solution was concentrated to dryness under reduced pressure and further dried under reduced pressure (*ca.* 1 mmHg) for 1 h at room temperature. To the resultant residue were successively added a D_2O solution (200 μL) of KCl (100 mM) and a D_2O solution (10 μL) of NaOH (1.25 M). The mixture was heated up to 70 °C, vortexed, cooled to 0 °C, and then vortexed. The heat–cool cycle was repeated at least three times until clear homogeneous solution was obtained.

Other bicellar mixtures were prepared in the same procedure, with varying surfactants, lipid, lipid/surfactant ratio and/or total lipid content.

5. Phase Behavior of a Bicellar Mixture of a Phospholipid and SC

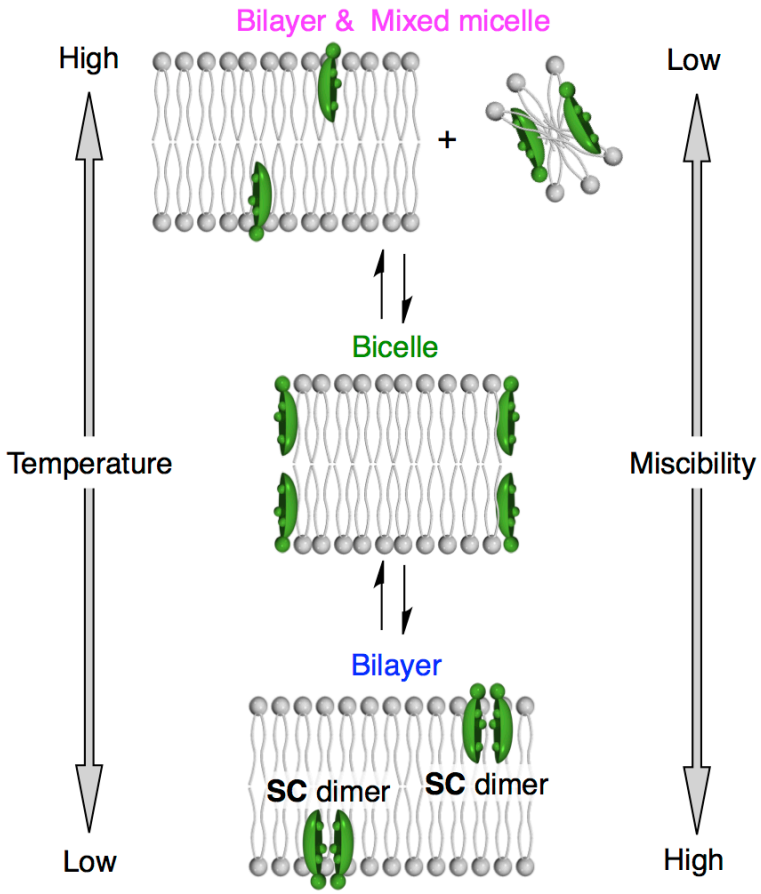

Figure S1. Schematic representation for the phase behavior of a bicellar mixture composed of a phospholipid and **SC**. Because of the dimer-formation nature characteristic of **SC**, phase behavior of this mixture at a low-temperature region is different from that of the SC-based surfactants bearing triethylene glycol chains at their hydrophilic side (Figure 1c in the main text).

6. ^{31}P NMR Spectra of a Bicellar Mixture with High ^{1}H Decoupling Power

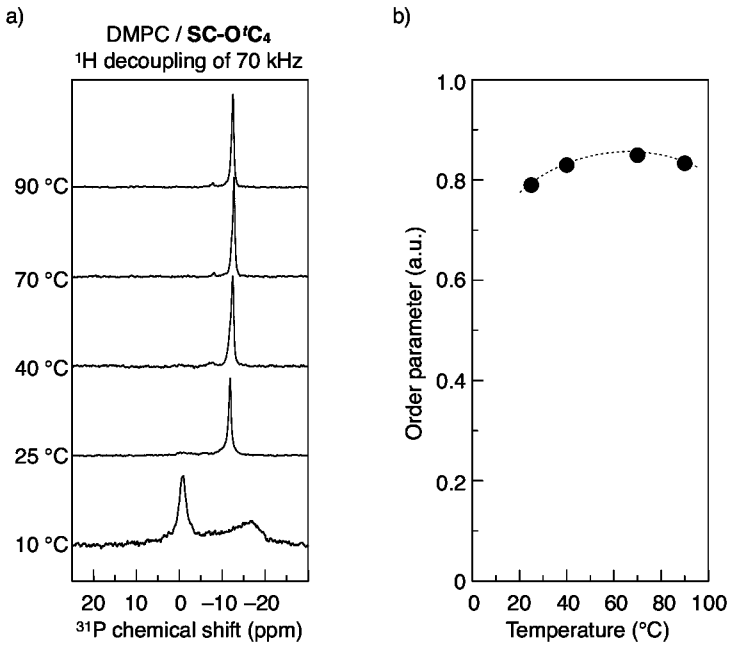

Figure S2. a) Variable temperature ^{31}P NMR spectra with a ^{1}H decoupling of 70 kHz for a bicellar mixture of DMPC and **SC-O^{t}C$_4$**. DMPC/**SC-O^{t}C$_4$** = 83:17 (mol/mol). Total lipid content (= DMPC + **SC-O^{t}C$_4$**) = 20% w/v. Medium: 100 mM KCl in D_2O. b) Temperature-dependent changes in order parameter of the bicellar mixture of a). The order parameter of the bicellar mixture ($S_{bicelle}$) was estimated as $S_{bicelle} = (\delta_{obs} - \delta_{iso}) / (\delta_{\perp} - \delta_{iso})$: δ_{obs} = chemical shit of the peak top in a). δ_{iso} = isotropic chemical shift (= 0 ppm). $\delta_{\perp}$ = perpendicular-edge chemical shift of the ^{31}P chemical-shift-anisotropy powder-pattern spectrum of unaligned DMPC in the liquid-crystalline phase (= 15 ppm).[15b]

7. Temporal Changes of the ^{31}P NMR Spectra of Bicellar Mixtures

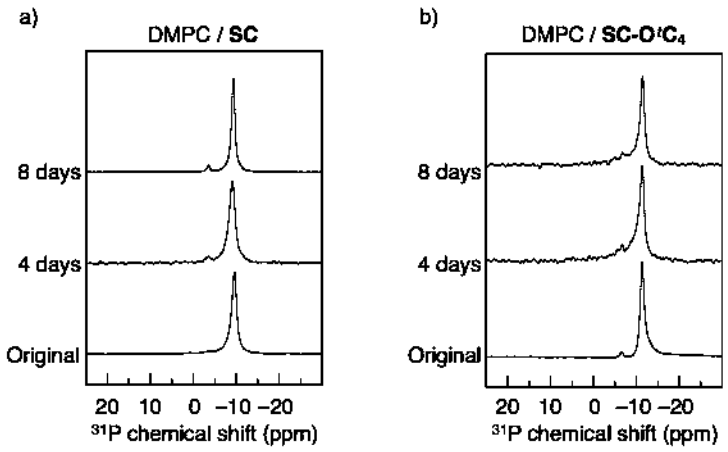

Figure S3. ^{31}P NMR spectra with a ^{1}H decoupling of 6 kHz for bicellar mixtures of DMPC with a) **SC** and b) **SC-O^{t}C$_4$**. DMPC/surfactant = 83:17 (mol/mol). Total lipid content (DMPC + surfactant) = 20% w/v. Medium = 100 mM KCl in D_2O. Measurement temperature = 40 °C. The ^{31}P NMR spectra were measured immediately after the preparation of bicelles (lower) and after being kept at 40 °C for 4 days (mid) and 8 days (upper).

Reference

[1] a) Sanders, C. R.; Prosser, R. S. *Structure* **1998**, *6*, 1227–1234. b) Marcotte, I.; Auger, M. L.; *Concepts Magn. Reson.* **2005**, *24A*, 17–37. c) Dürr, U. H. N.; Gildenberg, M.; Ramamoorthy, A. *Chem. Rev.* **2012**, *112*, 6054–6074.

[2] a) Sanders. II, C.; Prestegard, J. H. *Biophys. J.* **1990**, *58*, 447–460. b) Orädd, G.; Lindblom, G. *Magn. Reson. Chem.* **2004**, *42*, 123–131.

[3] a) Tjandra, N.; Bax, A. *Science* **1997**, *278*, 1111–1114. b) Yan, J.; Delaglio, F.; Kaerner, A.; Kline, A. D.; Mo, H.; Shapiro, M. J.; Smitka, T. A.; Stephenson, G. A.; Zartler, E. R. *J. Am. Chem. Soc.* **2004**, *126*, 5008–5017. c) Opella, S. J.; Marassi, F. M. *Chem. Rev.* **2004**, *104*, 3587–3606. d) Prestegard, J. H.; Bougault, C. M.; Kishore, A. I. *Chem. Rev.* **2004**, *104*, 3519–3540. e) Prosser, R. S.; Evanics, F.; Kitevski, J. L.; Al–Abdul–Wahid, M. S. *Biochemistry* **2006**, *45*, 8453–8465. f) Vlach, J.; Saad, J. S. *Proc. Natl. Acad. Sci. USA* **2013**, *110*, 3252–3530.

[4] a) Walther, T. H.; Grage, S. L.; Roth, N.; Ulrich, A. S. *J. Am. Chem. Soc.* **2010**, *132*, 15945–15956. b) Cho, M.-K.; Gayen, A.; Banigan, J. R.; Leningr, M.; Traaseth, N. J. *J. Am. Chem. Soc.* **2014**, *136*, 8072–8080. c) Song, Y.; Mittendorf, K. F.; Lu, Z.; Sanders, C. *J. Am. Chem. Soc.* **2014**, *136*, 4093–4096. d) Durr, U. H. N.; Yamamoto, K.; Im, S. C.; Waskell, L.; Ramamoorthy, A. *J. Am. Chem. Soc.* **2007**, *129*, 6670–6671. e) Wang, T.; Hong, M.; *Biochemistry*, **2015**, *54*, 2214–2226.

[5] a) Raffard, G.; Steinbruckner, S.; Arnold, A.; Davis, J. H.; Dufourc, E. J. *Langmuir* **2000**, *16*, 7655–7662. b) Arnold, A.; Labrot, T.; Oda, R.; Dufourc, E. J. *Biophys. J.* **2002**, *83*, 2667–2680.

[6] a) Yamamoto, K.; Pearcy, P.; Ramamoorthy, A. *Langmuir* **2014**, *30*, 1622–1629. b) Yamamoto, K.; Pearcy, P.; Lee, D.-K.; Yu, C.; Im, S.-C.; Waskell, L.; Ramamoorthy, A.; *Langmuir* **2015**, *31*, 1496–1504.

[7] a) King, V.; Parker, M.; Howard, K. P. *J. Mag. Res.* **2000**, *142***,** 177–182. b) Loudet, C.; Manet, S.; Gineste, S.; Oda, R.; Achard, M.-F.; Dufourc, E. J. *Biophys. J.* **2007**, 3949–3959.

[8] a) Losonczi, J. A.; Prestegard, J. H. *J. Biomol. NMR*, **1998**, *12***,** 447–451. b) Sasaki, H.; Fukuzawa, S.; Kikuchi, J.; Yokoyama, S.; Hirota, H.; Tachibana, K. *Langmuir* **2003**, *19*, 9841–9844. c) Lu, J.-X.; Caporini, M. A.; Lorigan, G. A. *J. Mag. Res.* **2004**, *168*, 18–30. d) Shapiro, R. A.; Brindley, A. J.; Martin, R. W. *J. Am. Chem. Soc.* **2010**, *132*, 11406–11407.

[9] a) Wang, H.; Eberstadt, M.; Olejniczak, E. T.; Meadows, R. P.; Fesik, S. W. *J. Biomol. NMR* **1998**, *12*, 443–446. b) Sanders, C. R.; Prestegard, J. H. *Biophys. J.* **1990**, *58*, 447–460. c) McKibbin, C.; Farmer, N. A.; Jeans, C.; Reeves, P. J.; Khorana, H. G.; Wallace, B. A.; Edwards, P. C.; Villa, C. Booth, P. J. *J. Mol. Biol.* **2007**, *374*, 1319–1332. d) Morales, H. H.; Saleem, Q.; Macdonald, P. M.; *Langmuir* **2014**, *30*, 15219−15228.

[10] a) Ahuja, S.; Jahr, N.; Im, S.-C.; Vivekanandan, S.; Popovych, N.; Le Clair, S. V.; Huang, R.; Soong, R.; Xu, J.; Yamamoto, K.; Nanga, R. P.; Bridges, A.; Waskell, L.; Ramamoorthy, A. *J. Biol. Chem.* **2013**, *288*, 22080–22095. b) Yamamoto, K.; Dürr, U. H. N.; Xu, J.; Im, S.-C.; Waskell, L.; Ramamoorthy, A. *Sci. Rep.* **2013**, *3*,

2538. c) Yamamoto, K.; Gildenberg, M.; Ahuja, S.; Im, S.-C.; Pearcy, P.; Waskell, L.; Ramamoorthy, A. *Sci. Rep.* **2013**, *3*, 2556.
[11] Koynova, R.; Caffrey, M. *Biochim. Biophys. Acta* **1998**, *1376*, 91–145.
[12] a) Müller, K.; *Biochemistry* **1981**, *20*, 404–414. b) Mazer, N. A.; Benedek, G. B.; Carey, M. C. *Biochemistry* **1980**, *19*, 601-615.
[13] Matsui, R.; Ohtani, M.; Yamada, K.; Hikima, T.; Takata, M.; Nakamura, T.; Koshino, H.; Ishida, Y.; Aida, T. *Angew. Chem. Int. Ed.* **2015**, *54*, 13284–13288.
[14] Cox, C.; Lectka, T. *J. Org. Chem.* **1998,** *63,* 2426–2427.
[15] a) Sanders, C. R.; Schwonek, J. P. *Biochemistry* **1992**, *31*, 8898–8905. b) Yamamoto, K.; Soong, R.; Ramamoorthy, A.; *Langmuir* **2009**, *25*, 7010–7018.
[16] Wang, H.; Eberstadt, M.; Olejniczak, E. T.; Meadows, R. P.; Fesik, S. W. *J. Biomol. NMR.* **1998**, *12*, 443–446.
[17] King, V., Parker, M.; Howard, K. P. *J. Magn. Reson.* **2000**, *142*, 177–182.
[18] Cho, H. S., Dominick, J. L.; Spence, M. M. *J. Phys. Chem. B.* **2010**, *114*, 9238–9245.
[19] Shimaoka, H.; Kuramoto, H.; Furukawa, J.; Miura, Y.; Kurogochi, M.; Kita, Y.; Hinou, H.; Shinohara, Y.; Nishimura, S. *Chem. Eur. J.* **2007**, *13*, 1664.
[20] Tang, W.; Fang, S. *Tetrahedron Lett.* **2008**, *49*, 6003.
[21] Wilson, C. P.; Webb, S. J. *Chem. Commun.* **2008**, *34*, 4007.
[22] Benett, A. W.; Rienstra, C. M.; Auger, M.; Lakshmi, K. V.; Griffin, R. G. *J. Chem. Phys.* **1995**, *103*, 6951–6958.

Chapter 2

Chemically Locked Bicelles with High Thermal and Kinetic Stability

Abstract

In situ polymerization of a bicellar mixture composed of a phospholipid and polymerizable surfactants afforded unprecedented stable bicelles. The polymerized composite showed an aligned phase over a wide thermal range (25 to > 90 ºC) with excellent ^{2}H quadrupole splitting of the solvent signal, thus implying versatility as an alignment medium for NMR studies. Crosslinking of the surfactants also brought favorable effects on the kinetic stability and alignment morphology of the bicelles. This system could thus offer a new class of scaffolds for biomembrane models.

Introduction

Bicelles (bilayered micelles) are aqueous lipid–surfactant assemblies, in which lipid bilayer fragments are edge-stabilized with certain surfactants.[1] Since bicelles take an intermediate morphology between lipid vesicles and lipid– surfactant mixed micelles, they offer a new class of biomembrane models that combine the attractive features of both of these classic model systems. In addition, bicelles spontaneously align in magnetic fields and can therefore be used as aligned media for modern NMR techniques to obtain 3D structural information on biomolecules.[2] More recently, bicelles have been used as templates for forming composite materials through hybridization with polymers and inorganics.[3] Although various bicellar systems have been developed to date, their application has been limited owing to insufficient stability of their aligned phase. Most of the reported bicelles attain optimal alignment only under limited conditions in terms of temperature, lipid content, pH value, ionic strength, among other factors.[2e,4]

To increase the stability of the aligned phase of bicelles, a number of strategies have been proposed, including modification of the lipids and doping the lipid bilayers with cholesterol, its derivatives, or charged surfactants.[5] However, since these methods inevitably change the interior environment of lipid bilayers, an alternative approach solely based on the design of surfactant units is important. For the formation of stable bicelles, surfactants should meet two seemingly contradictory requirements. When the miscibility of the surfactant with the phospholipid is too high, their mixture is more prone to forming isotropic mixed micelles rather than bicelles. On the other hand, insufficient miscibility results in the separation of bicelles into vesicles and isotropic surfactant–phospholipid mixed micelles. Moreover, phospholipids generally show thermotropic phase transitions accompanied by drastic changes in their miscibility with surfactants,[6] which makes the design of surfactants more difficult.

As a conceptually novel approach, the author reports the stabilization of bicelles through in situ crosslinking of surfactants (Scheme 1). In bicellar assemblies, surfactants are considered to be localized at the edge of the lipid bilayer fragments.[7] If the in situ crosslinking of surfactants proceeds without serious alteration of the overall structure of bicelles, the resultant polymeric networks of surfactants should show enhanced affinity for the edges of lipid bilayers owing to multivalency effects, which

would lead to thermodynamic and kinetic stabilization of the bicelles. Indeed, similar strategies have been successfully applied for the stabilization of other membrane models, such as vesicles.[8] To demonstrate the validity of this concept, the author developed two types of polymerizable surfactants (SC-M_1 and SC-M_3; Scheme 1) derived from sodium cholate (SC). SC a representative surfactant for the formation of bicelles and possesses a quasi-planar rigid steroid skeleton with hydrophilic and hydrophobic faces residing back-to-back.[9] This characteristic two-faced structure provides SC with unique surface-active properties and enables efficient dispersal of various hydrophobic materials, including lipid bilayers, in aqueous media. By replacing the hydroxy group(s) of SC with hydrophilic chain(s) with a polymerizable terminus, the mono- and trifunctional monomers SC-M_1 and SC-M_3, respectively, were obtained.

Scheme 1. Schematic Structure of Polymerized Bicelle Composed of a Phospholipid (DMPC) and Polymerizable Surfactants (SC-M_1 and SC-M_3).

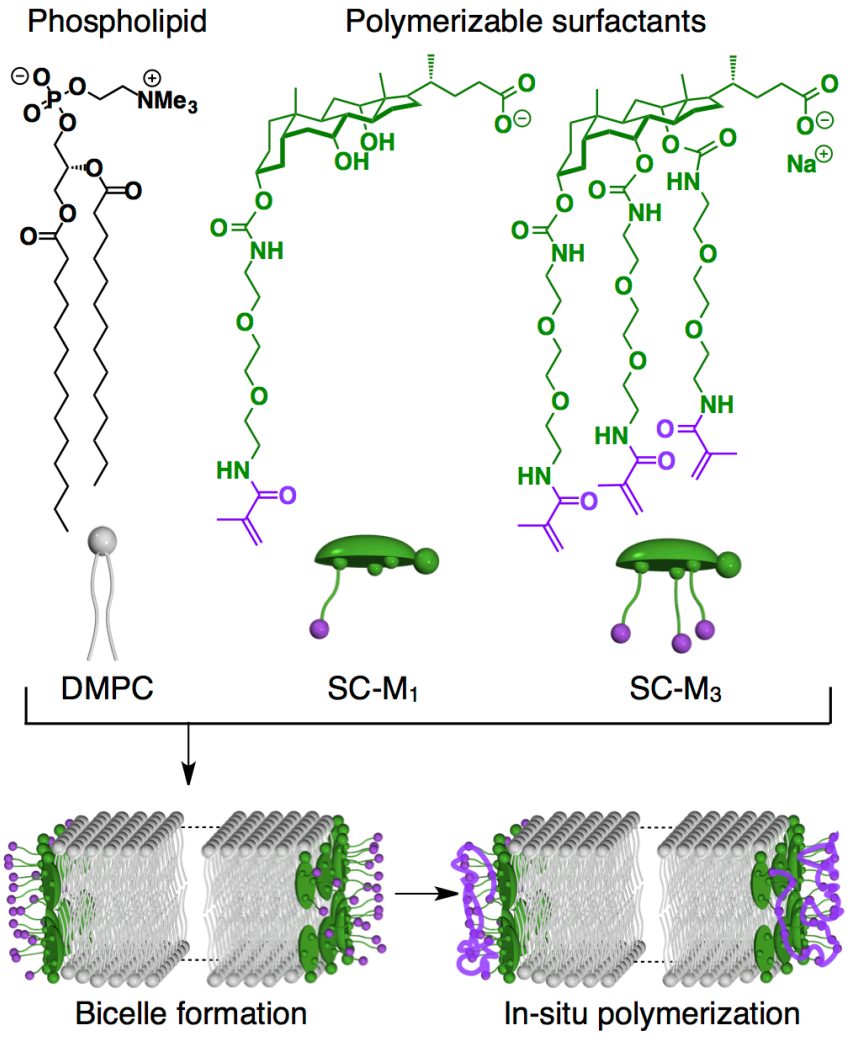

Results and Discussion

The phase behavior of aqueous mixtures of the polymerizable surfactants (SC-M_1, SC-M_3) and 1,2-dimyristoyl-sn-glycero-3-phosphatidylcholine (DMPC) was investigated in D_2O through measurement of the ^2H quadrupole splitting (Figure 1 a) and ^{31}P NMR with ^1H decoupling of 6 kHz (Figure 1 b). Typically, the author tested a sample with a molar ratio of DMPC/SC-M_1/SC-M_3 = 80 :19 :1 (10 % w/v total lipid con- tent, in D_2O containing 100 mm KCl). At temperatures lower than the phase transition of DMPC (24 ºC), where the phospholipid changes from the liquid-crystalline to the gel state, the mixture showed a nonaligned phase (Figure 1 a (i)). In the gel state, DMPC was highly miscible with the surfactants (SC-M_1 and SC-M_3), so the mixture formed isotropic mixed micelles, giving a ^{31}P NMR signal at 0 ppm (Figure 1 b (i)). When the mixture was heated in the range 25– 40 ºC, an obvious ^2H quadrupole splitting was observed (Figure 1 a (ii–iv)), thus indicating the formation of an aligned phase. In the ^{31}P NMR spectra, the signal at 0 ppm disappeared, while a new signal emerged at around -9 ppm, the chemical shift of which is in good agreement with magnetically aligned phospholipid bilayers with their normal perpendicular to the magnetic field (Figure 1 b (ii–iv)).[10] However, when the system was heated to more than 45 ºC, where the miscibility of the phospholipids and surfactants is insufficient to maintain the homogeneity, the bicellar assemblies separated into vesicles and isotropic mixed micelles (Figure 1 b (v– vii)), which abruptly terminated the alignment ability (Figure 1 a (v–vii)).

With the expectation of stabilizing the bicelles, in situ radical copolymerization of the surfactants SC-M_1 and SC-M_3 was performed at 40 ºC, which is the optimal temperature for the mixture to form alignable bicelles. Upon treating the bicellar mixture with potassium peroxodisulfate ($K_2S_2O_8$) and N,N,N',N'-tetramethylethylenediamine (1 mol % and 150 mol %, respectively, with respect to the acrylamide units), the acrylamides in the surfactants were quantitatively consumed within 15 min, as unambiguously confirmed by ^1H NMR measurement (Figure 2). After completion of the polymerization and subsequent aging, the system changed to a viscous translucent fluid.

Of particular interest is that the polymerized mixture showed an aligned phase over an unprecedentedly wide temperature range (Figure 1 c, d). According to the ^{31}P

NMR spectra, the system was composed solely of aligned bilayers from 25 ºC to over 90 ºC (Figure 1 d (ii–vii)), where the signals of isotropic mixed micelles or vesicles were not detected at all (Figure 1 d (ii–vii)). Before the present work, there have been only two bicellar systems that show an aligned phase at temperatures higher than 65 ºC, which were reported very recently.[5f,g] In addition, even when the system was cooled to 20 ºC, where DMPC is known to readily miscible with surfactants owing to the transition to a gel state, the author's bicellar mixture did not change to isotropic mixed micelles (Figure 1 d (i)). Most likely, the covalently crosslinked networks of the surfactants were able to strongly adhere to the bilayer edges, which prevented drastic structural reorganization of the lipid bilayers. Although the polymerized mixture did not align at temperatures lower than 25 ºC (Figure 1 c (i)), the alignment perfectly recovered when the mixture was heated to above 25 ºC. Upon repeating the temperature change across 25 ºC, the phase transition took place without any degradation.

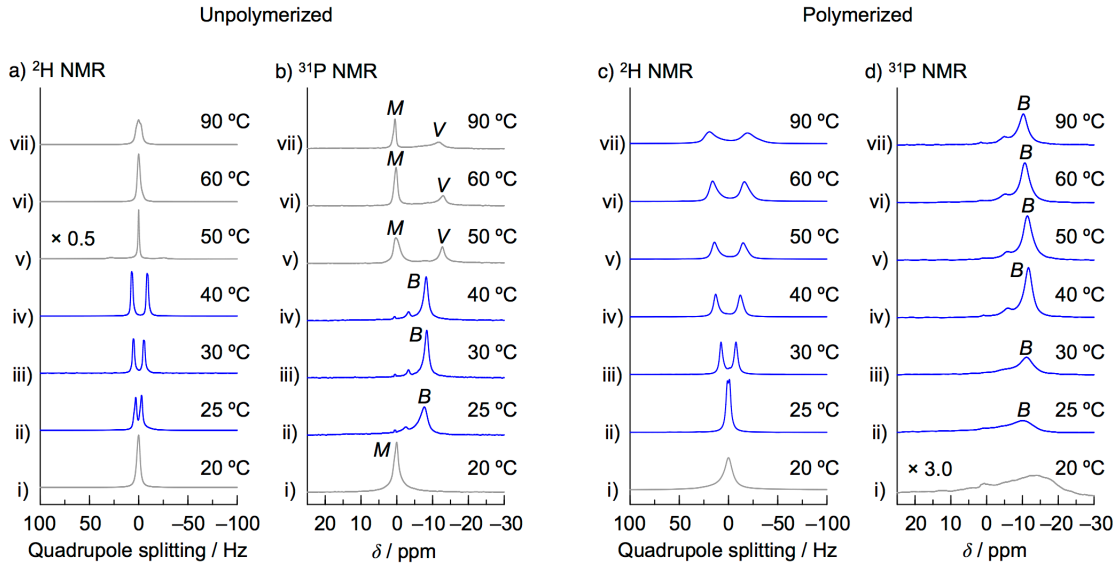

Figure 1. Variable temperature NMR spectra of bicellar mixtures composed of DMPC and polymerizable surfactants (SC-M_1 and SC-M_3) (a) before and (b) after the polymerization. ^{2}H quadrupole splitting (left) and ^{31}P NMR spectra (right) of mixtures with a molar ratio of DMPC/SC-M_1/SC-M_3 = 80/19/1 in D_2O containing 100 mM KCl (total lipid content, 10 % w/v). In ^{31}P NMR spectra, *M*, *B*, and *V* indicate signals assignable to micelles, bicelles, and vesicles, respectively.

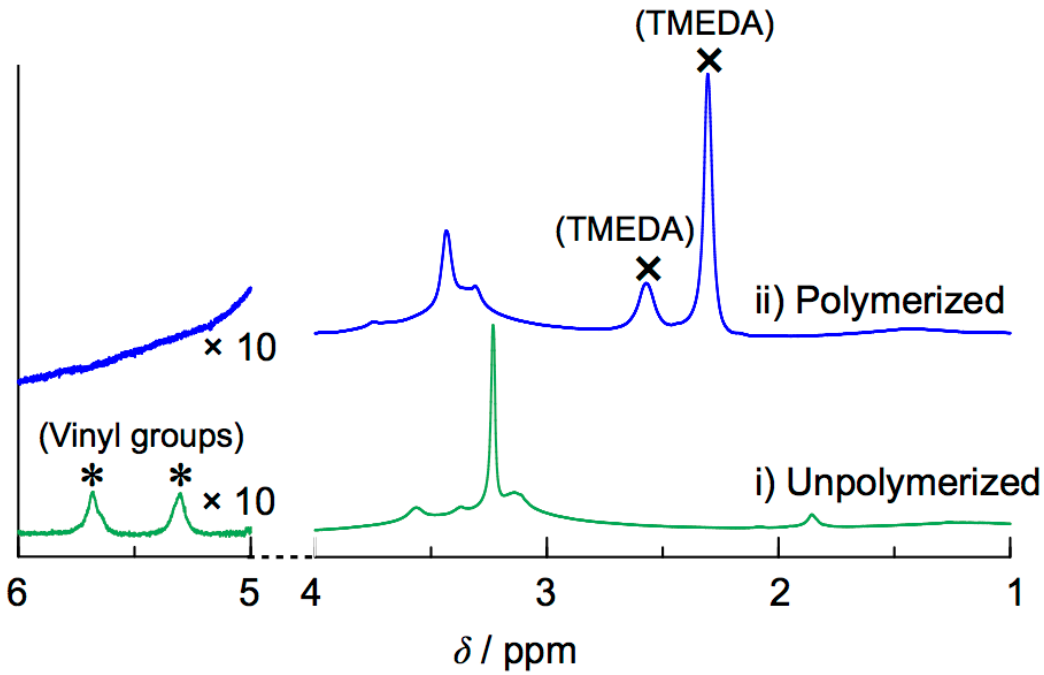

Figure 2. ^{1}H NMR spectra at 40 ºC of unpolymerized (i) and polymerized (ii) bicellar mixtures with a molar ratio of DMPC/SC-M_1/SC-M_3 = 80:19:1 in D_2O containing 100 mM KCl (total lipid content, 10% w/v). The resonances attributable to the vinyl protons in SC-M_1 and SC-M_3 and the protons of *N*,*N*,*N*',*N*'-tetramethylethylenediamine (TMEDA) are highlighted with asterisks (*) and crosses (×), respectively.

The magnitude of ^{2}H quadrupole splitting of the solvent signal is a reliable probe for evaluating the ability of bicelles to align the surrounding molecules, which is crucial for NMR structural studies of biomolecules through observing residual dipole couplings and chemical shift anisotropies.[1] In the case of common bicelles, the splitting is strongly dependent on temperature and is at a satisfactory level only within a narrow temperature range. Indeed, the author's bicellar mixture before polymerization showed meaningful ^{2}H quadrupole splitting (ca. 15 Hz) only within the thermal range 40–45 ºC (Figure 3 (i)). In sharp contrast, the polymerized bicellar mixture achieved 15 Hz splitting even at 30 ºC. Moreover, the splitting increased up to 40 Hz as the temperature was raised to 90 ºC (Figure 3 (ii)). Thus, the polymerized bicellar mixture that the author established serves as a useful alignable medium from 30 ºC to more than 90 ºC, which implies potential application for investigating the structure and dynamics of various proteins, including those that are thermally unstable and thermophilic, at their biologically relevant temperatures. It should also be mentioned that the present system has room for further improvement through alteration of the composition of the phospholipid bilayer parts, such as doping with cholesterol derivatives and the use of other phospholipids.[5]

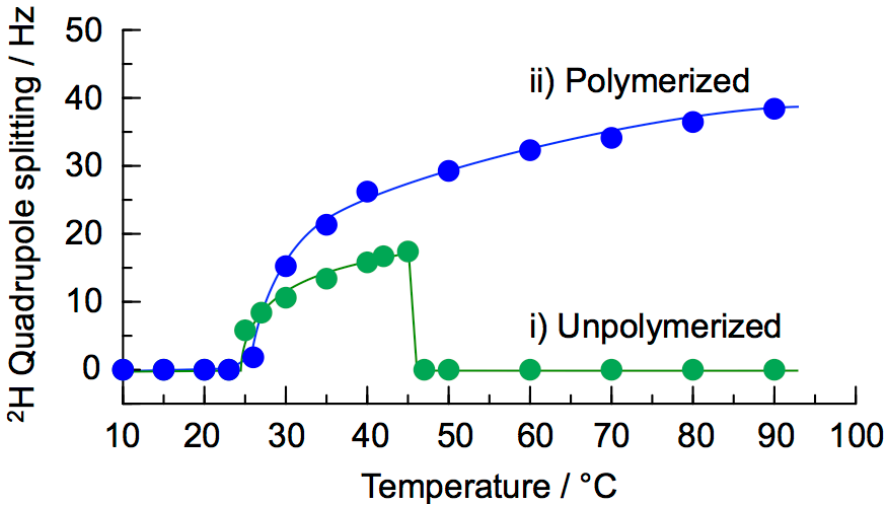

Figure 3. Temperature-dependent changes in the magnitude of ^{2}H quadrupole splitting of the D_2O signal in unpolymerized (i) and polymerized (ii) bicellar mixtures with a molar ratio of DMPC/SC-M_1/SC-M_3 = 80: 19: 1 in D_2O containing 100 mM KCl (total lipid content, 10% w/v).

In order to characterize the unpolymerized and polymerized bicelles further, ^{31}P NMR spectra were measured with higher ^{1}H decoupling (42 kHz; Figure 4). Consistent with the data with lower ^{1}H decoupling (6 kHz; Figure 1b,d), the unpolymerized mixture exhibited an aligned phase only within a narrow thermal range (Figure 4a), while the polymerized mixture showed a characteristic signal of aligned bicelles over a wide thermal range from 25 ºC to more than 90 ºC (Figure 4b). In terms of peak shape and chemical shift, the signal of the polymerized mixture was minimally dependent on temperature. Closer analysis of the data revealed that the signal of the polymerized mixture was gradually broadened and shifted upfield with increasing temperature. Based on these data, the bilayer order parameters of the bicelles were evaluated (Figure 5).[7a, 11] Bilayer order parameter of bicelles ($S_{bicelle}$) with respect to the pure DMPC bilayer was calculated from the ^{31}P NMR data measured with ^{1}H decoupling of 42 kHz (Figure 4), using the following equation;

$$S_{bicelle} = (\delta_{obs} - \delta_{iso}) / (\delta_{\perp} - \delta_{iso})$$

where δ_{obs} is the observed chemical shift, δ_{iso} is the isotropic chemical shift (0 ppm), and $\delta_{\perp}$ is the perpendicular edge chemical shift (15 ppm) of the ^{31}P chemical-shift-anisotropy powder pattern spectrum of unaligned DMPC in the liquid-crystalline phase.[12] Over the entire region from 25 to more than 90 ºC, the polymerized bicelles exhibited bilayer order parameter values ($S_{bicelle}$ = 0.68–0.80) comparable to typical bicelles. In addition, the polymerized bicelles always showed higher order parameter values than the unpolymerized bicelles ($S_{bicelle}$ = 0.48–0.64).

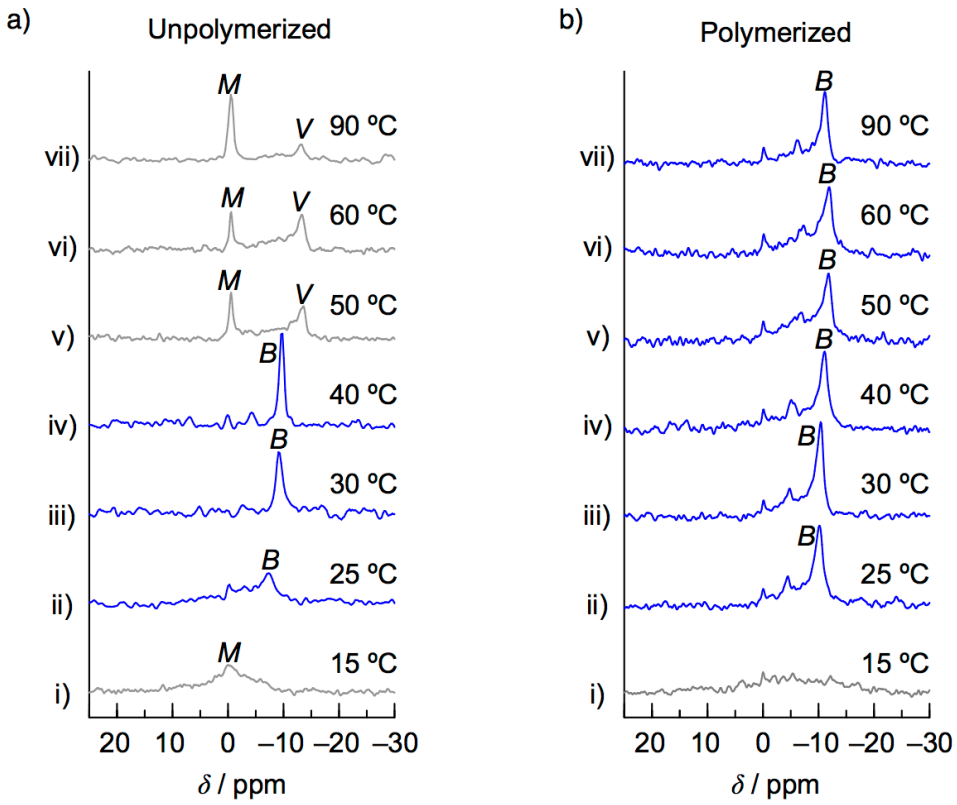

Figure 4. Variable temperature ^{31}P NMR spectra with ^{1}H decoupling of 42 kHz for the polymerized bicellar mixture with a molar ratio of DMPC/SC-M_1/SC-M_3 = 80:19:1 in D_2O containing 100 mM KCl (total lipid content, 10% w/v). *M*, *B*, and *V* indicate signals assignable to micelles, bicelles, and vesicles, respectively.

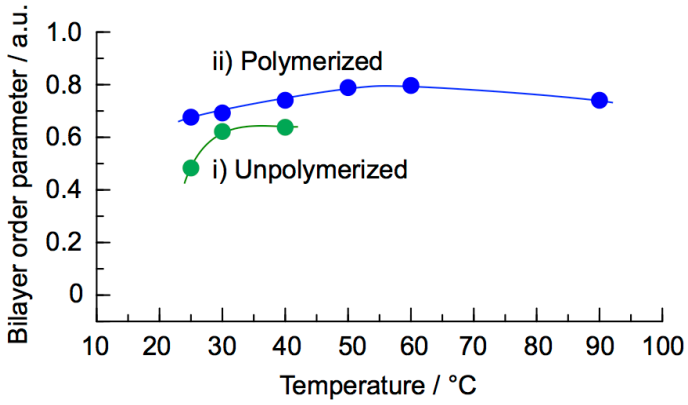

Figure 5. Temperature-dependent changes in bilayer order parameters of the unpolymerized (i) and polymerized (ii) bicellar mixtures with a molar ratio of DMPC/SC-M_1/SC-M_3 = 80:19:1 in D_2O containing 100 mM KCl (total lipid content, 10% w/v).

For the stabilization of polymerized bicelles, the multi- functional monomer SC-M_3 was found to play a crucial role. As a control experiment, the same in situ polymerization was conducted by using an SC-M_3-free mixture (molar ratio DMPC/SC-M_1=80:20). Before in situ polymerization, the SC-M_3-free system formed an aligned phase slightly more stable than that of the SC-M_3-doped mixture (DMPC/SC-M_1/ SC-M_3 = 80 :19 :1). When the in situ polymerization of the SC-M_3-free bicelles was conducted at 40 ºC, the resultant mixture again exhibited an aligned phase with an expanded thermal range (27–90 ºC). However, over the whole thermal range, a considerable amount of isotropic mixed micelles coexisted in the system, as confirmed by ^{31}P NMR (Figure 6). Most likely, the crosslinked networks of SC-M_1 and SC-M_3 were able to "freeze" the structure of bicelle templates more efficiently than the simple linear polymers of SC-M_1.

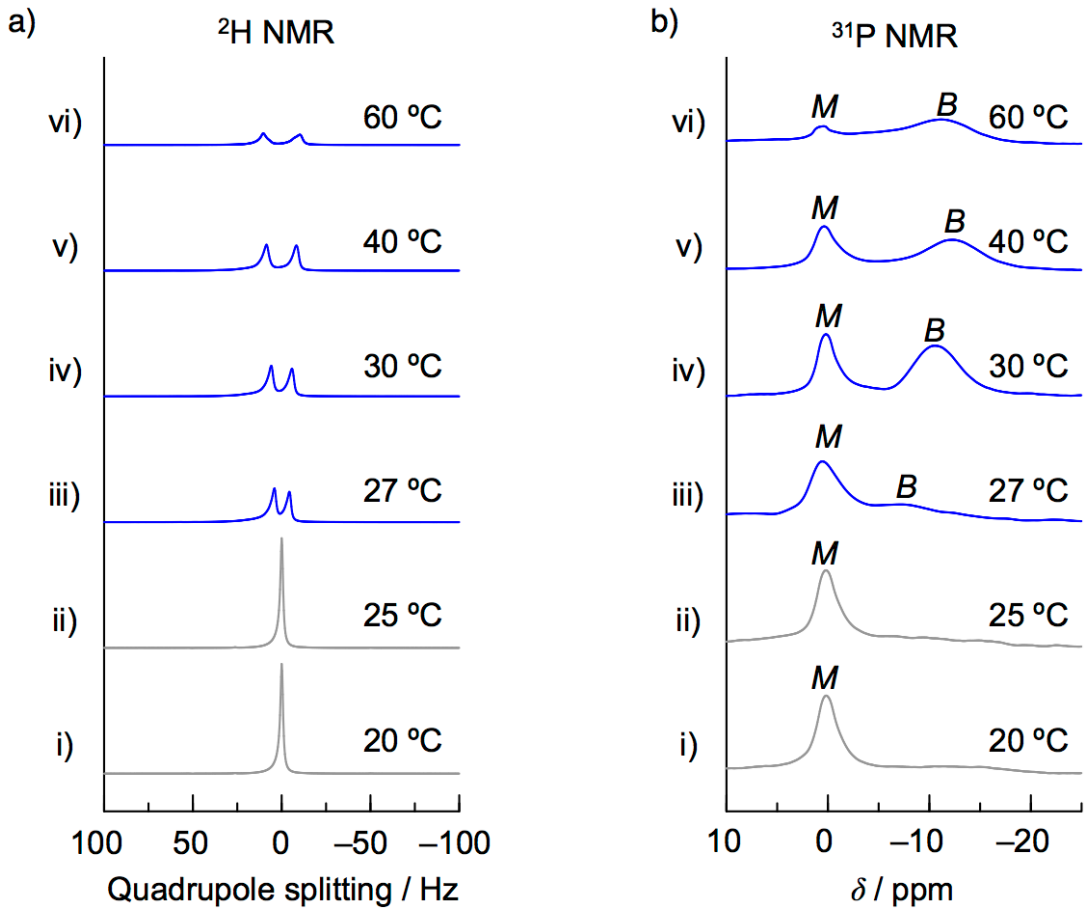

Figure 6. Variable temperature ^{2}H quadrupole splitting (a) and ^{31}P NMR spectra with ^{1}H decoupling of 6 kHz (b) for the polymerized bicellar mixture with a molar ratio of DMPC/SC-M_1 = 80:20 in D_2O containing 100 mM KCl (total lipid content, 10% w/v). *M*, *B*, and *V* indicate signals assignable to micelles, bicelles, and vesicles, respectively.

The in situ crosslinking method the author established was applicable to bicellar mixtures with various average sizes. In general, the size of the bicelles is tunable by changing the molar ratio of phospholipids and surfactants, where the size becomes smaller as the ratio of surfactants is increased.[9b, 13] For example, a mixture with a higher content of surfactants (molar ratio DMPC/SC- M_1/SC-M_3 = 33 :64 :3) is found to form small fast-tumbling bicelles (Figure 7a (i)). When this mixture was treated with the reagents for radical polymerization, the in situ crosslinking of the surfactants again proceeded smoothly without serious structural alteration of aggregates to afford smaller polymerized bicelles (Figure 7a (ii)). In both cases of the unpolymerized and polymerized bicelles, the double-logarithm plot of the small angle X-ray scattering data [ln(intensity) *vs.* ln(q)] at a region of q = <1 nm^{-1} shows a slope around –2, characteristic of disc-shaped objects, which indicates the formation of small bicelles.[14] Radius of gyration (R_g) can be estimated by Guinier plottings [ln(intensity) *vs.* q^2] at a small angle region (Figure 7b).[15] Based on the plottings, obtained radii of gyration for small bicelles before and after polymerization were 3.9 and 4.1 nm, respectively. According to the relation between the radius of a disk (R) and R_g [$R_g^2 = R^2/2$], the radii of small bicelles before and after polymerization were estimated to be 5.5 and 5.9 nm, respectively. These plottings and calculations indicate that the size of the small bicelles was retained after polymerization.

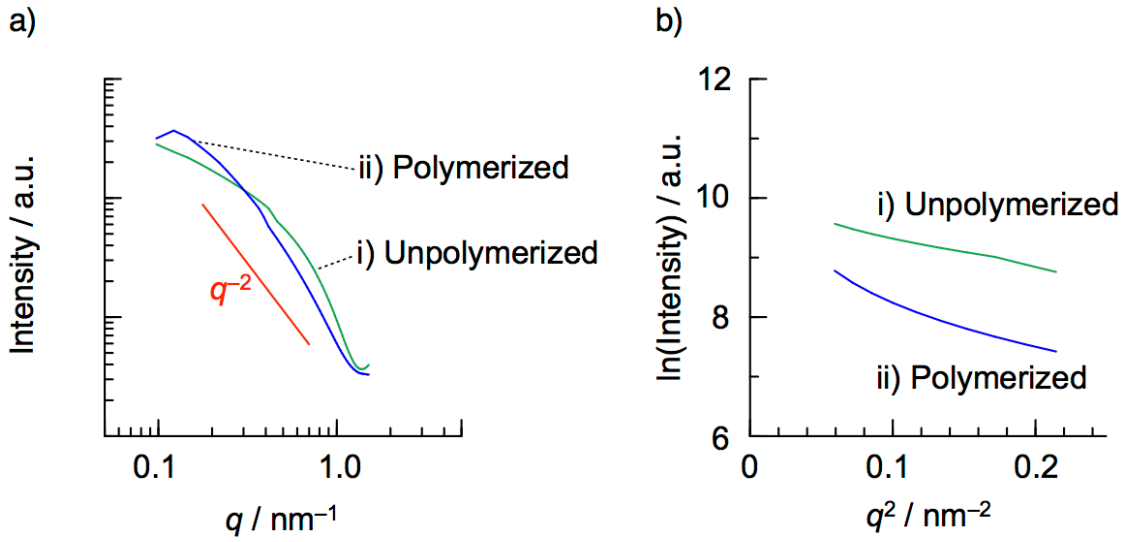

Figure 7. Small angle X-ray scattering (a) and Guinier representations of the low angle data (b) at 40 ºC of a bicellar mixture containing small tumbling bicelles. Unpolymerized (i) an polymerized (ii) bicellar mixtures with a molar ratio of DMPC/SC-M_1/SC-M_3 = 33:64:3 in D_2O containing 100 mM KCl (total lipid content, 5 % w/v).

As an additional benefit of crosslinking the surfactants, the author's polymerized bicelles showed notable kinetic stability. This is quite unlike the case of common bicelles, which are generally under rapid equilibrium of fission–fusion events. To detect the kinetics of bilayer fission and fusion, two samples of bicelles with different size distribution were prepared and then mixed (Figure 8 a). The smaller polymerized bicelles, prepared from a mixture with a higher content of surfactants (molar ratio DMPC/SC-M_1/SC-M_3 = 33 :64 :3), showed a ^{31}P NMR signal at around 0 ppm (Figure 8 c, (ii)), which could be easily distinguished from the ^{31}P NMR signal of the larger polymerized bicelles (DMPC/SC-M_1/SC-M_3 = 80 :19 :1; Figure 8 c (i)). Upon mixing the polymerized samples of the smaller and larger bicelles, their ^{31}P NMR signals were separately observed at their original chemical-shift regions (Figure 8 c (iii)). In sharp contrast, when the unpolymerized samples of the small (Figure 8 b (ii)) and large (Figure 8 b (i)) bicelles were mixed in the same manner, only a unimodal signal was observed in the ^{31}P NMR spectrum (Figure 8 b (iii)), thus suggesting that the relaxation of bicelles to their equilibrium size was completed just after the mixing of the samples. These observations clearly indicate that the fusion and fission of bicelles was significantly suppressed by crosslinking of the surfactants. Considering this enhanced kinetic stability, these polymerized bicelles could offer useful scaffolds for model membranes with complicated substructures, including lipid-raft domains.

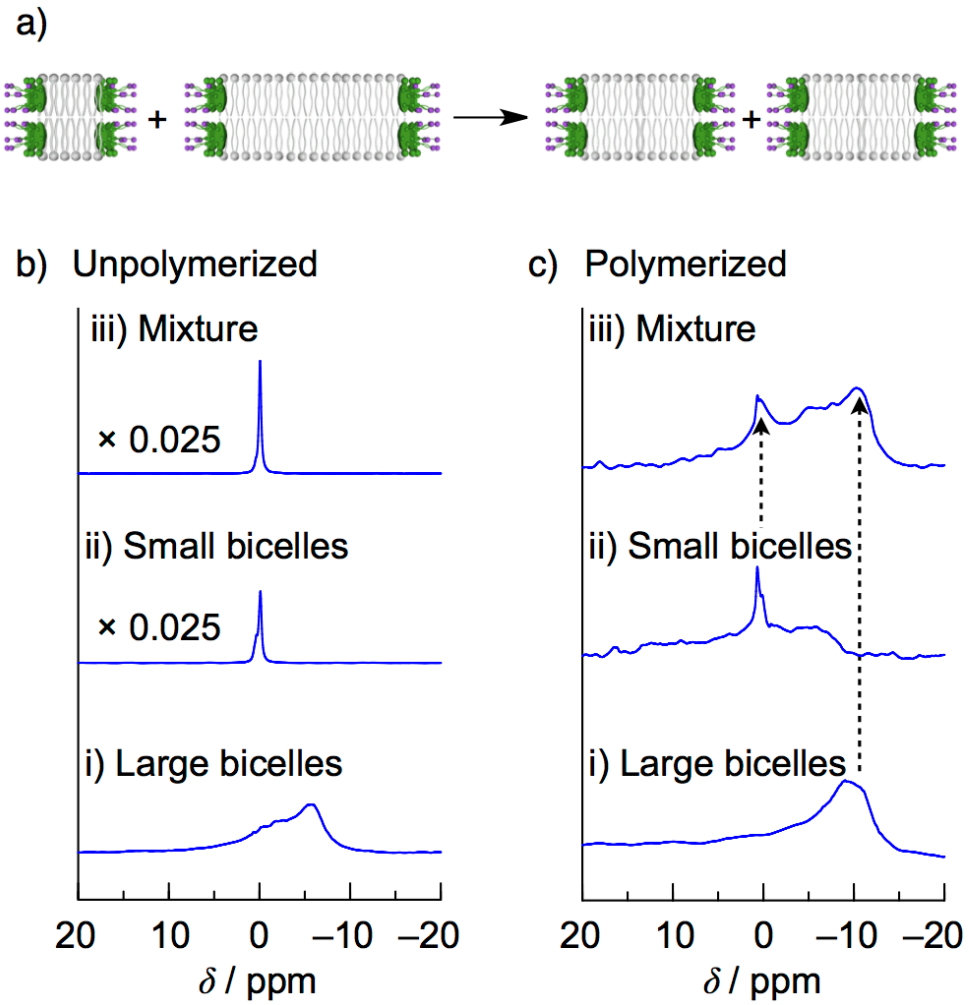

Figure 8. Kinetic studies of bilayer fission-fusion process of bicelles. (a) Schematic representation of the relaxation of bicelles to their equilibrium size. ^{31}P NMR spectra of (b) unpolymerized and (c) polymerized bicellar mixtures; (i) a mixture with a molar ratio of DMPC/SC-M_1/SC-M_3 = 80/19/1 in D_2O containing 100 mM KCl (total lipid content, 10% w/v), (ii) a mixture with a molar ratio of DMPC/SC-M_1/SC-M_3 = 33/64/3 in D_2O containing 100 mM KCl (total lipid content, 5% w/v), and (iii) a mixture of (i) and (ii) (3:5, v/v).

Last, small-angle X-ray scattering (SAXS) profiles of the polymerized bicelles were measured and they revealed the significant influence of the crosslinking of surfactants on the alignment morphology of bicelles. As shown in Figure 3 a, both the unpolymerized (i) and polymerized (ii) mixture showed a broad peak between q = 0.8 and 2.5 nm^{-1}, which is attributable to the scattering of single lipid bilayers with a thick of approximately 4 nm.[16] Interestingly, the polymerized mixture showed a strong sharp Bragg peak at q = 0.3 nm with a d-spacing of 20 nm (Figure 9 a (ii)). In the 2D SAXS pattern of an anisotropically oriented sample held in a thin capillary to induce macroscopic alignment by the anisotropic container-shape effect, the broad scattering (q = 0.8 and 2.5 nm^{-1}) and the Bragg peak (q = 0.3 nm) were observed in the regions with similar azimuthal angle (Figure 9 c, d). This observation unambiguously indicates smectic-type orientation, in which bicelles are cofacially aligned along the normal vector of bilayers (Figure 9 b, upper model). According to the half-width of the Bragg peak at q = 0.3 nm, the averaged number of spatially correlated bicelle sheets in the stack was estimated to be 13.[17] Contrary to this, the unpolymerized mixture showed a weak diffraction with an interlayer d- spacing of 6.2 nm (Figure 9 a (i)), which is attributable to close stacking of the bicelles (Figure 3 b, lower model), which is observed for common bicelles.[17b, 18] Overall, the newly established polymerized bicelles assembled in an unprecedented structure in terms of population of ordered bilayers, persistent length of alignment, and length of periodicity. Such unique alignment morphology is most likely the origin of the exceptional thermal stability and alignment-inducing ability of the author's polymerized bicelles. Also noteworthy is the distance between the polymerized bicelles (20 nm), which is five times as large as the thickness of single lipid bilayers (about 4 nm). This fact indicates that lipid bilayers in the polymerizable mixture are in a well-hydrated state (Figure 9 b, upper model), which is expected to provide more realistic biomembrane models compared with densely stacked multilamellar vesicles.

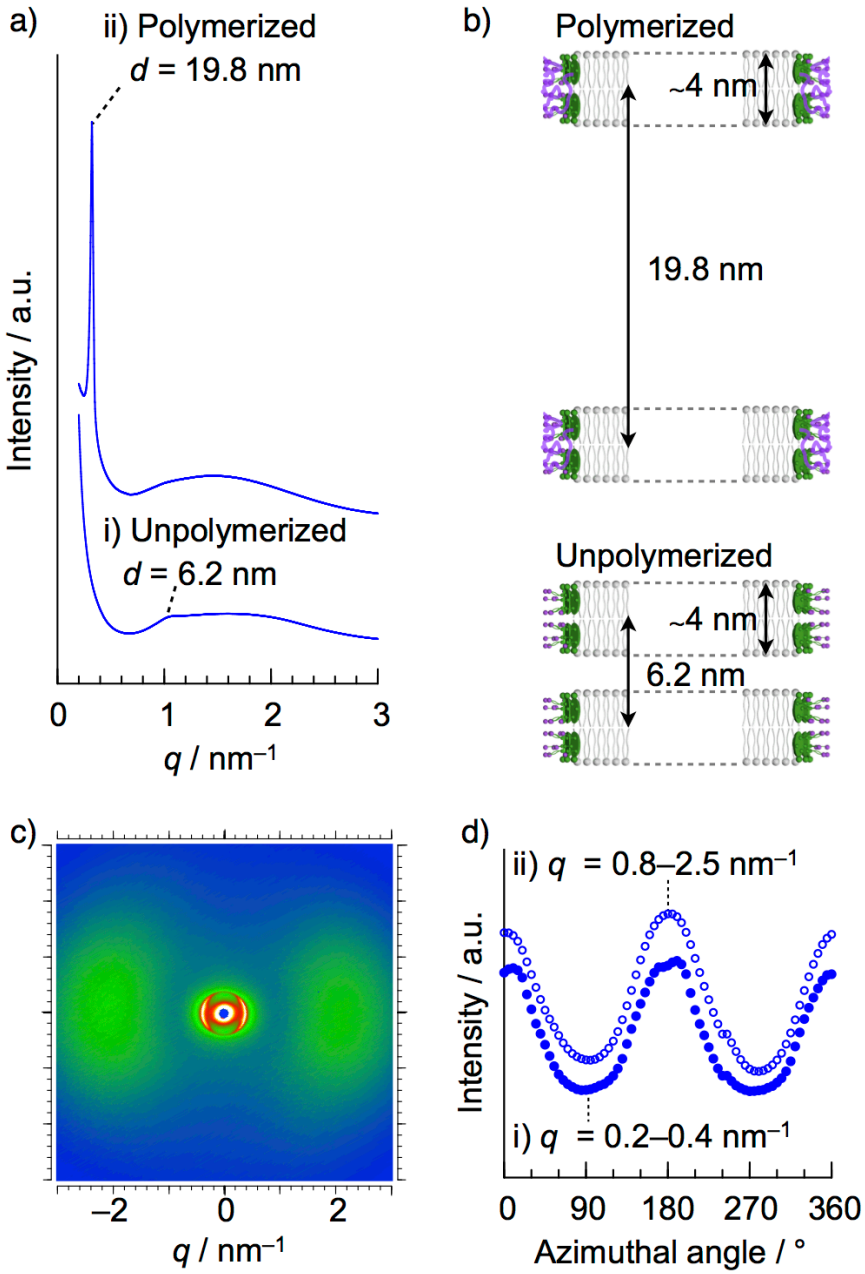

Figure 9. Alignment morphology of bicelles. a) SAXS profile of unpolymerized (i) and polymerized (ii) bicellar mixtures with a molar ratio of DMPC/SC-M_1/SC-M_3 = 80:19:1 in D_2O containing 100 mM KCl (total lipid content, 10% w/v) at 40 °C. b) Schematic representation of the long- (upper) and short-range (lower) ordering of stacked bicelles. c) 2D SAXS image of the polymerized bicellar mixture macroscopically aligned in a thin capillary. d) Plotting of total scattering intensities in the 2D SAXS of the aligned sample at q = 0.2–0.4 (i) and q = 0.8–2.5 nm^{-1} (ii) as a function of the azimuthal angle.

Conclusion

In conclusion, the author succeeded in stabilizing phospholipid bicelles through the in situ polymerization of the surfactants. The polymerized bicellar mixture showed an aligned phase over an unprecedentedly wide temperature range (from 25 to > 90 ºC) with large ^{2}H quadrupole splitting of the solvent D_2O signal, which suggests utility as an alignment medium for NMR measurements. In addition, the chemical locking of the surfactants improved the kinetic stability and alignment morphology of the resultant fragmented lipid bilayers, which means that this approach could offer a new class of scaffolds for biomembrane models.

Experimental Section

1. Materials and General Methods

All the reagents and chemicals used were obtained from commercial sources and used as received, unless otherwise noted. Dichloromethane (CH_2Cl_2), diethyl ether (Et_2O) and tetrahydrofuran (THF) were dried by activated alumina column in an Innovative Technology, Inc., PureSolv system. 1,2-Dimyristoyl-*sn*-glycero-3-phosphatidylcholine (DMPC) was used as purchased (Wako Chemicals) and used as received. *N*-(2-(2-Aminoethoxy)ethoxy)-ethyl-methacrylamide was prepared according to the literature.[19]

Solution state ^{1}H, ^{2}H, ^{13}C, and ^{31}P NMR spectra were recorded on a JEOL model EXcalibur 500 or ECA-500 spectrometer, operating at 500, 75, 125, and 202 MHz, respectively. Chemical shifts are given with respect to an internal (^{1}H and ^{13}C, tetramethylsilane) or external (^{31}P, 85% aqueous H_3PO_4) standard. For ^{31}P NMR measurement, WALTZ proton decoupling was used during a signal acquisition with the proton decoupler field strength of 6.0 kHz, 90° pulse width of 9.8 μs, and recycle delay of 2.0 s. For ^{31}P NMR measurement with higher ^{1}H decoupling, a Chemagnetics model CMX Infinity 400 operating at 161.4 MHz was used, with the proton decoupling field strength of 41.67 kHz, 45° pulse width of 3.0 μs, and recycle delay was 20 s. To the FID data of ^{31}P NMR thus obtained, an exponential line broadening of 50 Hz was applied to prior to Fourier transformation. High-resolution Mass (HRMS) spectrometry was performed on a JEOL model JMS-T100LC ESI-TOF-MS instrument with reserpine as an internal standard. Small-angle X-ray scattering (SAXS) was carried out at BL45XU in SPring-8 (Hyogo, Japan)[20] with a Rigaku imaging plate area detector model R-AXIS IV++. Scattering vector q ($q = 4\pi\sin\theta/\lambda$; 2θ and λ= scattering angle and wavelength of the incident X-ray beam [1.00 Å], respectively) and position of an incident X-ray beam on the detector were calibrated using several orders of layer reflections from silver behenate (d = 58.380 Å). The sample-to-detector distance was 2.5 m, where recorded scattering/diffraction images were integrated along the Debye-Scherrer ring, affording a one-dimensional scattering profile using a Rigaku model R-AXIS Display software.

2. Synthesis of the Polymerizable Cholate Derivative 4 (Free-acid Form of SC-M_1)

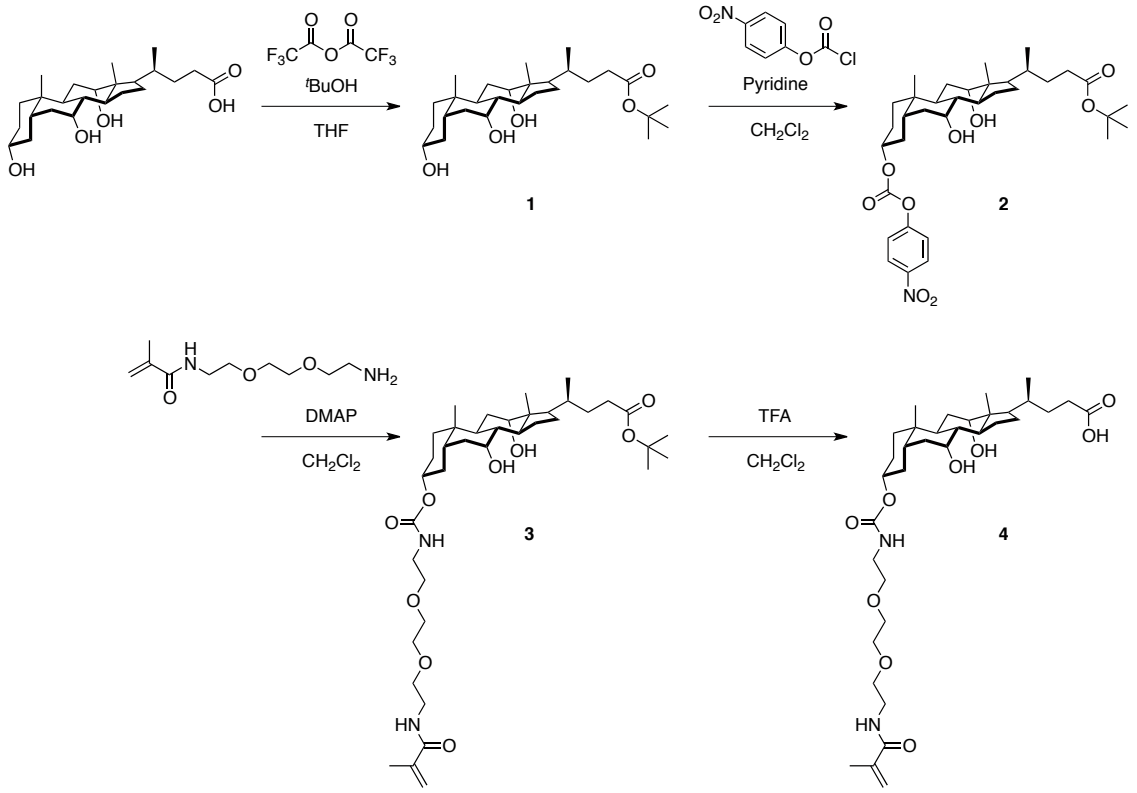

Scheme S1. Synthesis of the Polymerizable Cholate Derivative **4** (Free-acid Form of **SC-M_1**)

***tert*-Butyl cholate (1):**

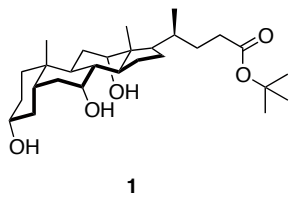

To a THF solution (100 mL) of cholic acid (5.00 g, 12.3 mmol) was added dropwise trifluoroacetic anhydride (20 mL, 90.1 mmol) at 0 ºC. After being stirred at room temperature for 1.5 h, the mixture was treated with ^{t}BuOH (30 mL, 316 mmol) and then stirred at the temperature for 7 h. To the resultant mixture was slowly added saturated aqueous NH_3 (25 mL) at 0 ºC. After being left to stand at the temperature for 12 h, the reaction mixture was diluted with Et_2O (200 mL) and successively washed with aqueous NaOH (1 M, 100 mL) and water (2 × 100 mL). The organic layer was dried over Na_2SO_4 and concentrated to dryness under reduced pressure. The resultant residue was crystallized from acetonitrile to give **1** as a white solid (5.24 g, 11.3 mmol, 92 %).

^{1}H NMR ($CDCl_3$): δ 0.69 (s, 3H), 0.89 (s, 3H), 0.97 (d, 3H, J = 6.4 Hz), 1.08–2.48 (m, overlapped, 24H), 1.44 (s, 9H), 3.45 (m, 1H), 3.85 (m, 1H), 3.98 (m, 1H).

^{13}C-NMR ($CDCl_3$): δ 12.7, 17.5, 22.7, 23.3, 26.8, 27.6, 28.5, 30.7, 31.1, 32.7, 34.7, 34.8, 35.2, 35.4, 39.8, 39.9, 41.6, 42.1, 46.7, 47.4, 68.5, 72.1, 73.1, 80.1, 173.8.

HRMS (ESI-TOF, positive-ion mode, MeOH): *m/z* found 487.3407 ([M + Na^+] calcd. for $C_{28}H_{48}O_5Na$: 487.3399).

***tert*-Butyl 3-((4-nitrophenoxy)carbonyl)oxy)cholate (2):**

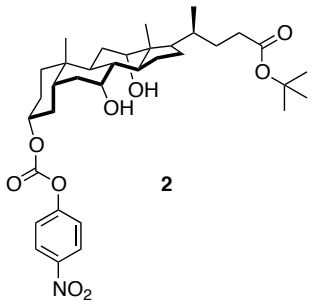

2

To a CH_2Cl_2 solution (40 mL) of **1** (2.00 g, 4.30 mmol) and 4-nitrophenyl chloroformate (867 mg, 4.30 mmol) was added pyridine (2 mL, 25 mmol) at room temperature. After being stirred at the temperature for 8 h, the reaction mixture was diluted with CH_2Cl_2 (40 mL) and successively washed with aqueous $NaHSO_4$ (1 M, 60 mL), water (2 × 60 mL) and brine (60 mL). The organic layer was dried over $MgSO_4$ and concentrated under reduced pressure to dryness. The resultant residue was subjected to silica gel column chromatography eluted with EtOAc/hexane (1:2, v/v) to afford **2** as a white solid (1.18 g, 1.87 mmol, 44%).

^{1}H NMR ($CDCl_3$): δ 0.70 (s, 3H), 0.93 (s, 3H), 0.99 (d, 3H, J = 6.3 Hz), 1.04–2.54 (m, overlapped, 24H), 1.45 (s, 9H), 3.87 (m, 1H), 4.02 (m, 1H), 4.57 (m, 1H), 7.37 (d, 2H, J = 9.2 Hz), 8.27 (d, 2H, J = 9.2 Hz).

^{13}C NMR. ($CDCl_3$): δ 12.4, 17.3, 22.2, 23.1, 26.3, 27.3, 28.0, 30.8, 32.4, 34.2, 34.6, 34.7, 34.8, 35.1, 39.3, 41.1, 41.5, 46.4, 47.2, 68.1, 72.9, 79.9, 80.2, 121.6, 125.1, 145.1, 151.8, 155.6, 173.7.

HRMS (ESI-TOF, positive-ion mode, MeOH): *m/z* found 487.3407 ([M + Na^+] calcd. for $C_{35}H_{51}NNaO_9Na$: 487.3399).

***tert*-Butyl 3-((2-(2-(2-methacrylamidoethoxy)ethoxy)ethyl)carbamoyloxy)cholate (3):**

To a CH_2Cl_2 solution (30 mL) of **2** (560 mg, 2.59 mmol) were successively added dropwise 4-(dimethylami-no)pyridine (316 mg, 2.59 mmol) and a CH_2Cl_2

solution (5 mL) of *N*-(2-(2-aminoethoxy)ethoxy)-ethyl)methacryl amide (791 mg, 1.26 mmol) at room temperature.

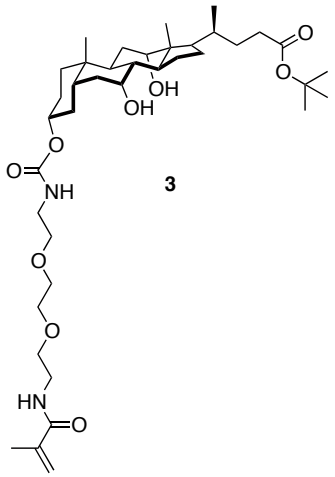

3

After being stirred at the temperature for 12 h under N_2, the reaction mixture was diluted with CH_2Cl_2 (20 mL) and successively washed with water (3 × 30 mL) and brine (40 mL). The organic layer was dried over $MgSO_4$ and concentrated to dryness under reduced pressure. The resultant residue was subjected to silica gel column chromatography eluted with EtOAc to afford **3** as a white solid (889 mg, 1.26 mmol, 99%).

^{1}H NMR ($CDCl_3$): 0.69 (s, 3H), 0.92 (s, 3H), 0.99 (d, 3H, J = 6.4 Hz), 1.03–2.40 (m, overlapped, 24H), 1.44(s, 9H), 1.97 (s, 3H) 3.34–3.63 (m, 12H), 3.84 (m, 1H), 3.97 (m, 1H), 4.46 (m, 1H), 5.38 (s, 1H), 5.70 (s, 1H), 7.96 (m, 1H).

^{13}C NMR ($CDCl_3$): δ 12.5, 17.3, 18.6, 22.5, 23.1, 26.5, 26.9, 27.4, 28.1, 28.3, 30.9, 32.6, 34.3, 34.6, 34.9, 35.1, 35.6, 39.6, 40.5, 41.1, 41.8, 46.5, 47.2, 68.2, 69.6, 69.8, 70.1, 72.9, 74.5, 77.2, 79.9, 119.9, 139.8, 156.4, 168.7, 173.7.

MALDI-TOF-MS: *m/z* calcd. for $C_{39}H_{66}N_2O_9Na$ ($[M + Na]^+$) 729.4666, found 729.4209.

3-((2-(2-(2-Methacrylamidoethoxy)ethoxy)ethyl)carbamoyloxy)cholic acid (4):

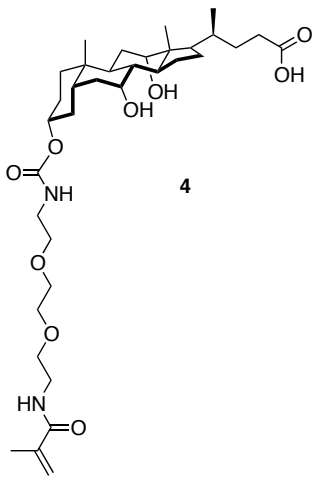

4

To a CH_2Cl_2 solution (5 mL) of **3** (298 mg, 0.42 mmol) was added trifluoroacetic acid (2 mL, 27 mmol) at room temperature. After being stirred at the temperature for 30 min, the mixture was concentrated to dryness under reduced pressure. The resultant residue was subjected to preparative thin-layer chromatography of silica gel developed with $CHCl_3$/MeOH (9:1, v/v) to afford **4** as a white solid (228 mg, 0.350 mmol, 83%).

^{1}H NMR ($CDCl_3$): δ 0.69 (s, 3H), 0.89 (s, 3H), 1.00 (d, 3H, J = 6.4 Hz), 1.03–2.43 (overlapped, 24H), 1.97 (s, 3H), 3.24–3.63 (m, 12H), 3.84 (m, 1H), 3.98 (m, 1H), 4.46 (m, 1H), 5.34 (s, 1H), 5.38 (m, 1H) 5.72 (s, 1H), 6.53 (m, 1H).

^{13}C NMR ($CDCl_3$, 125 MHz): 12.6, 17.3, 18.7, 22.5, 23.2, 26.5, 27.0, 27.5, 28.3, 30.8, 31.0, 34.4, 34.7, 34.9, 35.3, 35.7, 39.6, 40.5, 41.2, 41.8, 46.5, 46.9, 68.3, 69.8, 70.0, 70.1, 72.9, 74.7, 77.3, 120.1, 139.8, 156.5, 168.9, 178.3.

MALDI-TOF-MS: *m/z* calcd. for $C_{35}H_{58}N_2O_9Na$ ($[M + Na]^+$) 673.4040, found 673.4747.

3. Synthesis of the Polymerizable Cholate Derivative 7 (Free-acid Form of SC-M_3)

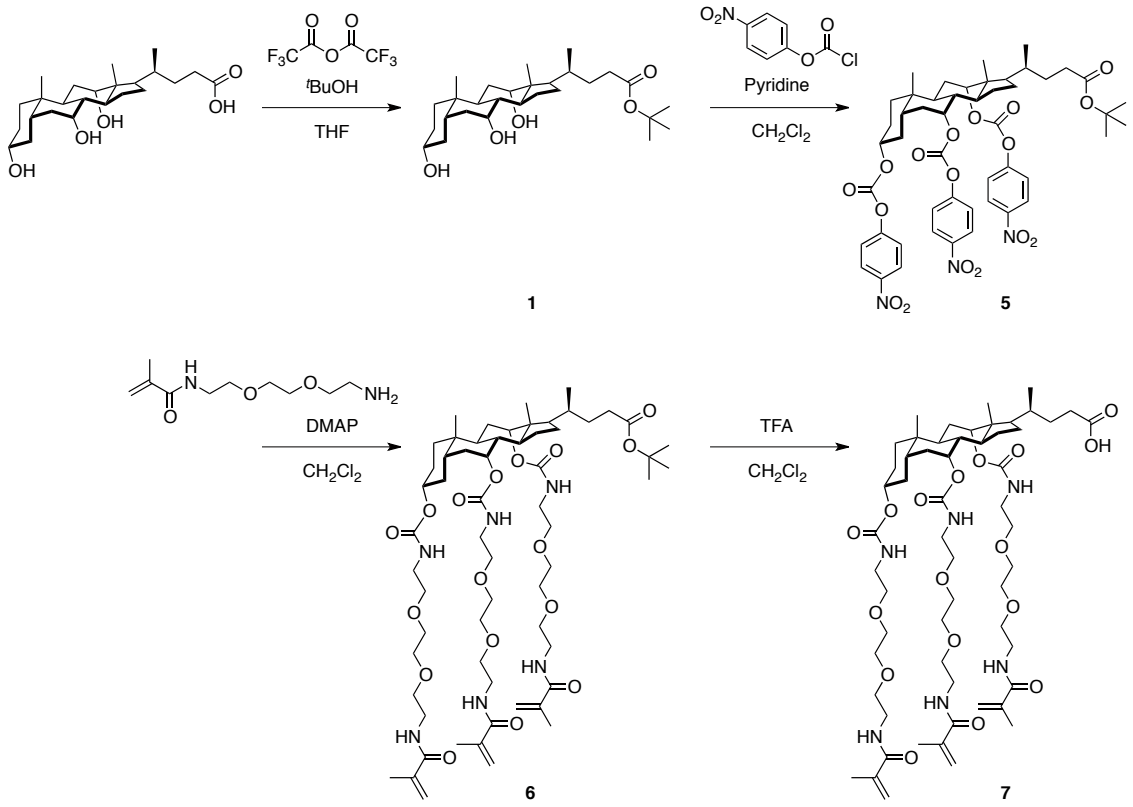

Scheme S2. Synthesis of the Polymerizable Cholate Derivative **7** (Free-acid Form of **SC-M_3**)

***tert*-Butyl 3,7,12-tris((4-nitrophenoxy)carbonyl)oxy)cholate (5):**

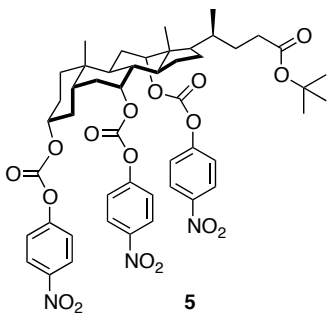

To a CH_2Cl_2 solution (150 mL) of **2** (3.00 g, 6.46 mmol) and 4-nitrophenyl chloroformate (7.00 g, 34.7 mmol) was added dropwise pyridine (3.0 mL, 37.3 mmol) at room temperature. After being stirred at the temperature for 24 h under Ar, the reaction mixture was diluted with CH_2Cl_2 (100 mL) and successively washed with aqueous $NaHSO_4$ (1 M, 2 × 100 mL) and brine (100 mL). The organic layer was dried over Na_2SO_4 and concentrated under reduced pressure to dryness. The resultant residue was subjected to silica gel column chromatography eluted with CH_2Cl_2 to afford **5** as a white solid (5.73 g, 5.97 mmol, 92%).

^{1}H NMR ($CDCl_3$): δ 0.81 (s, 3H), 0.94 (d, 3H, J = 6.1 Hz), 0.99 (s, 3H), 1.13–2.48 (m, overlapped, 24H), 1.45 (s, 9H), 4.59 (m, 1H), 4.96 (m, 1H), 5.15 (m, 1H), 7.40 (d + d + d, overlapped, 2H + 2H + 2H), 8.30 (d + d + d, overlapped, 2H + 2H + 2H).

^{13}C-NMR ($CDCl_3$): δ 12.2, 17.8, 22.3, 22.9, 25.5, 26.5, 27.1, 28.1, 28.7 30.7, 31.1, 32.5, 34.0, 34.3, 34.5, 38.0, 40.4, 43.1, 45.5, 47.6, 79.2, 80.2, 81.2, 121.7, 121.9, 122.0, 125.3, 125.3, 125.4, 145.6, 151.5, 151.8, 151.9, 155.4, 155.6, 173.3.

HRMS (ESI-TOF, positive-ion mode, MeOH): *m/z* calcd. for $C_{49}H_{57}N_3O_{17}Na$ ([M + Na^+]) 982.3586, found 982.3598.

***tert*-Butyl 3,7,12-tris((2-(2-(2-methacrylamidoethoxy)ethoxy)ethyl)carbamoyloxy)-cholate (6):**

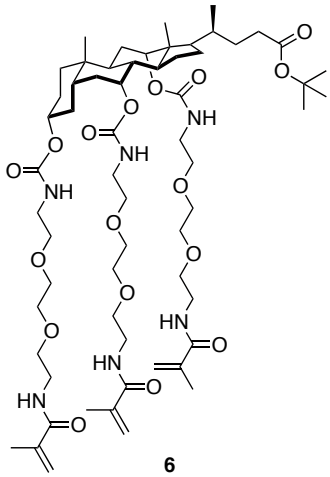

6

To a CH_2Cl_2 solution (100 mL) of **5** (5.00 g, 5.21 mmol) and *N*-(2-(2-aminoethoxy)ethoxy)ethylmethacrylamide (5.00 g, 23.0 mmol) was added 4-(dimethylamino)pyridine (2.74 g, 22.5 mmol) at room temperature. After being stirred at the temperature for 24 h under Ar, the reaction mixture was diluted with CH_2Cl_2 (200 mL) and successively washed with aqueous hydrochloric acid (0.1 M, 2 × 100 mL) and brine (200 mL). The organic layer was dried over Na_2SO_4 and concentrated under reduced pressure to dryness. The resultant residue was subjected to silica gel column chromatography eluted with CH_2Cl_2 to afford **6** as colorless oil (6.10 g, 5.120 mmol, 98%).

^{1}H NMR ($CDCl_3$): δ 0.71 (s, 3H), 0.85 (d, 3H, J = 7.1 Hz), 0.90 (s, 3H), 1.01–2.44 (m, overlapped, 24H), 1.45 (s, 9H), 1.96 (s, 9H), 3.30–3.67 (m, 36H), 4.47 (m, 1H), 4.80 (m, 1H), 4.95 (m, 1H), 5.34 (s, 3H), 5.71 (s, 3H), 5.25–5.80 (m, 3H), 6.40–6.55 (m, 3H).

^{13}C NMR ($CDCl_3$): δ 12.5, 17.6, 18.8, 22.7, 23.0, 26.3, 27.4, 27.5, 28.3, 29.2, 31.1, 31.7, 32.7, 34.4, 38.1, 39.5, 39.6, 40.9, 41.0, 41.1, 43.7, 45.5, 47.6, 69.9, 70.2, 70.2, 70.3, 70.4, 70.5, 70.5, 71.5, 74.8, 75.9, 77.4, 80.1, 119.7, 119.7, 140.2, 156.5, 168.8, 173.7.

HRMS (ESI-TOF, positive-ion mode, MeOH): *m/z* calcd. for $C_{61}H_{102}N_6O_{17}Na$ ([M + Na^+]) 1213.7199, found 1213.7182.

3,7,12-Tris((2-(2-(2-methacrylamidoethoxy)ethoxy)ethyl)carbamoyloxy)cholic acid (7):

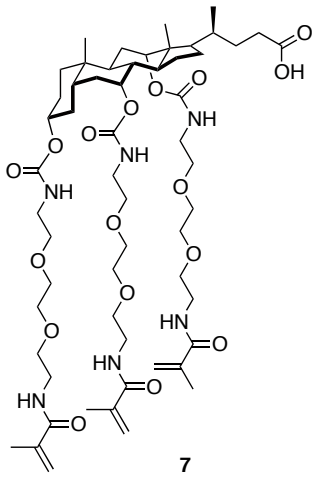

7

To a CH_2Cl_2 solution (100 mL) of **6** (6.00 g, 4.94 mmol) was added dropwise trifluoroacetic acid (1 mL) at 0 ºC. After being stirred at room temperature for 24 h, the reaction mixture was concentrated to dryness under reduced pressure to afford **7** as colorless oil (5.60 g, 4.936 mmol, 98%).

^{1}H NMR ($CDCl_3$): δ 0.72 (s, 3H), 0.85 (d, 3H, J = 6.1 Hz), 0.90 (s, 3H), 1.0X–2.25 (m, overlapped, 24H), 1.97 (s, 9H), 3.25–3.80 (m, 36H), 4.46 (m, 1H), 4.80 (m, 1H), 4.96 (m, 1H), 5.35 (s, 3H), 5.52 (m, 1H), 5.62 (m, 1H), 5.73 (m, 3H), 5.85 (m, 1H), 6.65–6.87 (m, 3H).

^{13}C NMR ($CDCl_3$): δ 12.4, 14.4, 17.6, 18.4, 18.8, 22.6, 23.0, 25.5, 26.1, 27.4, 29.1, 31.0, 31.1, 31.7, 34.4, 34.8, 35.2, 38.0, 39.5, 40.8, 41.0, 43.7, 45.4, 47.4, 50.9, 51.7, 53.6, 69.9, 70.2, 70.2, 70.3, 70.4, 70.5, 70.6, 71.5, 120.0, 140.1, 156.1, 156.6, 168.8, 174.8.

HRMS (ESI-TOF, positive-ion mode, MeOH): *m/z* calcd. for $C_{57}H_{94}N_6O_{17}Na$ ([M + H^+]) 1157.6573, found 1157.6587.

4. Typical Procedure for the Preparation of Bicellar Mixtures

1,2-Dimyristoyl-*sn*-glycero-3-phosphatidylcholine (DMPC: 62.5 mg, 0.092 mmol), **4** (free-acid form of SC-M_1: 14.2 mg, 0.022 mmol), and **7** (free-acid form of SC-M_3: 1.3 mg, 1.1 μmol) were dissolved in $CHCl_3$/MeOH (9:1, v/v, 1 mL). The solution was concentrated to dryness under reduced pressure and further dried under reduced pressure for 1 h at room temperature. To the resultant residue were successively added a D_2O solution (0.7 mL) of KCl (100 mM) was and a D_2O solution (18 μL) of NaOH (1.25 M). The mixture was heated up to 40 ºC, vortexed, cooled to 0 ºC, and vortexed. The heat–cool cycle was repeated at least three times until clear homogeneous solution was obtained.

Other bicellar mixtures were prepared in the same procedure, with varying the lipid/surfactant ratio and/or total lipid content.

5. Typical Procedure for the in-situ Polymerization of Bicelles

A bicellar mixture containing DMPC (62.5 mg, 0.092 mmol), SC-M_1 (14.2 mg, 0.022 mmol), and SC-M_3 (1.3 mg, 1.1 μmol) dispersed in a D_2O solution (320 μL) of KCl (100 mM) was cooled in ice/water bath, held in a Shigemi NMR tube, and purged with N_2 by bubbling. To the mixture was successively added a D_2O solution (9 μL) of potassium persulfate (24.8 mM) and then *N*,*N*,*N*',*N*'-tetramethylethylenediamine (5.0 μL, 0.034 mmol) at 0 ºC with N_2 flow. The mixture was vigorously shaken, heated to 40 ºC, and left to stand at the temperature for 1 h. Completion of the polymerization was confirmed by monitoring the ^{1}H NMR signals attributable to the vinyl groups of SC-M_1 and SC-M_3. To ensure the homogeneity, the resultant mixture was treated with a D_2O solution (380 μL) of KCl (100 mM) and left at room temperature for 1.5 h to afford a viscous translucent fluid.

The in-situ polymerization of other bicellar mixtures was conducted in the same procedure, with varying the lipid/surfactant ratio, total lipid content, and/or polymerization temperature.

Reference

[1] a) Sanders, C. R.; Prosser, R. S. *Structure* **1998**, *6*, 1227–1234. b) Marcotte, I.; Auger, M. L. *Concepts Magn. Reson.* **2005**, *24A*, 17–37. c) Dürr, U. H. N.; Gildenberg, M.; Ramamoorthy, A. *Chem. Rev.* **2012**, *112*, 6054–6074.

[2] a) Tjandra, N.; Bax, A. *Science* **1997**, *278*, 1111–1114. b) Yan, J.; Delaglio, F.; Kaerner, A.; Kline, A. D.; Mo, H.; Shapiro, M. J.; Smitka, T. A.; Stephenson, G. A.; Zartler, E. R. *J. Am. Chem. Soc.* **2004**, *126*, 5008–5017. c) Opella, S. J.; Marassi, F. M. *Chem. Rev.* **2004**, *104*, 3587–3606. d) Prestegard, J. H.; Bougault, C. M.; Kishore, A. I. *Chem. Rev.* **2004**, *104*, 3519–3540. e) Prosser, R. S.; Evanics, F.; Kitevski, J. L.; Al–Abdul–Wahid, M. S. *Biochemistry* **2006**, *45*, 8453–8465. f) Vlach, J.; Saad, J. S. *Proc. Natl. Acad. Sci. USA* **2013**, *110*, 3252–3530. g) Cho, M.–K.; Gayen, A.; Banigan, J. R.; Leninger, M.; Traaseth, N. J. *J. Am. Chem. Soc.* **2014**, *136*, 8072−8080.

[3] a) Song, Y.; Dorin, R. M.; Garcia, R. M.; Jiang, Y.–B.; Wang, H.; Li, P.; Qiu, Y.; van Swol, F.; Miller, J. E.; Shelnutt, J. A. *J. Am. Chem. Soc.* **2008**, *130*, 12602–12603. b) Tekobo, S.; Pinkhassik, E. *Chem. Commun.* **2009**, 1112–1114. c) Yasuhara, K.; Miki, S.; Nakazono, H.; Ohta, A.; Kikuchi, J. *Chem. Commun.* **2011**, *47*, 4691–4693. d) Yang, P.–W.; Lin, T.–L.; Lin, T.–Y.; Yang, C.–H.; Hu, Y.; Jeng, U.–S. *Soft Matter* **2013**, *9*, 11542–11548. e) Ikeda, A.; Kiguchi, K.; Hida, T.; Yasuhara, K.; Nobusawa, K.; Akiyama, M.; Shinoda, W. *Langmuir* **2014**, *30*, 12315−12320.

[4] a) Raffard, G.; Steinbruckner, S.; Arnold, A.; Davis, J. H.; Dufourc, E. J. *Langmuir* **2000**, *16*, 7655–7662. b) Arnold, A.; Labrot, T.; Oda, R.; Dufourc, E. J.; *Biophys. J.* **2002**, *83*, 2667–2680.

[5] a) Sanders, C. R.; Prestegard, J. H. *Biophys. J.* **1990**, *58*, 447–460. b) Wang, H.; Eberstadt, M.; Olejniczak, E. T.; Meadows, R. P.; Fesik, S. W. *J. Biomol. NMR* **1998**, *12*, 443–446. c) Sasaki, H.; Fukuzawa, S.; Kikuchi, J.; Yokoyama, S.; Hirota, H.; Tachibana, K. *Langmuir* **2003**, *19*, 9841–9844. d) Shapiro, R. A.; Brindley, A. J.; Martin, R. W. *J. Am. Chem. Soc.* **2010**, *132*, 11406–11407. e) Yamamoto, K.; Pearcy, P.; Ramamoorthy, A. *Langmuir* **2014,** *30*, 1622–1629. f) Morales, H. H.; Saleem, Q.; Macdonald, P. M. *Langmuir* **2014**, *30*, 15219−15228. g) Yamamoto, K.; Pearcy, P.; Lee, D.-K.; Yu, C.; Im, S.-C.; Waskell, L.; Ramamoorthy, A. *Langmuir* **2015,** *31*, 1496–1504.

[6] Koynova, R.; Caffrey, M. *Biochim. Biophys. Acta* **1998**, *1376*, 91–145.

[7] a) Sanders, C. R.; Schwonek, J. P. *Biochemistry* **1992**, *31*, 8898–8905. b) Nieh, M.–P.; Raghunathan, V. A.; Pabst, G.; Harroun, T.; Nagashima, K.; Morales, H.; Katsaras, J.; Macdonald, P. *Langmuir* **2011**, *27*, 4838–4847.

[8] Ringsdorf, H.; Schlarb, B.; Venzmer, J. *Angew. Chem.* **1988**, *100*, 117–162. *Angew. Chem. Int. Ed. Engl*. **1988**, *27*, 113–158.

[9] a) Mazer, N. A.; Benedek, G. B.; Carey, M. C.; *Biochemistry* **1980**, *19*, 601–615. b) Müller, K.; *Biochemistry* **1981**, *20*, 404–414; c) Pártay, L. B.; Jedlovszky, P.; Sega, M. *J. Phys. Chem. B* **2007**, *111*, 9886–9896.

[10] a) Picard, F.; Paquet, M.–J.; Levesque, J.; Bélanger, A.; Auger, M. *Biophys. J.* **1999**, *77*, 888–902. b) Triba, M. N.; Warschawski, D. E.; Devaux, P. F. *Biophys. J.*

2005, *88*, 1887–1901. c) Loudet, C.; Manet, S.; Gineste, S.; Oda, R.; Achard, M.–F.; Dufourc, E. J. *Biophys. J.* **2007**, *92*, 3949–3959.
[11] Yamamoto, K.; Soong, R.; Ramamoorthy, A. *Langmuir* **2009**, *25*, 7010–7018.
[12] Yamamoto, K.; Soong, R.; Ramamoorthy, A. *Langmuir* **2009**, *25*, 7010–7018.
[13] a) van Dam, L.; Karlsson, G.; Edwards, K. *Biochim. Biophys. Acta* **2004**, *1664*, 241–256. b) Glover, K. J.; Whiles, J. A.; Wu, G.; Yu, N.; Deems, R.; Struppe, J. O.; Stark, R. E.; Komives, E. A.; Vold, R. R. *Biophys. J.* **2001**, *81,* 2163–2171.
[14] Yang, P.–W.; Lin, T.–L.; Hu, Y.; Jeng, U.; *Chinese J. Phys.* **2012**, *50*, 349–356.
[15] Lipfert, J.; Columbus, L.; Chu, V. B.; Lesley, S. A.; Doniach, S. *J. Phys. Chem. B* **2007**, *111*, 12427–12438.
[16] a) Brzustowicz, M. R.; Brunger, A. T. *J. Appl. Crystallogr.* **2005**, *38*, 126–131. b) Pabst, G.; Kučerka, N.; Nieh, M.–P.; Rheinstädter, M. C.; Katsaras, J. *Chem. Phys. Lipids* **2010**, *163*, 460–479.
[17] a) Martin, J. E.; Hurd, A. J. *J. Appl. Crystallogr.* **1987**, *20*, 61–78. b) Bolze, J.; Fujisawa, T.; Nagao, T.; Norisada, K.; Saitô, H.; Naito, A. *Chem. Phys. Lett.* **2000**, *329*, 215–220.
[18] a) Jeworrek, C.; Uelner, S.; Winter, R. *Soft Matter* **2011**, *7*, 2709–2719. b) Loudet–Courreges, C.; Nallet, F.; Dufourc, E. J.; Oda, R. *Langmuir* **2011**, *27*, 9122–9130.
[19] Shimaoka, H.; Kuramoto, H.; Furukawa, J.; Miura, Y.; Kurogochi, M.; Kita, Y.; Hinou, H.; Shinohara, Y.; Nishimura, S. *Chem. Eur. J.* **2007**, *13*, 1664–1673.
[20] Fujisawa, T.; Inoue, K.; Oka, T.; Iwamoto, H.; Uruga, T.; Kumasaka, T.; Inoko, Y.; Yaga, N.; Yamamoto, M.; Ueki, T.; *J. Appl. Cryst.* **2000**, *33*, 797–800.

Conclusions and Perspectives

Throughout the thesis, the author developed design methodology of novel surfactants that affords extraordinary stabilization and additional functionalization of bicellar systems. With the elaborately designed cholic acid derivatives, the author developed unprecedented thermally stable magnetically oriented bicelles and kinetically stable magnetically oriented bicelles.

In ***Chapter 1***, the author achieved extraordinarily stable bicelle in high temperature by elaborately designed surfactants. Here the author focused on derivatives of cholic acid for a surfactant as a component of bicelles. Cholic acid bears three hydroxyl groups on the one side of a steroid skeleton, so the skeleton embraces two faces (hydrophilic face with three -OH group, and hydrophobic group). Hydrophobic face of Sodium Cholate easily interacts with hydrophobic edge of DMPC bilayer, so mixture of them forms magnetically oriented bicelle. Though cholic acid has such interesting character, temperature range of magnetically oriented bicelle formation is narrow. The author aimed establishment of proper molecular design guideline started from cholic acid, which hydroxyl groups can be easily modified. After several trials, the author found that the tailor-designed cholic acid derivative which hydroxyl groups are properly modified by long chain-like group with origoethylene glycol and appropriate alkyl units, can form extraordinarily thermally stable magnetically oriented bicelles (up to >90 °C) when they are mixed with DMPC. On the contrary, there is almost no example of thermally stable bicelles with an approach of molecular design of surfactants. Needless to say, this is a first example of thermally stable DMPC bicelle up to >90 °C.

Chapter 2 highlighted the first example of functionalization of bicelles using polymerizable surfactants, which are designed based on findings of ***Chapter 1***. The system composed of DMPC and a surfactant based on cholic acid derivatives with polymerizable units is able to form magnetically oriented bicelles in a narrow temperature range. To fix the morphology of magnetically oriented bicelles, the author tried to *in situ* polymerization of the surfactant at the temperature under which the system forms magnetically oriented bicelles. The author found that thermal stability of the bicelle is unprecedentedly improved after *in situ* polymerization of the surfactant. The surfactant is also found to have ability to fix morphology of isotropic

bicelles, indicating that the polymerization method has versatility to morphology of bicelles that are fixed to some extent. In addition, the author also found that when polymerized magnetically oriented bicelle and polymerized isotropic bicelle are mixed, exchange rate of lipids between two assemblies is quite slow, indicating that in situ polymerization of bicelles with various morphology is able to stabilize both thermally and kinetically. This is the first example of stabilization of bicelles by functionalization of surfactants, and this is also the first example of kinetic stabilization of bicelles.

The author expect that thermally and kinetically stable bicelles developed through the course of studies will be utilized for analysis for thermally stable proteins like proteins from thermophile bacteria, or more complicated analyses of reaction mechanisms like enzymatic events with multiple components. The author strongly believes that these studies will open the next door for analyses of membrane proteins and membrane acting molecules.

List of Publications

Original Papers

[1] "Chemically Locked Bielles with High Thermal and Kinetic Stability"
Ryoichi Matsui, Masataka Ohtani, Kuniyo Yamada, Takaaki Hikima, Masaki Takata, Takashi Nakamura, Hiroyuki Koshino, Yasuhiro Ishida, and Takuzo Aida.
Angew. Chem. Int. Ed,. **2015**, *54*, 13284–13288.

[2] "Magnetically Orientable Bicelles with Unprecedented Stability by Novel Surfactants Derived from Sodium Cholate"
Ryoichi Matsui, Noriyuki Uchida, Masataka Ohtani, Kuniyo Yamada, Arisu Shigeta, Izuru Kawamura, Takuzo Aida, and Yasuhiro Ishida.
ChemPhysChem, **2016***, In Press.*